Design of the Cathode, Field Cage and High Voltage Subsystems in the Far Detector Single Phase TPC

June 4, 2019

[DUNE-doc-10452]

Argonne National Laboratory: Frank Skrzecz, Ken Wood, Victor Guarino, Steve Magill
Brookhaven National Laboratory: Sergio Rescia**,** Rahul Sharma, Bo Yu, Manhong Zhao
CERN: Francesco Piertropaolo
FNAL: Sarah Lockwitz
Kansas State University: Glenn Horton-Smith
Louisiana State University: Thomas Kutter
Stony Brook University: Mike Wilking
University of Minnesota: Bill Miller
Princeton: Bill Sands

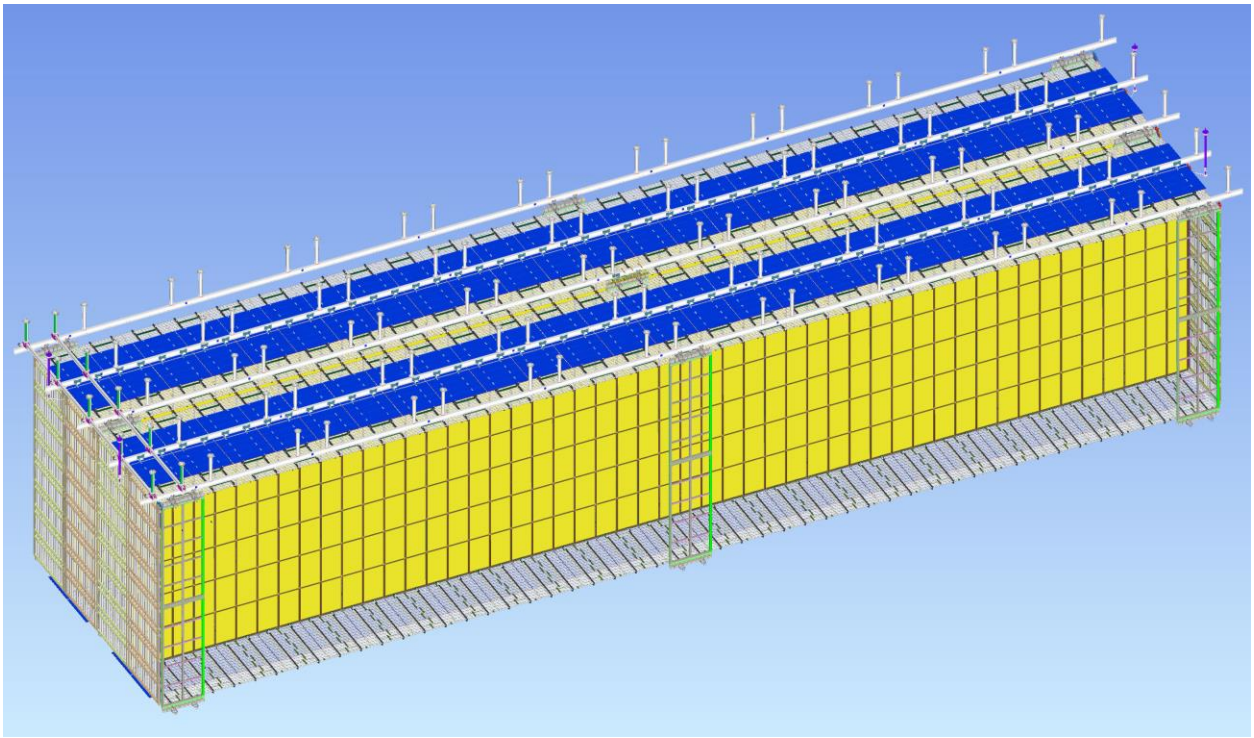

Approvals and Version Control

This version of the document may not be the current or approved revision. The current revision is maintained in LBNF/DUNE's document Management system (DocDB) where all internal Project document approvals are managed. DocDB can be accessed through the web by authorized users (http://docs.dunescience.org) and this document can be identified by the document and version number as indicated in the Version Control Table below. Note that the version number in the table below and DocDB may not match. The current approved version is always available in DocDB.

Approvals for this document will be required from:

Responsible Person:	Victor Guarino
Project Director	Eric James
Project Manager	Jolie Macier
Proto-DUNE Detector	Regina Rameika

DocDB	Version	Responsible Person	Version Date	Description of Changes

Contents

List of Figures

List of Tables

Acronyms and Abbreviations

XXXXX **Definition of Acronym**

YYYYY **Definition of Acronym**

Note that the list above text uses the format “List of Items”. And the title uses “Unnumbered 1”.

1 Introduction

The first detector of the DUNE long-baseline neutrino experiment will be located in the Homestake Mine at the Sanford Underground Research Facility (SURF) in Lead, South Dakota. The detector is a 10 kton Single Phase (SP) Time Projection Chamber (TPC) completely submerged in liquid argon with 3-wire Anode Plane Assembly (APA) readout. The complete TPC volume is approximately 12 m tall by 58 m long by ~14 m in the electron drift direction approximately perpendicular to the direction of the incoming neutrino beam. The elements which make up the HV Field Cage are the Cathode Plane Assembly (CPA) opposite the APA in the drift direction, the top and bottom Field Cage (FC) units, and the two EndWalls (EW) at the beginning and end of the 58 m long structure. The TPC is made up of 25 rows of the field cage elements between the two EWs, each row configured as APA-CPA-APA-CPA-APA where the APA-CPA connections are made at the top and bottom of the 12 m tall structure by the FCs in the drift direction. Fig. 1 shows this configuration with the central APA and two symmetric drift volumes on both sides.

The TPC, shown in Figure 1 has a central APA facing two symmetric drift volumes on both sides. Two cathode planes, 3.5 m away from the anode, terminate the central drift volumes. Two APA's 3.5 m from left and right CPA respectively delimit the two external drift volumes. At the open sides of each drift volume (top, bottom, upstream and downstream) , field cage modules are installed to define the uniform drift field of 500V/cm (nominal value). To reach this field, the cathode planes are biased at -180kV, with the anode planes at ground. The cathode bias is provided by an external high voltage power supply with a HV feedthrough connecting the cathode inside the cryostat.

Each anode plane is tiled from 25 side by side Anode Plane Assemblies (APAs). An APA has a 2.3m x 12m active area, with 3 layers of sense wires strung over stainless steel frames, and front-end readout electronics mounted on the top edge of the frame. Each APA is suspended from a rail above with a single link.

Each cathode plane is constructed from 50 side by side CPA (Cathode Plane Assembly) Panels. Each CPA Panel is 1.15m in width and 12m tall, formed from 6 vertically stacked modules, and supported by the CPA installation rail above through a single link.

The field cage modules have two distinctive styles: the top/bottom, and the end wall. Each module is constructed from an array of extruded aluminum open profiles supported by two FRP (fiber reinforced plastic) structural beams. A resistive divider chain interconnects all the metal profiles to provide a linear voltage gradient between the cathode and anode planes. The top/bottom modules are nominally 2.3m wide by 3.5m long. A ground plane in the form of tiled perforated stainless steel sheet panels is mounted on the outside surface of the top/bottom field cage module with a 20cm clearance. The T/B modules are supported by the CPAs and APAs. The end wall modules are 1.5m tall by 3.6m long. They are stacked 4 units high to cover the 6m height of the TPC. These modules are supported by the installation rails above the APAs and CPAs.

This paper describes the design, construction, methods of installation, structural, electrostatic analyses and thermal concerns for all key components of the cathode, field cage and high voltage subsystems in the PC.

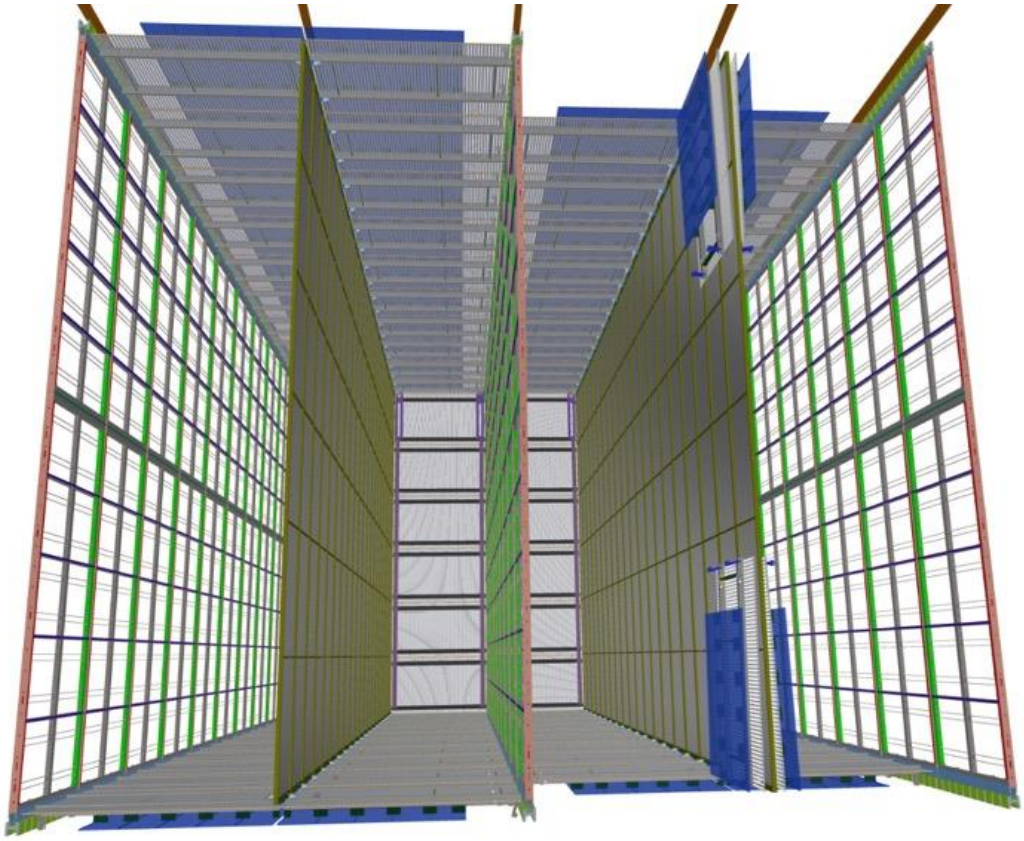

Figure 1. Geometry of TPC in DUNE-SP far detector cryostat. The central APA, and two external ones are shown interleaved with two CPA's. The top and bottom field cage modules are also present (each equipped with field blocking ground plane modules); on the right in the picture, the front most FC modules are not deployed. For Clarity only the furthermost Endwall panels are shown.

2 Lessons Learned and New Design Concepts

ProtoDUNE-SP [Dune-DocDB 1504] is the prototype for the DUNE SP far module. With approximately one twentieth the size of a far detector SP module, this detector implements an APA-CPA-APA configuration with one CPA array that bisects the TPC and two APA arrays, one along each side. The CPA array consists of six CPA panels, each 1.15 m wide by 6.0 m high (half-height relative to a SP module), and is positioned 359 cm away from each APA array, matching the maximum drift distance of a SP module.

Six top and six bottom FC modules connect the horizontal edges of the CPA and APA arrays, and four endwall FCs connect the vertical edges (two per drift volume). Each endwall FC comprises of four endwall modules (half-height relative to a SP module). A Heinzinger −300 kV 0.5 mA HV power supply delivers voltage to the cathode. Two HV filters in series between the power supply and HV feedthrough filter out high-frequency fluctuations upstream of the cathode.

The ProtoDUNE-SP HV experience was, in general, very encouraging, having demonstrated the ability to operate the TPC at the nominal drift field of 500 V/cm with a detector live-time higher than 98%.

Throughout the run the system experienced some instabilities, the sources of which are under investigation with the long stability run during 2019. Systematic studies of the HV system are underway that could lead to further design optimization for a reliable operation of a scaled-up version in the DUNE-SP far detector.

Figure 2 – CPA and FC in ProtoDUNE-SP

The instrumented Ground Planes on the top and bottom FCs proved invaluable for collecting information during moments of instability. A dedicated data acquisition (DAQ) read out the signals from the GP monitoring system, the beam plug current monitor, and the power supply at a rate of 20 kHz on a trigger provided useful information for diagnosing the HV behavior inside the TPC. This system was not operated continuously due to correspondingly large data disk storage requirements. Toroid signals from the HV filters were also helpful in localizing sources of instability, specifically for distinguishing issues on the warm side from issues inside the TPC. As mentioned, undesired current draws implicated unknown but consistent grounding pathways, these weak points evident with an increase in the number of tracks traversing a TPC during periods with increased beam halo. Given the consistent location of the ground path, these weak points are likely inadvertent features rather than design flaws. There is some evidence that the rate at which energy is deposited into the LAr impacts the rate of instabilities, which would be good news for DUNE.

Two classes of instabilities are recorded. They come in the form of (1) fast discharges (~10 ms in duration) and (2) persistent excessive current draw from the PS (current streamer) with accompanying excessive current detected on a specific ground plane and the beam plug termination. The frequency of both classes of instabilities increase over time after the system is powered on, until a steady state of about ten fast discharges/day and an instance of persistent current excess approximately once every 4 to 6 hours is achieved. Nonetheless, during operation, the HV system is able to consistently achieve >98% uptime (with automatic streamer suppression routine which takes about 4 minutes).

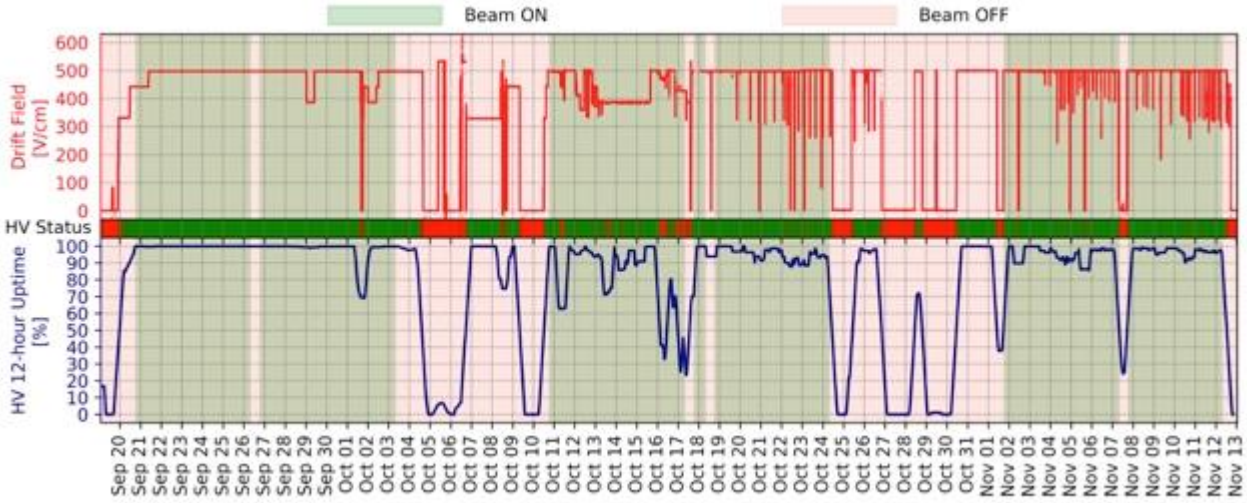

Figure 3 - ProtoDUNE-SP UpTime

Understanding the origin of the “localized current streamers” is one of the goals of the long term operation of ProtoDUNE-SP in 2019 exposed to cosmic rays. As of this writing, it appears confirmed that "current streamer" effect emerges as a charging-up process with its frequency increasing with time after a long HV-off period. The “current streamer” rate stabilizes at 3-4 per day and the location is essentially always on the same GP. Rate and location are approximately independent from the voltage applied on the CPA (in the 90 to 180 kV range).

A DAQ trigger signal, based on the HV power supply excess current and/or on the GP signals, has been implemented. It will be used to study the effect of "current streamers" or "blips" on the front end electronics and on the Photon Detectors. This trigger will also help studying the "current streamer" localization, in case extra noise/light is detected only on specific detector portions.

Furthermore, the possible role of macroscopic impurities (metallic or insulating dust) circulation with the LAr is still to be understood and specific running conditions will be implemented in ProtoDUNE SP to better investigate this issue as well.

The success of ProtoDUNE-SP validates the general design of the DUNE HV system. However various opportunities for improvement during its construction and operation were found. In particular,

- improve HV stability by increasing the distance between the GPs and field cage profiles and eliminating direct paths for potential surface currents.
- adopt a dry filter resistor design (either in-line as in the present filter design on as “pot-stile” with input and output cables on the same end) as already experienced in ICARUS;

- raise the HV feedthrough cable insert to be above the cold insulation space, if space allows (to allow cable removal while preventing moisture to enter and freeze on the walls, which could affect electrical contact);

- add toroid signals to the feed-through.

The production and handling of HV components must be approached with great care to avoid scratching and potentially compromising the electrical components. Part production should be carried out in such a way to avoid introducing sharp edges wherever possible. The corners of the ground plane panels had to be smoothed after some buckling was introduced during the pressing process, and a number of support hinges and clevises had sharp features removed by polishing. The aluminum field-shaping profiles are particularly prone to scratches and must be packaged and handled so as to avoid direct contact with other profiles and materials. Kapton strips were used to separate the profiles from the FRP of the FC frames as they were being inserted to protect against scratching or removal of the profile coating. Any scratches found in the FRP beams were covered with epoxy to prevent fibers from escaping into the LAr. Various quality control (QC) tests were conducted on HV modules and individual components at every step: part procurement, assembly, integration, and installation. To ensure that nothing was compromised during transport, QC tests were repeated on individual components and assembled pieces after shipping. Resistance between steps on the voltage divider boards were measured and verified to be within specification both after their production at LSU and after they were shipped to CERN. Once the voltage divider boards were mounted onto an assembled FC module, the resistance between adjacent profiles was measured to verify sound electrical connection. In a similar way, the connections between CPA modules and between CPA and FC modules were verified after integration. The scale of DUNE will make dedicated QC tools essential. It was a tedious process to measure each voltage step individually several times each. For example, designing a rig that can latch onto the FC modules in such a way to make contact with all electrodes and control their voltages independently, would allow for an automated loop across all steps. Such dedicated equipment and automated procedures will be required en route to a full SP module.

The ProtoDUNE-SP experience allowed for a realistic estimation of the time involved to produce various HV components for a SP module. The time involved for ProtoDUNE-SP was approximately as follows:

- FC module assembly - 1.5 days/module with 2 workers,

- EW module assembly - 1.5 days/module with 2 workers,

- CPA Plane - 2 days/Plane with 4 workers,

- CPA Plane + FC integration - 1 day/assembly with 4 workers,

- EW building - 4 hours/wall with 4-6 workers.

During installation there were some concerns about various alignment issues with the TPC, but essentially all issues were corrected once the entire detector was in place. The ProtoDUNE-SP installation sequence had the beam right drift volume deployed before the beam left. Asymmetries in the weight distribution before the beam left drift was deployed produced subtle misalignments which propagated throughout the entire detector. The process of connecting individual endwall modules to build an endwall exposed another alignment issue. The first endwall turned out significantly bowed initially. A tool was built to adjust the angle between adjacent modules, which straightened out the wall. The tool was also used while connecting modules for the remaining three endwalls and no significant bowing was observed.

In addition to ProtoDUNE-SP, two other large liquid argon TPCs have been successfully operated: ICARUS T600 and MicroBooNE. Both TPC constructions are very similar. ICARUS T600 has a 1.5m drift distance and is designed to operate at 75kV. The distance of the field cage from the ground planes as well as the shapes of all the electrodes were chosen to satisfy the requirement that the maximum electric field strength everywhere in LAr was less than 30 kV/cm, at the nominal operating voltage on the Cathode. In addition, ground planes were introduced below the LAr surface to avoid electric field leakage into the Gas phase. The T600 LAr-TPC had no difficulty holding that voltage continuously for about four years at LNGS, and furthermore, was also tested at 150kV for a brief period of time (several days at the end of the ICARUS rune at LNGS with a LAr electron lifetime exceeding 10 ms) without issues. MicroBooNE has a 2.5m drift distance and a 128kV nominal voltage. It was designed using a published LAr breakdown strength of >1MV/cm, and an overly aggressive HV to ground clearance of ~ 10cm in order to maximize the rectangular active detector cross section inside of a cylindrical cryostat. During the TPC construction period of MicroBooNE, a series of reports surfaced from several noble liquid experiments and tests that the breakdown strength of liquid argon is significantly lower than the 1 MV/cm figure, and it also shows anti-correlation with the liquid argon purity. The published breakdown strength results put the lower threshold slightly under 40kV/cm (https://arxiv.org/abs/1408.0264, https://arxiv.org/abs/1401.6693). These results prompted several studies by the MicroBooNE collaboration on the mitigation methods to reduce the maximum E field in the TPC under construction, and to harden the existing design to withstand HV breakdowns. From these studies, the DUNE LAr-TPC established a design threshold of 30kV/cm on the maximum allowed electric field inside the liquid argon, and included surge suppressors as necessary components in the field cage.

The discharge mitigation studies continued under the DUNE project focusing on the system behavior of the DUNE SP Far Detector, in particular the cathode plane. The details of this study are included in the "Discharge Mitigation" section of this document. One of the key findings is that if the cathode plane is made from a good conductor, the charge injection from the cathode plane into the front end electronics channels during a high voltage discharge, when the cathode voltage is suddenly pulled to ground at a time scale of 10s of ns, is dangerously close to the threshold of causing damage to the electronics despite of the input protections in the system. One solution to this problem is to implement a highly resistive cathode structure such that the RC time constant of the cathode is sufficiently long to limit the instantaneous voltage swing to a very local area near the discharge site, and the rest of the cathode area follows at a much longer time scale.

The cathode design described in this paper is one implementation of this solution. A commercially available resistive Kapton film from DuPont was identified as the candidate to provide the necessary resistivity on the cathode surfaces. This film can be laminated on insulating FR4 sheets using commercial printed circuit board process.

The cathode plane in the DUNE FD has a continuous area of 58m long by 12m deep. The minute pressure differential caused by the convective flow of the liquid argon on the cathode plane adds up to a non-negligible force. In addition, the cathode structure must also support the field cage modules on the top and bottom edges of the cathode. To prevent deformation of the cathode plane from the convective force of the liquid, and to provide support of the field cage, the CPA modules are designed with a robust frame using solid FR4 bars with grooves to mount the resistive panels. Since the frame protrude significantly beyond the thin cathode surface, it would have caused distortion of the drift field due to its higher dielectric constant and possible surface charging in the electric field. To eliminate this local field distortion, another layer of

resistive strip is placed on the surfaces of the frame facing the anode plane. This resistive strip is biased at a different potential to restore the uniform field near the frame surfaces.

Both ICARUS and MicroBooNE use stainless steel tubes as the field cage electrodes. Each field cage node is assembled from tube sections and corner pieces to form a continuous mechanical and electrical "ring" or "race track". There are disadvantages to scale this design to multi-kiloton scale LArTPCs such as the DUNE FD: mechanically, the field cage cannot be built as completely independent modules and therefore requires labor intensive steps to interconnect the electrode, many at great heights inside the cryostat; electrically, linking electrodes spanning more than 100m in length also increases the stored energy each electrode has and increase the risk of damaging the field cage components in a HV discharge. The joints between electrodes must be carefully designed and fabricated to avoid local electrical field enhancement.

These considerations lead to the development of a field cage concept that is completely modular: both mechanically and electrically independent field cage modules tiled to form the entire field cage. Each module has its own resistive divider network, which minimizes the impact of the drift field in the event of a resistor failure.

Instead of using tubes as the field cage electrode, which must be vented frequently to avoid trapped volumes, aluminum extruded open profiles have been adopted as electrodes. The shape of the electrode profiles has been optimized to ensure uniform E field under the DUNE field cage configuration, allowing at the same time to minimize the distance of the field cage from the ground planes and keep the E-field outside of the active volume always below the critical value of 30 kV/cm (to minimize the probability of discharge initiations). The latter is beneficial to reduce the amount of inactive LAr surrounding the field cage in favor of the active volume.

Figure 4 shows a map of the E field amplitude in the region above the CPA side of the field cage built with this profile. With -180 kV maximum bias on the cathode, and a 30 cm FC to ground clearance, the E field above the profiles are under 10 kV/cm, well below the 30 kV/cm limit set for safe TPC operation.

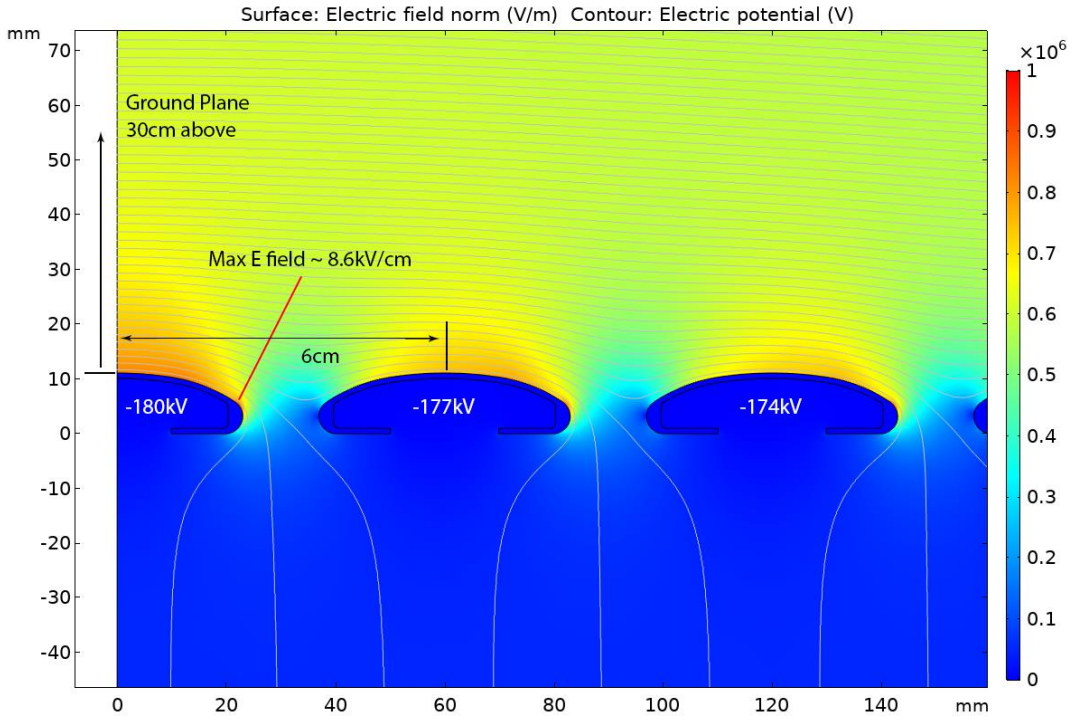

Figure 4 Electric field map (color) and equipotential contours of an array of extruded profiles biased up to -180kV and a ground clearance of 30cm.

Maintaining electrical isolation between side by side FC modules requires electrical insulation between ends of profiles up to the full bias voltage of 180 kV such that if one field cage element is discharging to the ground, the electrode from the neighboring modules will not arc over and transfer additional energy to the original discharge. The solution is to terminate the profiles ends with UHMW polyethylene caps. These caps are designed to have sufficient wall thickness (6 mm) to withstand the full voltage across their walls.

These caps also solved the problem with the field cage edges while a horizontal module meets a vertical one. The E field on the profile ends is significantly higher than that of the flat portion of the profile surface. Due to the thickness and the rounded edges of the caps, the E field at the outer surface of the caps is greatly reduced to below the E field threshold. Figure 5 shows some results of the FEA on the corner caps for the DUNE operating condition.

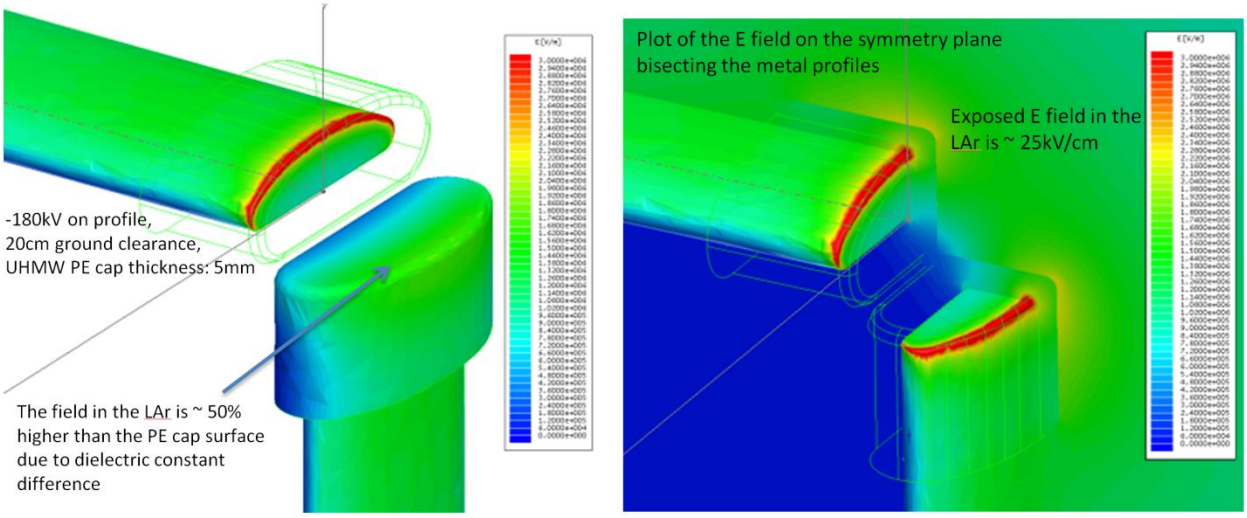

Figure 5 E-field amplitude in the region near the PE caps

3 CPA Design and Analysis

The CPA consists of a FR4 frame that encloses and supports the resistive panels. Each CPA Panel is approximately 1.15m wide and 12m long and is constructed from 6 separate modules. Two CPA Panels paired together form a CPA Plane. A CPA Plane with attached top and bottom Field Cage (FC) units is the basic installation unit for DUNE. Figure 6 shows a CPA Plane before attachment of Field Cage (FC) units. Details of the design and the stress analysis that has been performed are described below.

3.1 CPA Requirements

Below is a list of requirements the CPA must achieve:

		Parameter	Value	units
1	The CPA surface resistivity shall exceed the indicated minimum value.	CPA-resistivity-min	1	Mohm/square
2	The CPA surface resistivity shall not exceed the indicated maximum value.	CPA-resistivity-max	1	Gohm/square
4	All CPA elements will be cleaned according to guidelines established by the DUNE purity group.	CPA-cleaning		
5	All FC elements will satisfy radioactivity requirements as specified by the DUNE purity group.	CPA-radiopurity		
6	A CPA plane shall meet the material requirements of FNAL for DUNE.	**CPA-flammability**		
8	All CPA connections shall be able to withstand a peak instantaneous current given by the specification.	CPA-peak-power	?	kA
9	The CPA voltage shall drop to 10% of its operational value in a time meeting or exceeding the specification.	CPA-discharge-time-min	1	ms
11	CPA planes shall be able to support top/bottom Field Cage (FC) modules			
12	A CPA plane shall be able to withstand installation forces			
13	A CPA plane shall have no trapped volumes.			
14	A CPA plane shall provide support for the HV system.			
15	A CPA plane must stay within an envelope (including the HV) of 58000mm laterally and 12400mm vertically.			
17	CPA planes shall have a maximum deviation from flatness less than the given tolerance.	CPA-Flat	6	mm
18	No exposed electrically-floating conductors, and no sharp points or edges on any conductor.			

3.2 CPA Design

The CPA is composed of six modules that are bolted and pinned together with tongue/groove joints to form a CPA Panel. Figure 7 shows the basic geometry of a CPA Panel and Figure 8 shows a typical frame joint. Each module consists of a framework in which the resistive panel is captured inside a groove. Each module weighs roughly 80 lbs. for a total weight of the CPA Panel of 480 lbs.

The resistive panel is 1/8" thick FR4 and floats within the framework so that no external forces are applied to it. When hung vertically the weight of the resistive panel rests on the bottom cross bar of the module. The weight of the lower module is transferred through the side bars of the frame and up to the top cross bar. The resistive panel will have a layer of carbon-impregnated Kapton laminated on the front and back. The laminating will occur during the fabrication of the FR4 panel itself by an Italian company MDT.

The very top cross bar of the CPA Panel has a block attached to it through which the entire load is transferred to the strap which attaches to the supporting stainless steel I-beam. The FR4 strap extends through the FC and then makes a transition to a stainless steel threaded rod for connection to the roof. See Figure 9 and Figure 12. Integral to this main support block is the hinge which supports the top FC modules.

Each hinge must support half of the weight of a FC module (282lbs/2 = 141 lbs) during installation, and a fourth of its weight (282lbs/4 = 70lbs) after installation.

Figure 12 and Figure 13 shows the hinge connection for the bottom FC modules. A block is bolted and pinned to the bottom cross bar of the FC panel and a hinge attached to protruding wings.

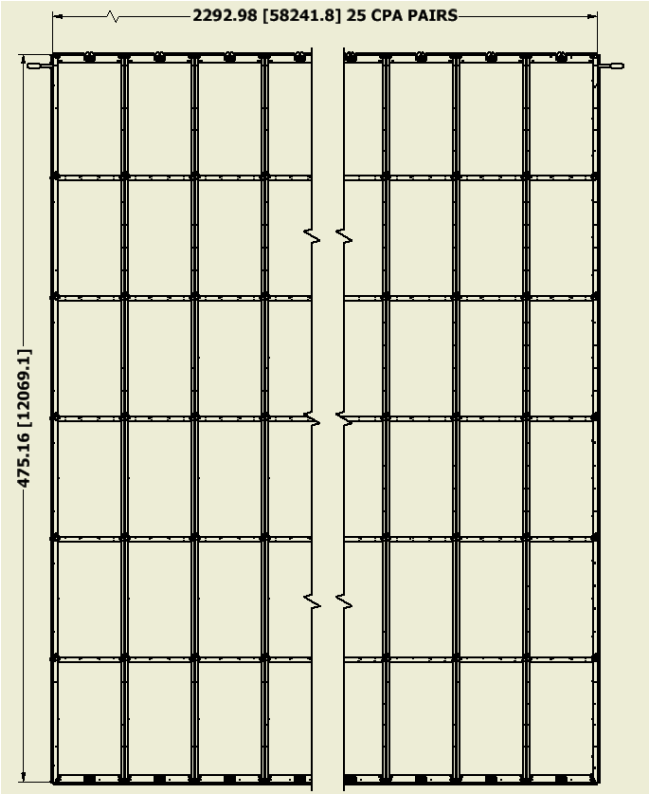

Figure 6 CPA Assembly

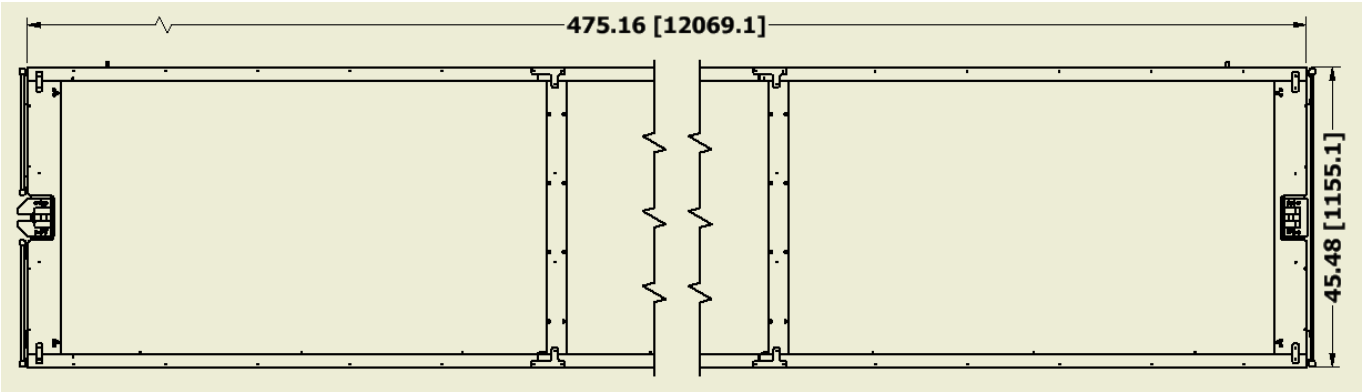

Figure 7 CPA Dimensions

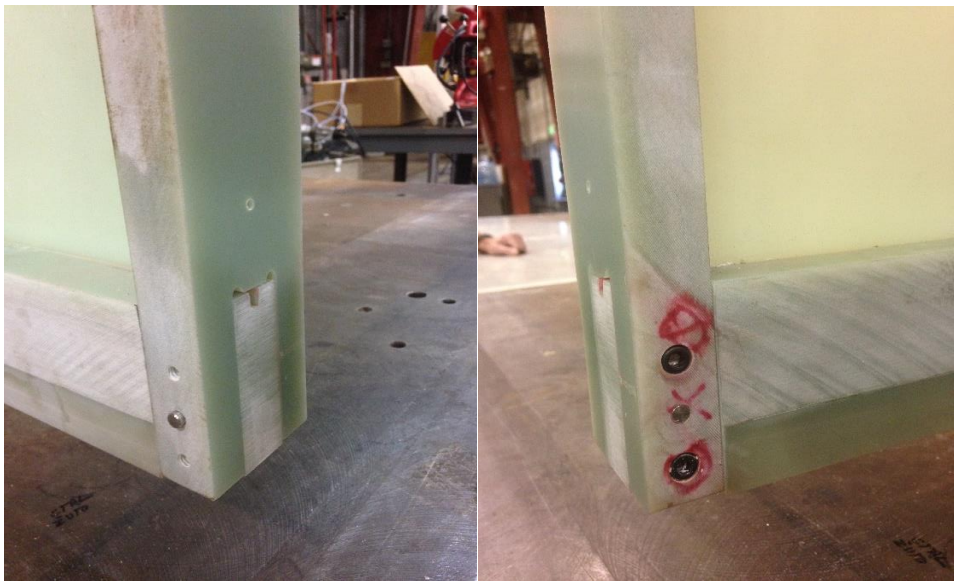

Figure 8 View of Tongue and Groove Joint

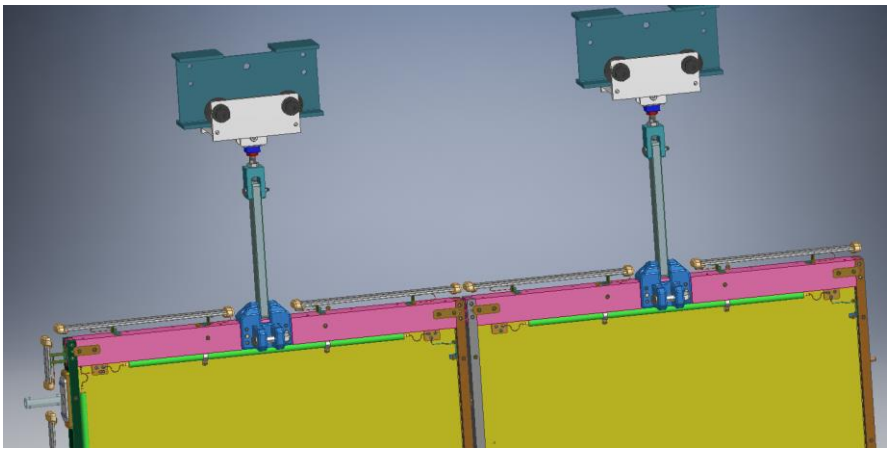

Figure 9 View of the interface between CPA Panels (Field Shaping Strips removed for clarity)

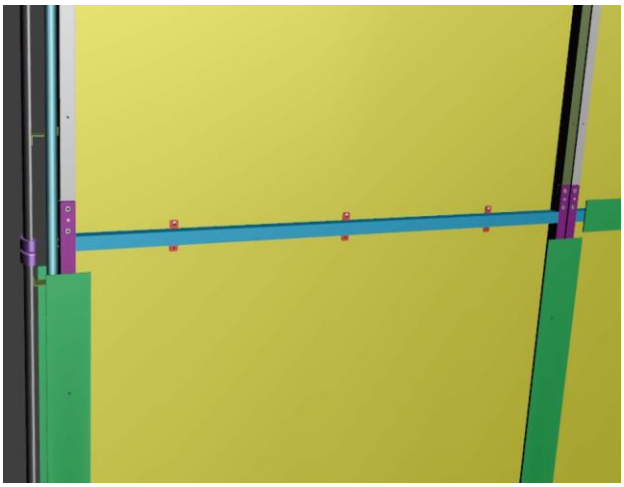

Figure 10 View of the interface between CPA modules. Upper Field Shaping Strips removed for clarity

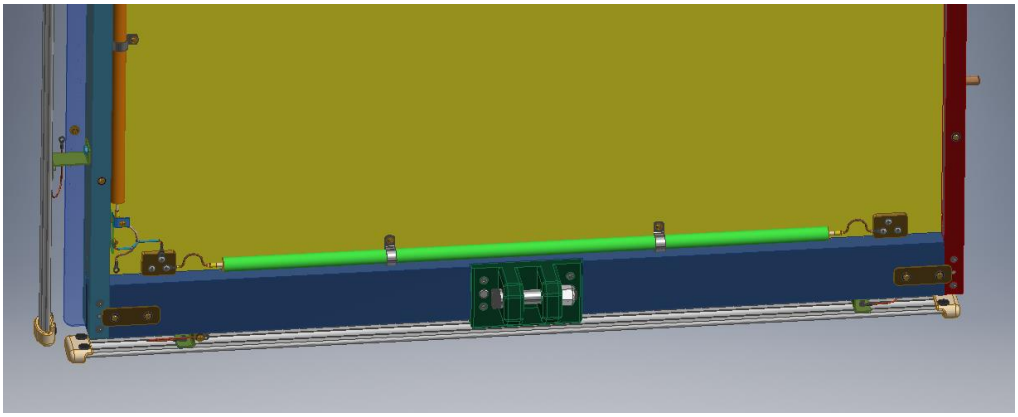

Figure 11 View of the bottom of CPA showing the HV connection and mounting for bottom FC modules. Field Shaping Strips removed for clarity

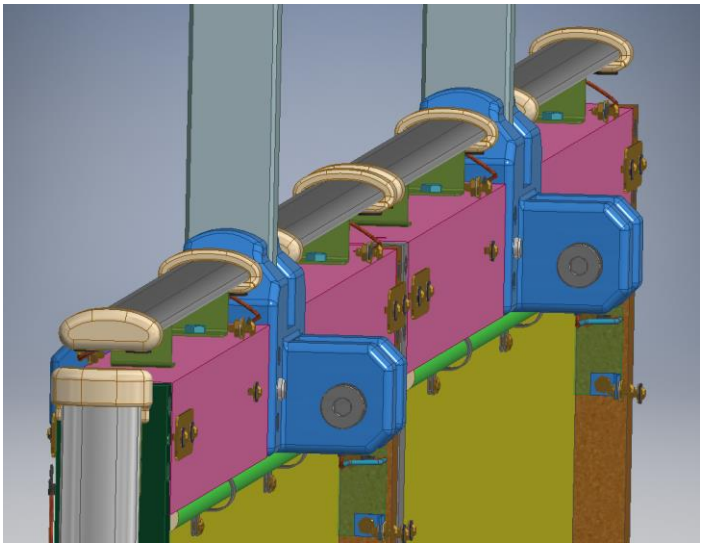

Figure 12 View of top of CPA Plane showing upper support block and hinge for mounting top FC modules. Field Shaping Strips removed for clarity

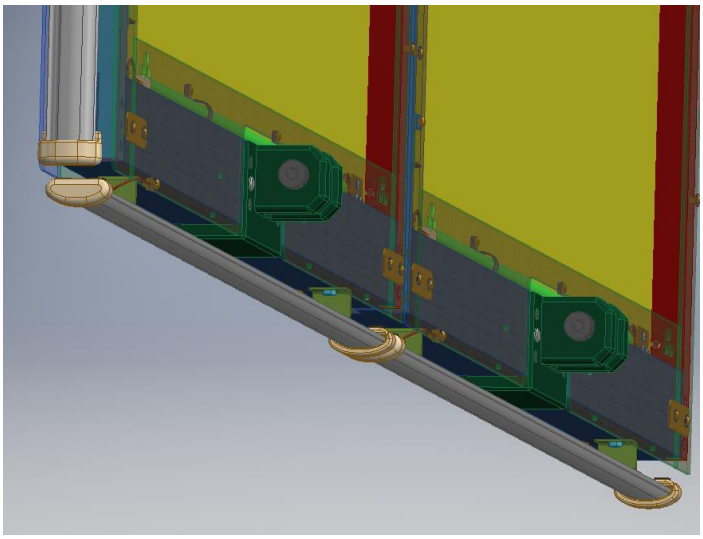

Figure 13 View of bottom of CPA and mounting for bottom FC Modules

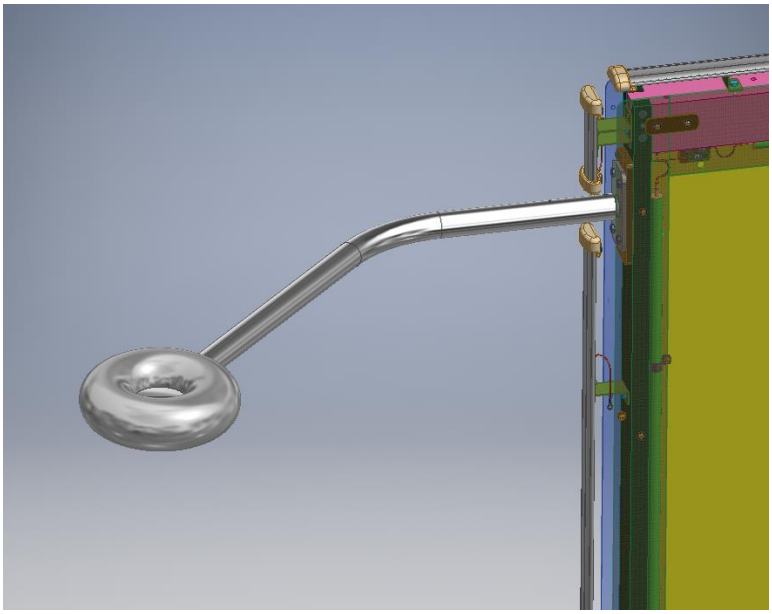

Figure 14 View of Electrical Connection to HV Cup

The HV will be fed to the CPA plane through a donut connection shown in Figure 14. HV cable will run along the top and bottom of each CPA panel as shown in Figure 9 and Figure 11. A HV cable will also run down the side of the first CPA as shown in Figure 10 and g to the bottom where a second HV cable will run across CPA's in the same manner as the top cable. The resistive coating on each module will be electrically connected together with stainless steel tabs that are bolted through the panel to matching tabs on the opposite side, and between panels by running a HV cable that has to be connected during installation, Figure 9.

The CPA's will also have field shaping strips attached to the outside surface of the frame. Each strip will overhang the sides of the frame by 1".

The assembled row of CPAs will have FC profiles attached to them around the outside perimeter and are shown in green in Figure 12, Figure 13, and Figure 14.

A complete drawing package is in Appendix 2 and in Docdb 10452.

3.3 Kapton Laminated Panels

The resistive CPA is composed of a thin FR4 panel laminated on both sides with DuPont resistive Kapton film (25 µm thickness, graphite loaded, available with resistivity in the 0.5 to 50 MOhm/square range, Figure 15). The main criteria for the selection of the resistive material to be used for the CPA panels included:

- Surface resistivity range.
- Compatibility with cryogenic temperatures
- Robustness to HV discharges, material ageing.
- Radio-purity.

- Availability on large area; achievable planarity

This option was selected out of few alternatives after extensive an intense R&D phase including radiological purity that was carried out in view of the ProtoDUNE SP design and construction (see ProtoDUNE docdb….).

Table 2
Electrical Properties of Kapton® 100XC10E7 and 100XC10E5 Polyimide Film

Property	Typical Value	Test Method
Film Type 100XC10E7		
Surface Resistivity Aim, mega ohm/sq.	5	ETS 870 electrometer at 100V
Resistivity Range, avg, mega ohm/sq.	.5-50	
Film Type 100XC10E5		
Surface Resistivity Aim, mega ohm/sq.	5	ETS 870 electrometer at 100V
Resistivity Range, mega ohm/sq.	0.1-1000	

Figure 15 Electric properties of resistive kapton by DuPont TM: 100XC10E7 has been chosen for the narrower resistivity range.

Kapton lamination on FR4/FR4 is well-established fabrication techniques (used for example in the construction of resistive Thick-GEM's) and are available on panels as large as to 2.1 x 1.2 m (well matching the required size of the CPA panels). Kapton exhibits a quite uniform surface and resistivity. Preliminary tests on large size panels have demonstrated that Kapton laminated FR4 survive without deformation or delamination to repeated immersions in LAr. The resistivity increase at LAr temperature is bounded to much less than a factor two from 6 MOhm/square at room temperature to 9 MOhm/square at LAr temperature.

Electrical contacts are performed with specific silver paint bonded on to the panel surface at high temperature and high pressure, making it highly stable at LAr temperature and resistant to mechanical scratches.

Tests on surface ageing when exposed to HV sparks indicate that Kapton is an appropriate solution because sparks are point-like inducing tiny localized carbonization on material surface, at the spark position, but no change in average resistivity is recorded (Figure 16).

Figure 16 Resistive Kapton behavior to continuous sparks. Robustness to sparks shows as localized carmonized spots that do not change the average surface resistivity.

The resistive CPA panel construction will rely on well-established PCB techniques developed at CERN for the resistive thick-GEM's detectors. The resistive kapton lamination procedure is summarized as follows:

- A stack composed of FR4/FR4 panel (3mm thick) with 75 um pre-preg and 25 um kapton foil on both sides is placed in between metallic sheets and un-moulding foils (for uniform pressure and temperature distribution).
- The stack undergoes a press cycle at 20 Kg/cm^2 for about 1 hour at 160-200°C.
- Unmoulding of outer metallic foils and cleaning is finally performed.
- Silver paste for electrical contacts is painted where required and stabilized at high temperature (~ 200°C) and pressure (~20 Kg/cm^2).

At least one press is available in EU (owned by the MDT company in Italy, a known CERN supplier) for dimensions exceeding 1.2 m x 2.1 m as requires for ProtoDUNE Single Phase CPA. A panel machining procedure has also been developed to assure sharp edges of holes and borders of the kapton layer, based on temporary gluing of copper foils before machining, to avoid delamination of kapton during drilling or cutting.

While the panel construction is a consolidated procedure at CERN, the cryogenic behaviour of the laminated elements required an extensive R&D test phase. This was performed on four panels 700mm x 600 mm area, fabricated at CERN: they have been immersed in LAr, in a open-air dewar, for few weeks and then underwent several thermal cycle from room to LAr temperatures without any sign of delamination. Moreover two smaller panels (350x350 mm2, Figure 17) were fabricated and machines to be used as cathode plane for the 50-liter LAr-TPC available at CERN. These panels have been already operated several times as cathode in various test runs of the 50-liter LAr-TPC, with behavior completely equivalent to that of the metallic planes in term of mechanical stability, electric field uniformity and LAr purity. MDT has at present produced a full prototype 1.2 m x 2.1 m. This panel has been machined into two smaller elements to be installed in the 35 ton HV test at FNAL.

The resistive strip elements, foreseen to cover the CPA frame to make a uniform electric field in the drift volume, will be built with the lamination a single kapton layer on one side only. Being these elements much smaller with respect to the CPA panels and requiring in addition more precise machining and hole drilling,

they will be fabricated at CERN. A first set has been already produced (See Figure 18) for the 35 ton HV test at FNAL.

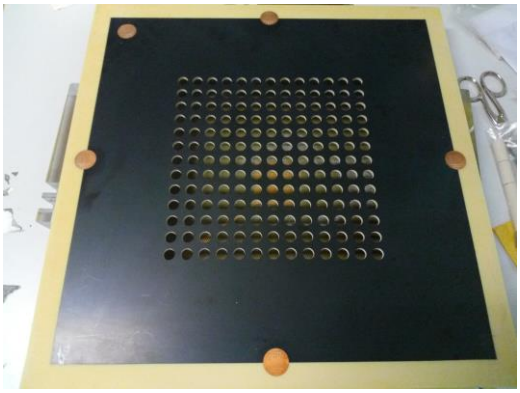

Figure 17 Double sided laminated cathode panel for the 50 liter LAr-TPC at CERN.

Figure 18 Strips for the CPA frame, obtained from a 700mm x 600mm panel laminated with resistive Kapton on a single side.

3.4 CPA Assembly

CPAs will be assembled at two factories in order to complete the production in ~6 months. Individual CPA modules (1.1m x 2m) will be mated with another module to form a basic CPA 2-module shipping Unit at the factories and will be shipped in the horizontal position. Each 2-module Unit will have attached all components of the final CPA Panel including FSSs, Profiles, HV Bus cables, wire jumpers and resistor boards. There will be six 2-module Units stacked per shipping crate making up the 2 CPA Panels of a Plane. Each crate will weigh roughly 800 lbs when full. Two crates per week will be shipped to the DUNE Logistics Warehouse (LW) on a flatbed truck. Each 2-module Unit weighs roughly 106 lbs and therefore can be lifted out by hand by 2-3 people and will not require special fixtures. Each Unit will be sealed in a plastic bag that will have to be removed. The resistive panel floats inside the module frame and during

handling the frame can be distorted and there is a potential for the panel to pop out of its retaining groove. In order to prevent this each module will have a single strap wrapped around it that can be removed after hanging. Complete CPA factory assembly and shipping procedures and checklists are available in docdb-10452.

CPA Panel assembly in the clean room at SURF will be done using a vertical assembly frame to assemble three Units together to form a full 12m tall CPA Panel which will then be hung from a transport beam. Two CPA Panels from one shipping crate will then be paired vertically to form a CPA Plane ready for attachment of the top and bottom FCs. Complete CPA/FC assembly and installation procedures and checklists are available in docdb-10452.

3.5 CPA Stress and Deflection Analysis

The CPA frame has been evaluated using empirical calculations. Detailed calculations are shown in Appendix 1. The CPA is a simple frame and the sections are tied together with a tongue and groove joint. Each module weighs only 58 lbs and is assembled on a table and then shipped in a stack horizontally under no load. Three 4m long modules are lifted out of the shipping crate from the horizontal to the vertical placing the section in bending, see Figure 20. Once vertical the 4m sections are attached to each other on an assembly fixture to form a full 12m long panel. Two panels are then brought together and the top FC modules are hung from them, see Figure 19. This configuration is the maximum loading during installation.

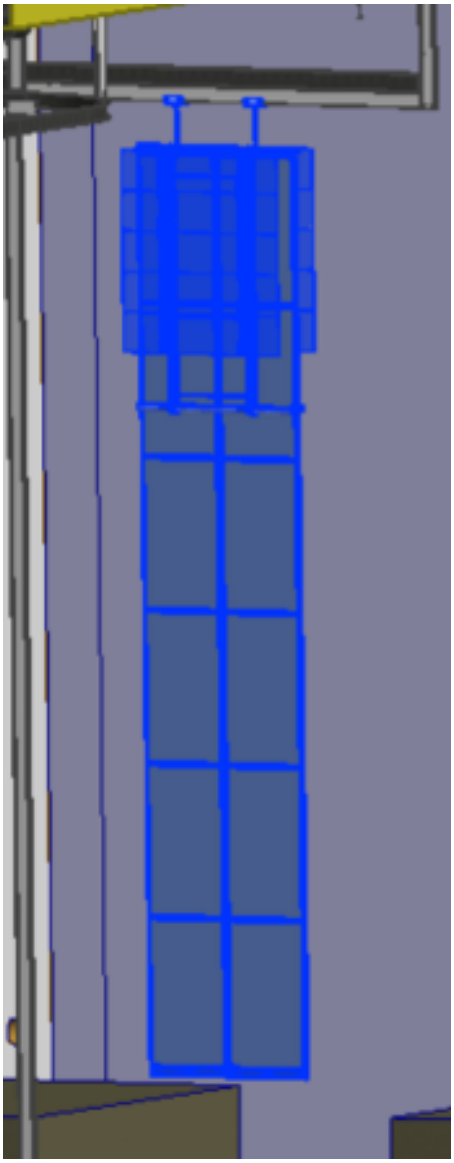

Figure 19 CPA with FC Attached During Installation

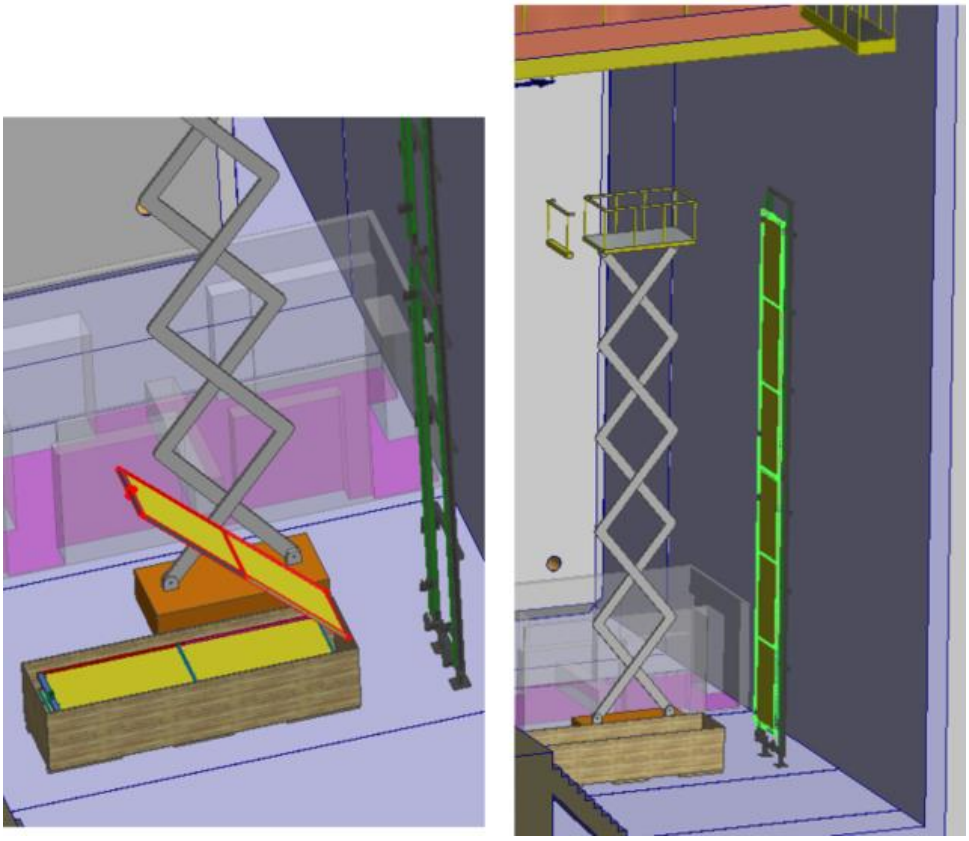

Figure 20 Assembly of CPA

The JRC Science for Policy Report "Prospect for New Guidance in Design of FRP" is used as a guide for the strength calculations. It specifies a strength reduction factor that has been calculated to be 3.75. It does not specify a load factor. In addition, a stress concentration factor of 2.3 has been applied to all pinned joints. See Section 1 of Appendix 1 for details.

The main loading occurs during rotation from the horizontal to the vertical orientation and when vertical and the

FC modules are hung from the CPA panel. Figure 19 shows a CPA module supporting the FC modules during installation. Each FC module weighs 282 lbs so a single CPA is loaded with 141 lbs on both sides at the top during installation.

The load cases that have to be considered are:

- Case 1: Lifting of the 4m long CPA module from horizontal to vertical during installation
- Case 2: CPA hanging while supporting two top FC modules that are not deployed.
- Case 3: CPA hanging while supporting four FC modules that are deployed and have a 200 lbs worker standing at the center of a FC bottom I-beam
- Case 4: Operational condition cold.

The highest stresses and deflections occur during assembly before the cryostat is filled with liquid. During installation the CPA must carry the full weight of the FC rather than sharing it with the APA and the buoyancy force which reduces the load from gravity is not present.

In all of the analysis the weight of the resistive panels was included but any additional strength or stiffness from them was not included. In the design of the CPA it is planned that the resistive panel will float within a frame and no load will be applied to it and therefore it does not contribute to the stiffness of the modules.

In all of the load cases the loads/stresses are below the allowable loads/stresses. The table below summarizes the extra margin above allowable for each Load Case which occurs for all load cases in the FR4 bar that connects the CPA to the DSS, see Section 6.1.2 of Appendix 1

Load Case	Margin above allowable
1	2.0
2	3.2
3	2.6
4	10.9

Load Case 1 - Lifting the CPA During Installation

During installation the three 4m frame sections that make up a CPA module will be lifted from the horizontal to the vertical and then attached together to form the full 12m module. Figure 20 shows a 4m long submodule being lifted from horizontal to vertical. The worst case loading occurs immediately after the crane begins to lift the top of the module when it is simply supported at its ends. The stresses are calculated in section 4 of Appendix 1. The plane will sag a maximum of 0.85" and the first principle stresses are below 1098psi which is a factor of 19 below the allowable stress.

Load Case 2 - CPA Hanging with Top FC Attached in Installation Position

During installation, the two top FC modules will be hung from a CPA pair. Once installed in the correct location in the detector the top FC modules will be deployed. The current estimate for the FC weight is 282 lbs. This load is carried by 2 CPA's so each hinge on the CPA will support 141 lbs from each FC in the installation position or a total of 282 lbs per CPA. The load of the top FC is transferred through the aluminum hinge directly to the center strap that supports the CPA.

The center main strap the supports the CPA has a load is 824 lbs, see Figure 21Figure 21. There is a margin of 3.2 above the allowable strength of the central strap when the pin connection is perpendicular to the fiber mesh but only 1.1 when the pin is parallel to the mesh, see Appendix 1 Section 6.1. Therefore, during fabrication of the top strap the pin must be oriented perpendicular to the mesh or the size of the strap should be increased so that the pin can be inserted in any direction. Tests on the strap strength, see Section 4.2, showed that the joint can withstand greater than 9000 lbs before failure.

The CPA frame joints only have to support the self weight of the CPA. The load at the top joint is 271 lbs. With the pin perpendicular to the mesh the design joint strength is 1831 lbs. See Section 6.2.2 of Appendix 1. Testing showed that the failure load of the joint is 6600 lbs, see Section 4.2 above.

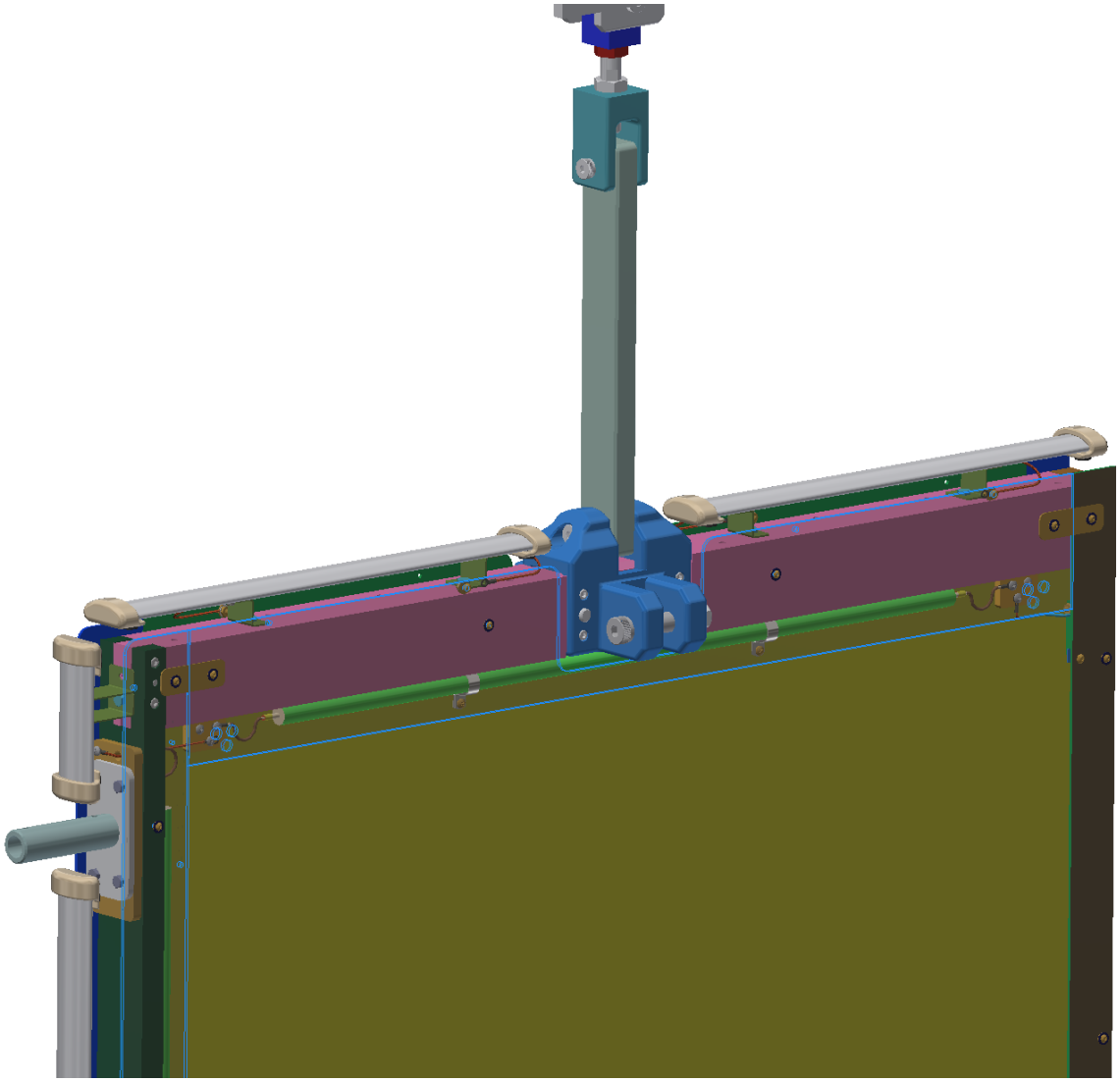

Figure 21 – Top Strap Connecting CPA to DSS

Load Case 3 - CPA Hanging with all FC Attached in Deployed Position with Weight of Workers on FC

The current estimate for the FC weight is 282 lbs. This load is carried by 2 CPA's and by the APAs after deployment so each hinge on the CPA will supposed 70.5 lbs in the installation position. In addition, in the worst case a 200 lbs worker could be standing directly over an I-beam on the FC directly next to a CPA. The top two hinges on the CPA will have 70.5 lbs applied. One of the bottom hinges will have a 70.5 lbs load also and the second bottom hinge will have 70.5 lbs of the FC plus the 200 lbs of the worker applied.

The load on the top strap is 1024 lbs. The design load of the strap when the pin is perpendicular to the mesh is 2637 lbs which gives a margin of 2.6, see Section 6.1 of Appendix 1.

The load at the CPA top frame joint is 512 lbs and the design strength is 1831 lbs which gives a margin of 3.6, see Section 6.2 of Appendix 1.

Load Case 4 - Operational Condition

The weight of the CPA and FC is substantially lower in the wet condition due to buoyancy. The CPA weighs 122 lbs and the FC weighs 119.7 lbs. The top two hinges on the CPA will have 30 lbs applied. One of the bottom hinges will have a 30 lbs load also and the second bottom hinge will have 30 lbs of the FC.

The load on the top strap is 242 lbs. The design load of the strap when the pin is perpendicular to the mesh is 2637 lbs which gives a margin of 10.9, see Section 6.1 of Appendix 1

The load at the CPA top frame joint is 121 lbs and the design strength is 1831 lbs which gives a margin of 15.1, see Section 6.2 of Appendix 1.

In the cold condition the CPA will shrink 24.9mm. In Section 9.4 of Appendix 1 a calculation was done to find the forces acting on the TPC members and DSS connections after shrinkage which showed that the forces remain virtually unchanged.

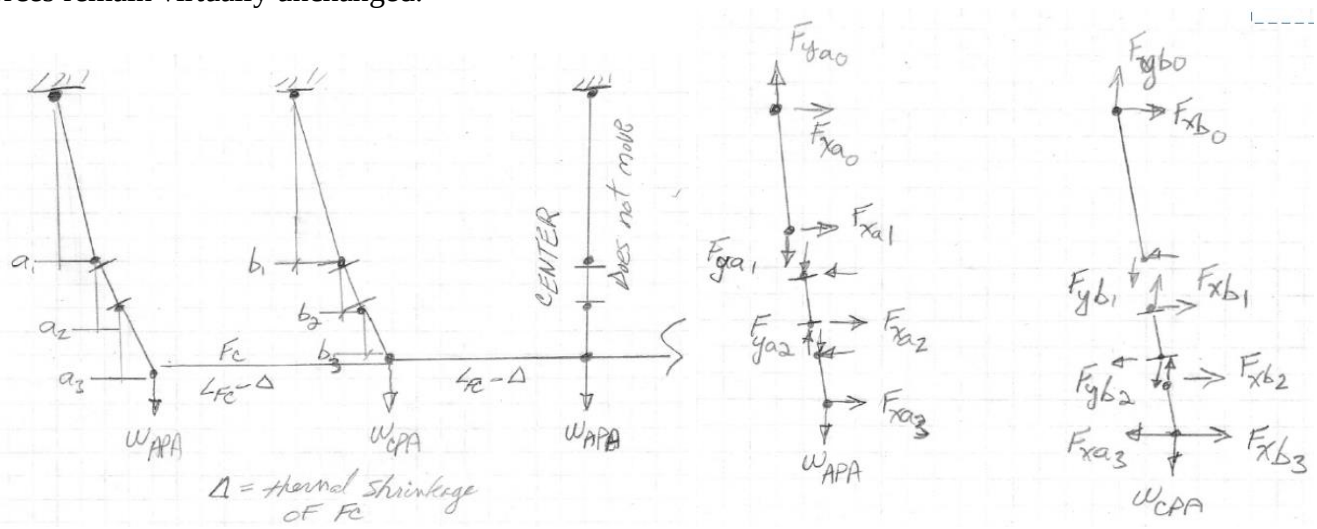

Figure 22 Lateral motion of TPC

Analysis of Effect of Pressure from Circulating Liquid Argon

Calculations done at Fermi Lab (see docdb 886) indicate that a linearly varying pressure during cool down will be applied to the resistive panels. Calculations show that this will result in 0.14" deflections of the panel at its center. The CPA/FC/APA assembly will displace 1.9mm laterally as a result of the net force from this pressure, see Section 5 of Appendix 1.

3.6 CPA Thermal Considerations

There is a significant difference in the thermal contraction coefficients between the orthogonal orientations of fibers in the FR4 material that makes up the CPA frame.

There are several areas where compensation is needed to account for differential shrinkage between the FR4 and stainless steel as well as the differences in FR4 direction: differential shrinkage between the support beam and CPA width; differential shrinkage between the stainless beam and the FC length;

potential differential shrinkage between the CPA panel and the frame if the fiber orientations are not aligned.

The material for the top member of the CPA frame will be specified so that the warp direction runs in the direction of the width of the CPA. When the CPA modules are cooled their width will shrink by up to -2.4 mm if the top cross beam has the main fibers oriented in the warp direction of the fibers and -7.3 mm if the fibers are oriented in the normal direction. The supporting stainless steel beam will shrink by -3.1mm over the width of the CPA. The CPA strap is attached to the supporting stainless steel beam so an interference of potentially 3.1mm – 2.4mm = .7mm will occur. In order to prevent this interference an initial gap of 3mm between CPA's is required which will ensure that the CPAs are in contact after cool down and account for alignment and fabrication tolerances.

Another thermal consideration is the steel beam between the CPA and APA which will cool and shrink by 9.7mm. The FC I-beams will shrink by roughly 7mm. The joint between the FC and the CPA must be able to accommodate this shrinkage differential. The hinge between the FC and CPA will a slot to accommodate this shrinkage. See section 2 of Appendix 1.

Section 9.4 of Appendix 1 calculates the movement of the detector cross section. The center APA hangs vertically because of symmetry while the adjacent CPAs will move towards the center by 7.5mm and the outer APAs move towards the center 15mm. There are several pivot joints that support the CPA and APA and allow this motion to occur. As shown in Section 9 of Appendix 1 the resulting increase of loads on the DSS because of this movement is negligible.

4 FC Design and Analysis

FC are constructed from pultruded FR4 I-beam and box beams and extruded aluminum profiles. Details of the design are described below and the analysis that has been performed.

4.1 FC Requirements

Below is a list of requirements the FC must achieve:

		Parameter	Value	units	notes
1	The FC shall maintain its integrity for the specified lifetime.	FC-lifetime	1	years	
2	The FC integrity shall be defined by the maximum allowable resistance over a bar length that can develop over the specified lifetime.	FC-Qfactor	1	Ohm	
3	A FC profile shall have a maximum sagitta less than the specified tolerance.	FC-bar-straightness	5	mm	
4	A FC profile shall have no surface defect with a depth exceeding the tolerance.	FC-bar-smooth	100	microns	
5	A FC bar shall have an end-to-end resistance less than the tolerance.	FC-bar-resistabce	0.1	Ohm	

		Parameter	Value	units	notes
6	Each resistor in a FC voltage divider chain shall have a resistance within the tolerance of the value specified in the voltage divider design.	FC-divider-resistance	1	percent	
7	All FC elements will be cleaned according to guidelines established by the DUNE purity group.	FC-cleaning			Need input
8	All FC elements will satisfy radioactivity requirements as specified by the DUNE purity group.	FC-radioprity			Need input
9	A FC voltage divider shall be protected by surge protection circuit elements even in the case where the specified number of elements fail at any voltage divider leg	FC-divider-surge-number	2		
10	FC elements shall have only one resistive path to ground through the FC voltage divider circuit.	FC-max-current	1	nA	total bias current limit at 500 V/cm operation.
11	All FC elements shall hold voltage up to the specified value.	FC-max-voltage	150	percent	of bias corresponding to 500 V/cm drift field
12	All FC voltage dividers must have correct resistances as specified in design.	FC-resistance-tolerance	1	percent	measure electrode-to-electrode resistances with multimeter
13	The FC voltage divider chain must have the design resistance within tolerance.	FC-total-resistance	1	%	warm resistance
14	FC unit bars shall maintain a constant separation with respect to neighbors over their full length within the tolerance.	FC-bar-separation	1	mm	
15	FC units shall have a maximum deviation from flatness less than the given tolerance.	FC-Flat	3	mm	Frame flatness tolerance. Mechanically achievable.
16	All conducting elements of the FC shall be held at a defined voltage.	FC-no-float			

4.2 Design Description

The main structure of the Top/Bottom Field Cage is constructed of two main I-Beams that are 3.5 m long, and three cross I-beams that connect main I-beams for structural stability as shown in Figure 23

Main I-beams have cutouts of the shape of profiles. All field cage components are made of insulating material, except for the field shaping profiles, the nuts and bolts holding them, and the ground planes. The material selected for the structural components is FRP. This is to prevent binding when the fiberglass structure is under cryogenic temperatures. The ground planes are made of stainless steel. The bottom face of the ground planes is approximately 30 cm away from the top of the field shaping profiles. The ground planes are mounted at a fixed distance from the field shaping profiles using standoffs, as shown in Figure 23.

To avoid interfering with the natural convection of the liquid argon flow, the ground planes are designed with perforation holes (6mm diameter), which are used to connect them to the main structure using 5/16" FRP bolts. Please note that perforations are not shown in the 3D model.

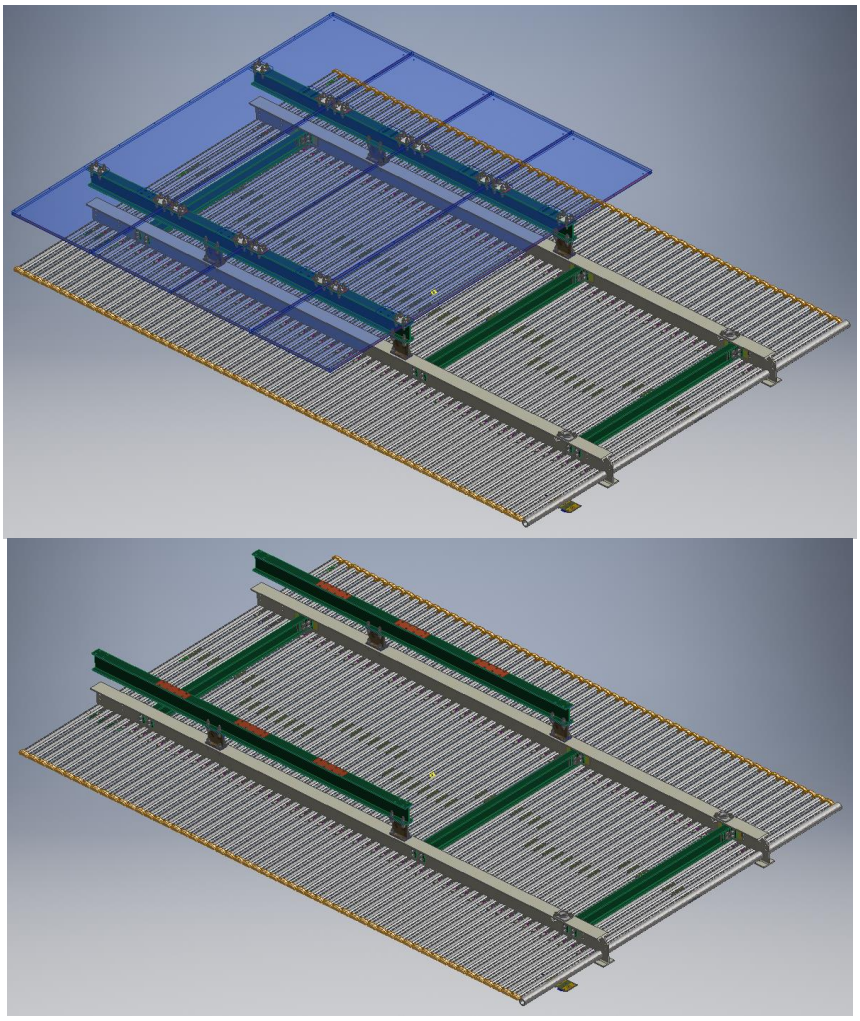

Figure 23 Field Cage with and without Ground Planes

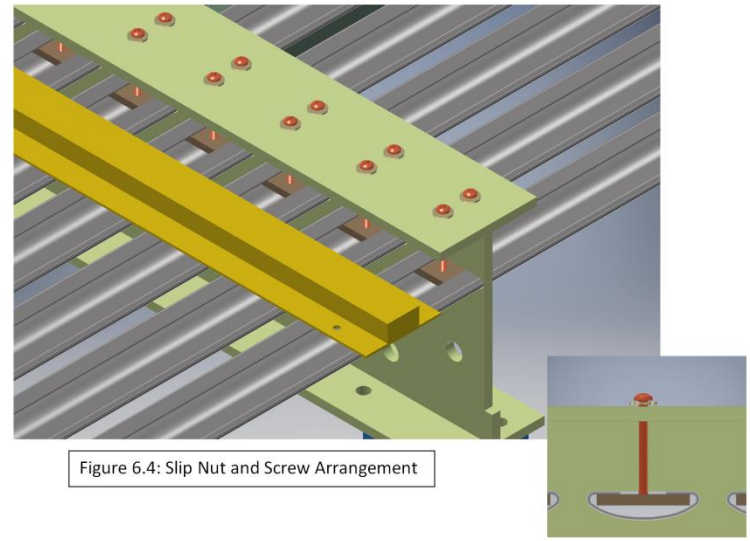

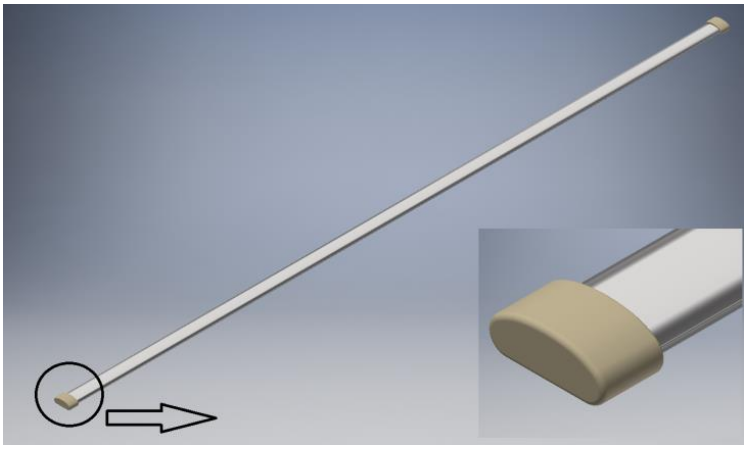

Figure 24 Field Shaping Profiles, endcaps and profile locking

The field shaping profiles as shown in Figure 24 are constrained using custom slip nut and screw arrangement. These profiles are only constrained on the first main I-beam and are allowed to move freely in the slots of the second main I-beam.

In order to confine the electric field in the liquid argon region, it is foreseen to install a metallic plane, set to ground potential, between the upper field cage module and the liquid-gas interface. The design of such Ground Plane (GP) is inspired by the one from the ICARUS T600 detector, and it is meant to limit the residual electric field in the gas phase above the TPC to prevent HV discharges. The design details of the planes are verified to comply with the requests on residual electric field with FEA. Identical GPs are implemented on the bottom field cage modules to shield the field in the region where cryostat pipes are running. The distance between the cryostat walls and the end-wall field cage are deemed sufficiently large that GP shielding is not necessary.

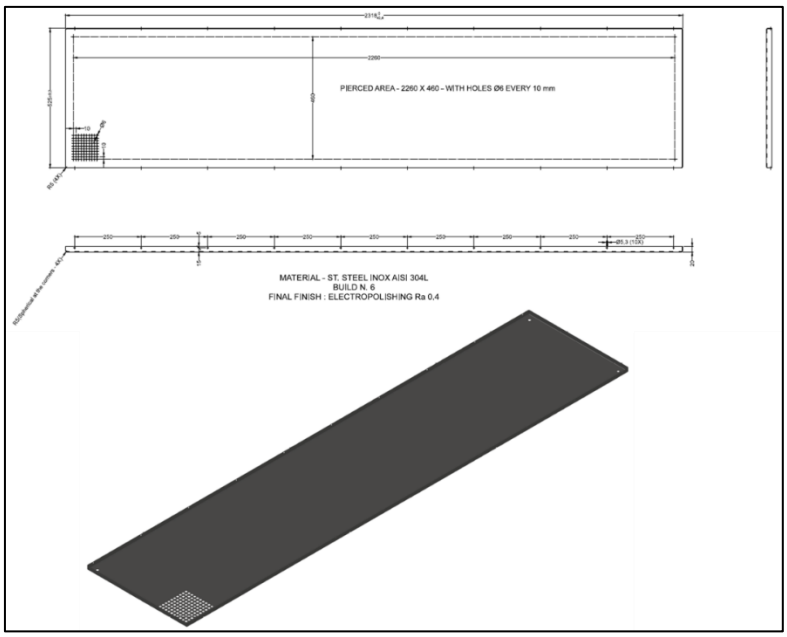

Figure 25 Top: Technical Drawing of the Ground Plane panels for ProtoDUNE. At present it is expected to adopt the same design for DUNE. Bottom: 3D model of one panel.

One module will be made of 4 GP pieces, put next to each other along the 2318 mm direction: this dimension is made to match the APA and FC module widths. The planes are connected to the FC beam with further FR4 pieces that are used also to connect two neighboring GP panels. The electrical continuity between consecutive panels can be performed with metallic screws (with holes on the planes edges) or with looser connections, like copper strips, that better adapt to the shrinking of the structure during cool-down. Copper strips were successfully employed on the ProtoDUNE-SP modules. As for most detector systems, the GP should be referenced to the detector ground, set at cryostat top. The grounding anyway should ensure that possible discharges do not affect at all the cold electronics boards.

The GP modules will be installed on the corresponding FC modules in the clean room outside the cryostat, to facilitate the connections.

Three small GP filler pieces are needed to fill the gap directly above the CPA around the two CPA lifting straps. These filler pieces are connected on the GP modules on one side of the CPA so that, once in position, they should clear the CPA straps and cover the CPA frame.

Ideally, the ground plane should extend beyond the endwall field cage modules such that the GP edges terminated in a low field region. However, since the GPs are rigidly mounted on the top/bottom FCs, and must rotate passing the EWFC during their final deployment, the GP must clear the EWPC. This configuration exposes the outer edges of the ground plane (1mm thick stainless steel) to high electric field. Figure 26 shows the E field profile in this region. A solution we used in NP04 was to weld a 3mm stainless steel rod to the top rim of the GP panel facing the cryostat wall, effectively increasing the edge radius of the stainless steel sheet.

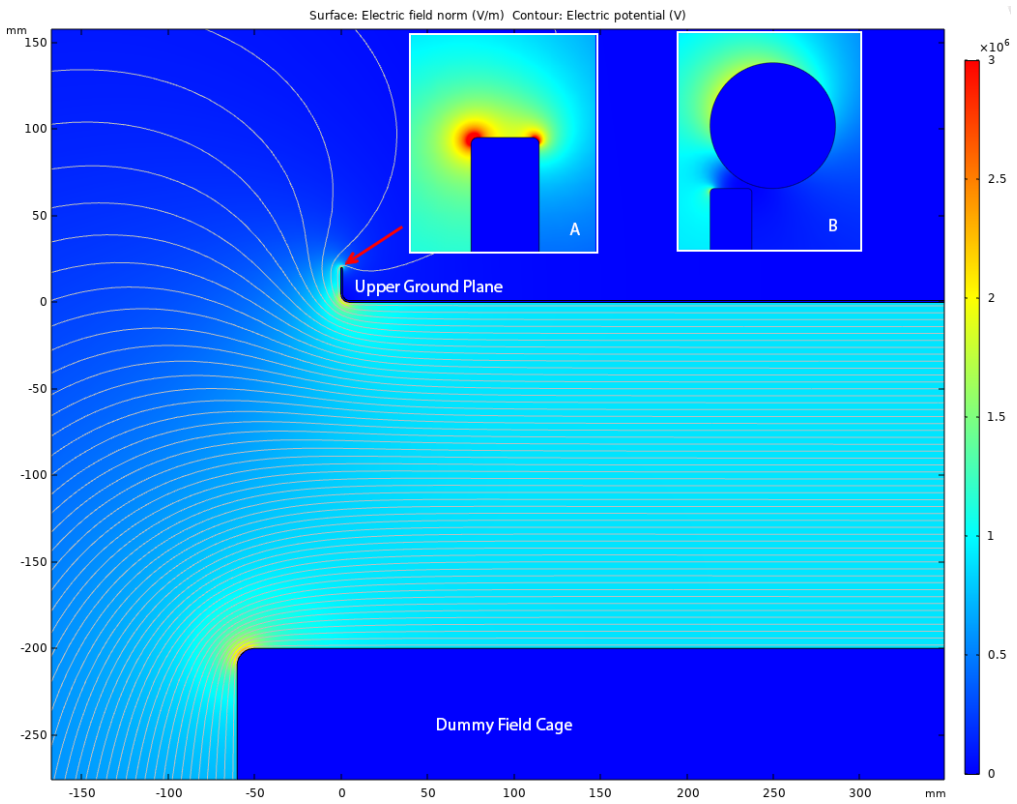

Figure 26 Electrostatic FEA of the region above a corner of the upper field cage including the ground plane. Due to the specific deployment scheme of the combined FC+GP, the GP cannot extend beyond the EWFC. As a result, the edge of the GP has very high E field (>40kV/cm, see inset A). To reduce the field at the edges of the GP panels, in NP04, we added a stainless steel rod, 3mm OD, directly along the top edges of the GP tiles (E<20kV/cm, see inset B).

4.3 FC End Wall Design Description

The End Wall Field Cage (EWFC) assembly consists of eight panels. There are 3 different types of EW panels due to various design features needed.

The feature for the topmost panel is that it holds the weight of the entire end wall assembly. The EWFC structure consists of two main box beams which are 3.5 m long. The box beam design also incorporates cutouts on the outside face to minimize charge build up. Box beams are connected using ½" thick FRP plates on either side. The plates are connected to the box beams using a shear pin and bolt arrangement. The inside plate for the splice joint facing the active volume is connected using special slip nuts and stainless steel bolts. The field shaping profiles are connected to the top box beam using slip nuts, an FRP angle, and two screws each. The profiles are connected to the bottom box beam with a single slip nut that is held in place by friction and compression. The lift plates (both inside and outside), as shown in Figure 28, are used to connect the field cage panel to the panel right above it.

All eight panels are attached to one another using the connecting plates. The top panel has the hanger design incorporated in it as shown in the left panel of Figure 27.

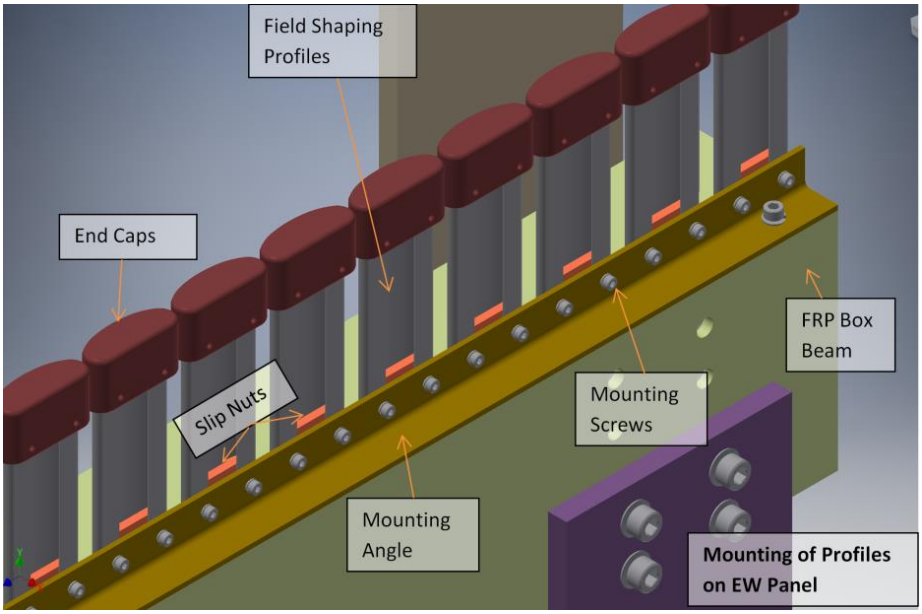

Figure 27--Mounting Profiles

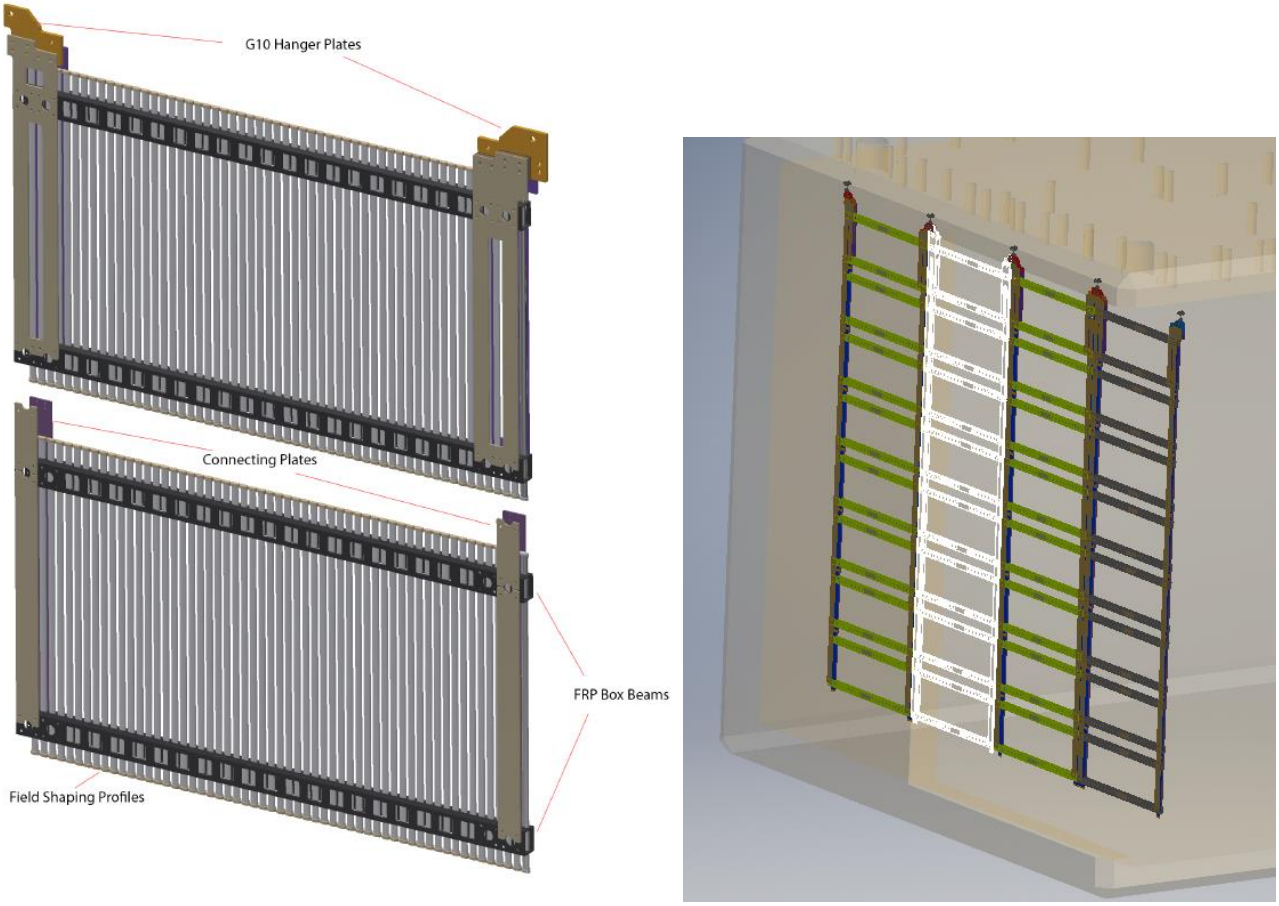

Figure 28 End Wall Panels

4.4 FC Top/Bottom Assembly

The FC is constructed in several steps. First the main I-beams were set parallel to each other and connected together using the cross beams. The field shaping profiles were then inserted through the cutouts in the main I-beams and connected using a slip nut and screw arrangement. See Figure 29.

Next the plastic endcaps are secured onto the ends of field shaping profiles using nylon pins: The ground plane standoffs to the main I-beams are then attached by lining up the pre-drilled holes and slots in the standoffs and main I-beams. Mount the ground planes on the ground plane standoffs, leaving one off of the CPA side. This is to access the lifting plates, see Figure 30.

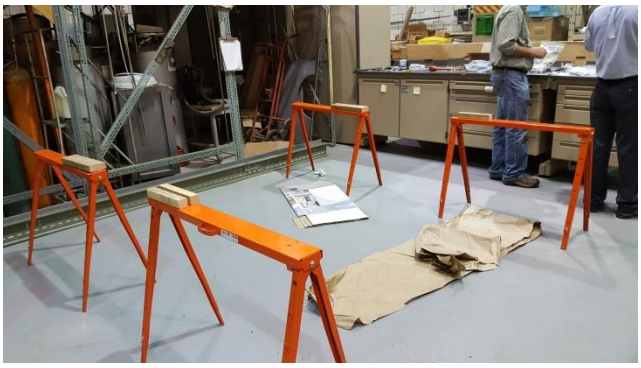

Placing the I beams on saw horses

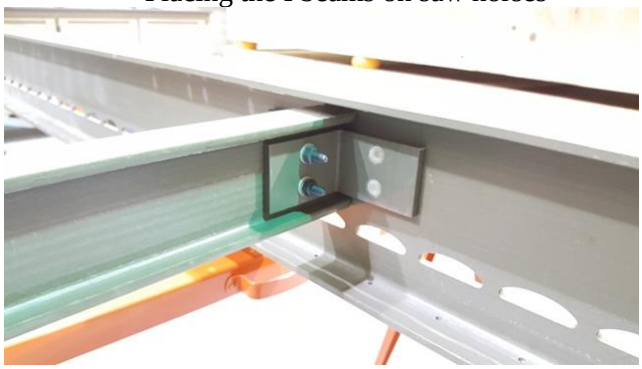

Attaching the cross beams

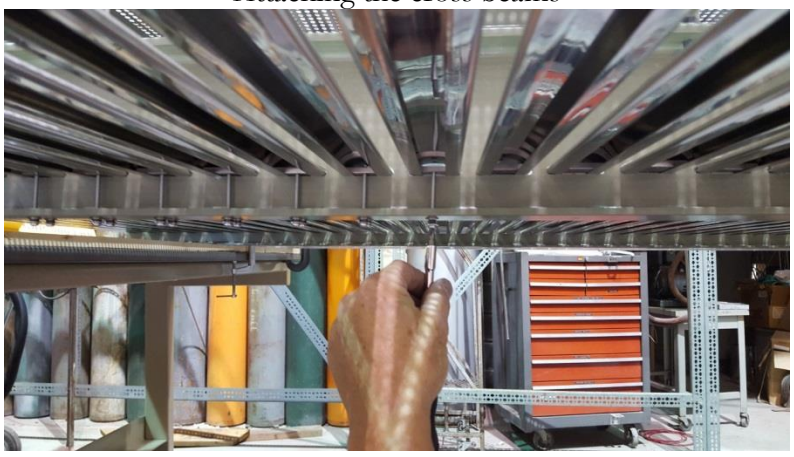

Figure 29 Securing the Profiles

Figure 30 Assembled FC (ProtoDUNE Style)

4.5 FC EndWall Assembly

Assembly is to be done inside the clean room. All the components are cleaned before delivery to the clean room. A custom made turntable is utilized to assemble the EndWall panels and is shown in Figure 31. The turntable allows to rotate the modules around its long axis and thereby provides access to both sides of a panel.

Connect the box beams on the inside face using stainless steel bolts and slip nut arrangement:

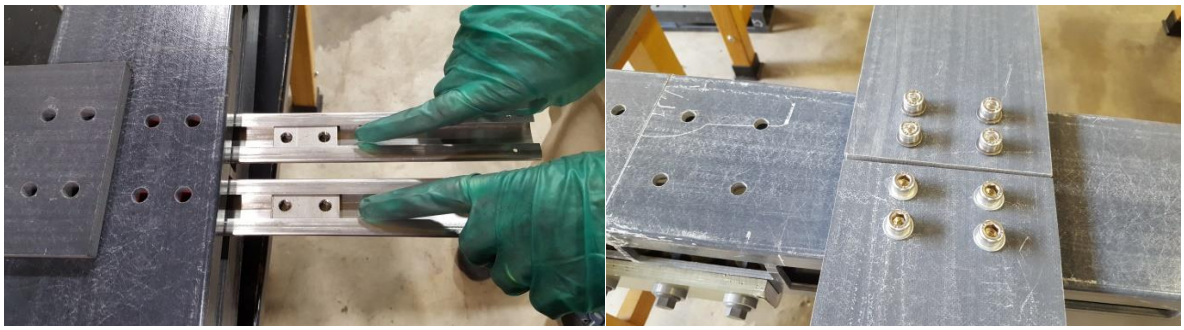

Slide the field-shaping profiles through the cutouts on both main box beams and connect them using a slip nut and screw arrangement on the first box-beam:

Attach the plastic endcaps onto the ends of field shaping profiles using nylon pins:

The turntable allows easy rotation of the FC endwall module.

Figure 31 Turntable for assembly of EndWall modules.

For the hanging test the top module is rotated into vertical position and attached to the crane hook by means of a spreader bar. Successive modules are then connected to the hanging modules, either while still in the turning table or while stored in vertical orientation using a roller base as shown for the bottom module of Figure 32.

Figure 32 Use of crane and spreader bar to connect successive EndWall modules.

4.6 FC Stress and Deflection Analysis

The Top/Bottom Panels consist of 2 FRP I beams connected to each other by 3 cross I beams, FRP Angles and G10 pins. There are 57 aluminum Profiles that pass through the cutouts of the I-beams. Load from the profiles and ground planes was calculated and applied on the model at appropriate locations. Standard earth's gravity was applied on all the models. The table below shows the load cases examined and resulting safety factor.

Load Case	Description	Safety Factor
1	Both ends support in the horizontal position (dry operational condition)	7 at hole stress concentration
2	Hanging vertically as supported during installation	7 at hole stress concentration
3	In wet operational condition	6.6 at hole stress concentration

Load Case #1

Load Case #1 is when the FC is in its operational position dry. The FC is simply supported at both ends and subjected to gravity. Figure 33 and Figure 34 show the deflections and stresses in the frame. The highest stresses occur in the FR4 pin. The results compare well with empirical results, see Appendix 4. The Safety Factor exceeds the required 3.75

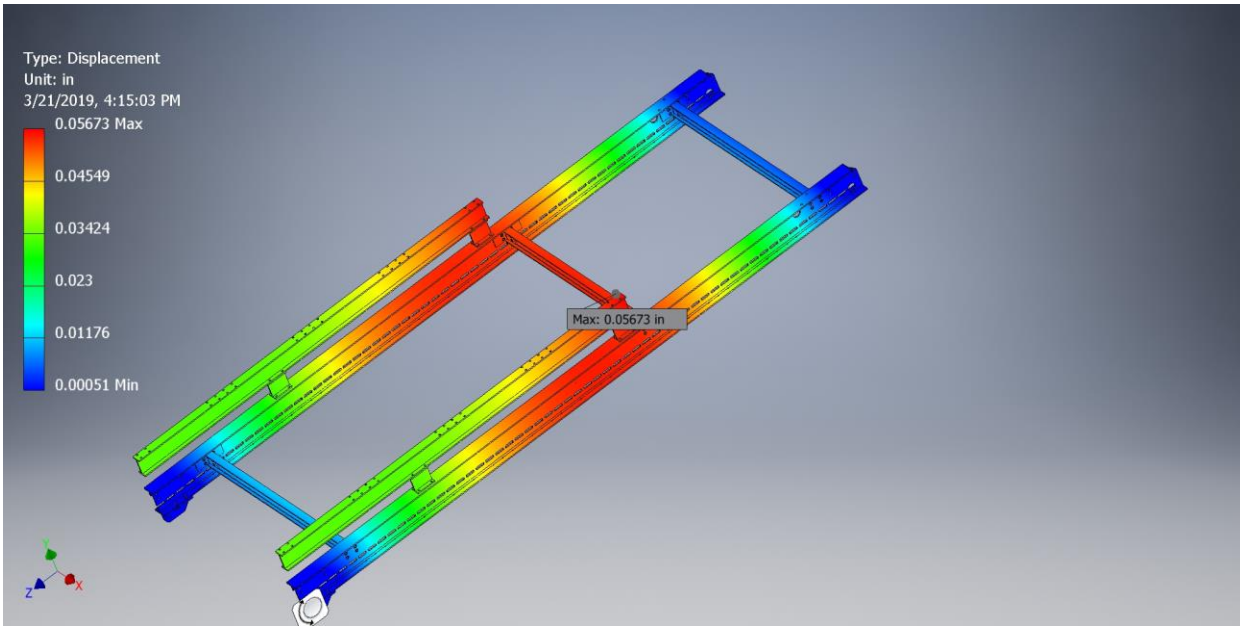

Figure 33 Case 1 Deflections

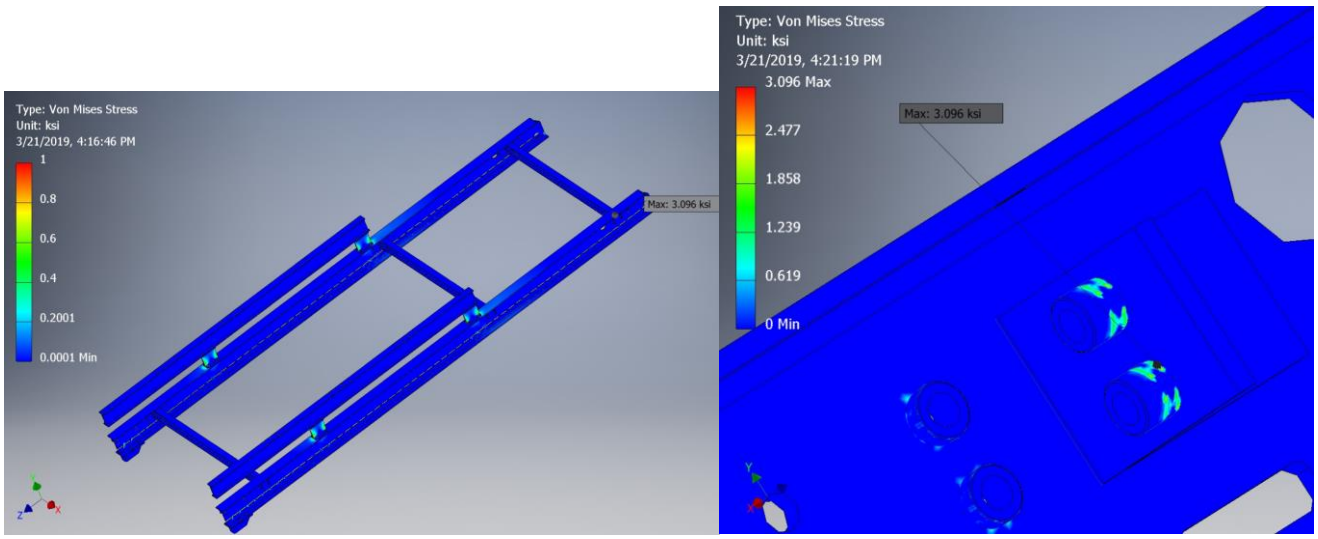

Figure 34 Case 1 Stresses

Load Case #2

During installation the FC is hung vertically from one end. Figure 35 shows the restraints and loads on the FEA model. Figure 36 shows the frame deflected a max of 0.08" (2mm). The stresses are very low and are a maximum of 1079 psi at a stress concentration located at a lifting hole, see Figure 37. Empirical calculations were also done (see Appendix 2) which show a maximum stress due to tension and bending from the off-axis GP load to be ~125psi which is consistent with the FEA results.

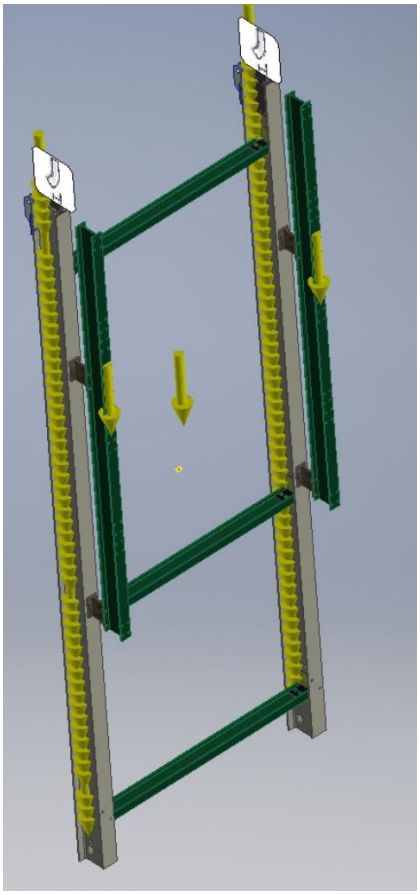

Figure 35 FC Module Hanging Vertically with Loads of GP and Profiles Applied

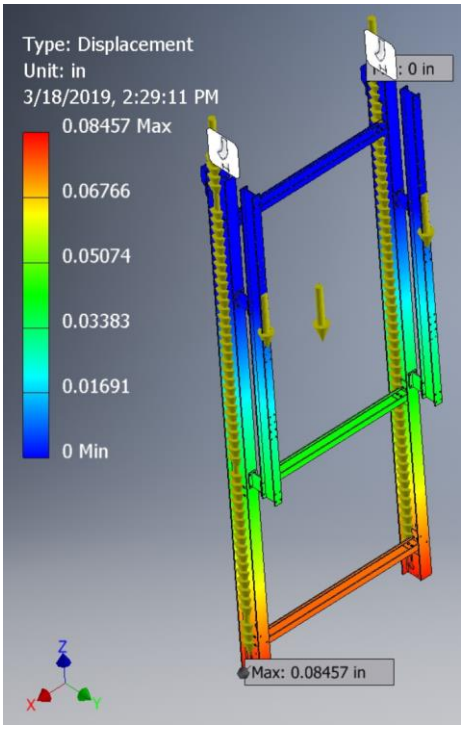

Figure 36 Load Case 2 Deflections

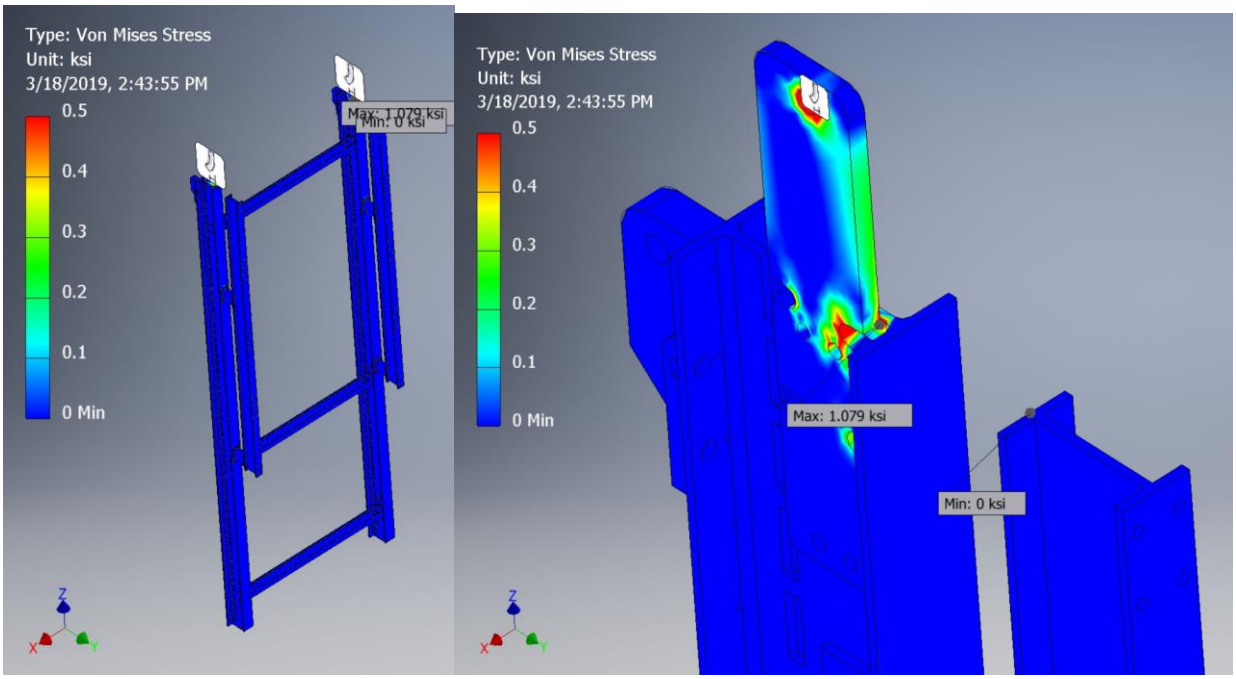

Figure 37 Load Case 2 Stresses

Load Case #3

Load case #3 is the FC in its operational position wet. The FC is simply supported at its ends. The location of the supports change by a few mm due to shrinkage (see Section 9 of Appendix 1) but the FC essentially remains horizontal and simply supported. Load Case #3 is essentially the same as Load Case #1 but with a smaller gravity loads due to the buoyancy force (calculated in Appendix 1, Section 1.6). The maximum stress is in the FR4 pins and is 1389 psi which results in a safety factor of 6.7.

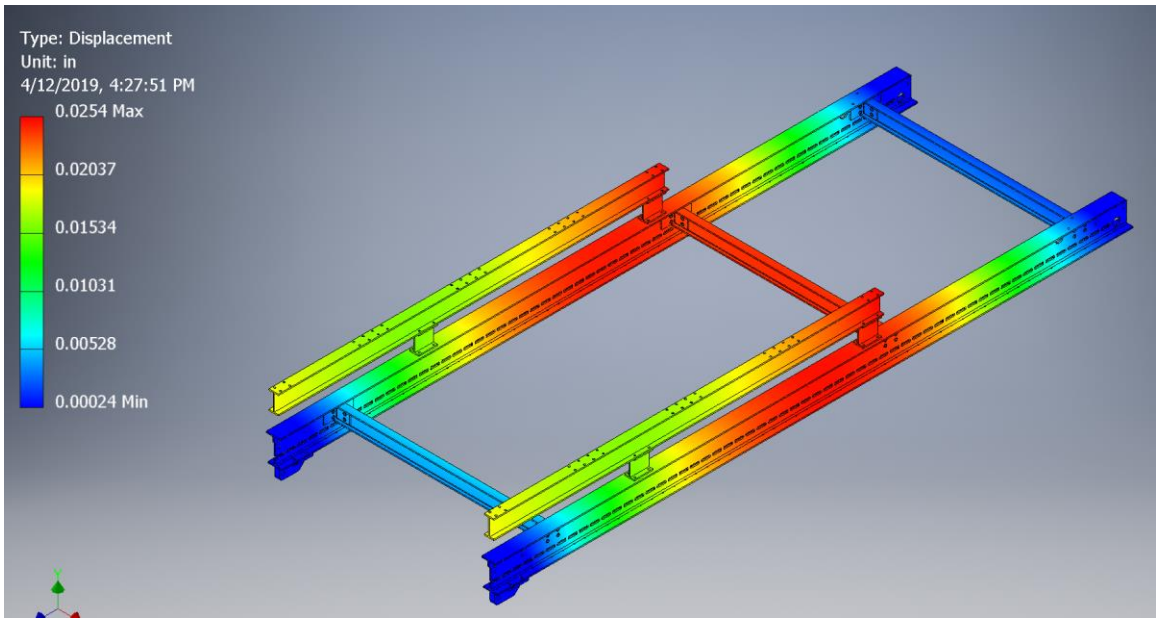

Figure 38 – Load Case 6 Deformation

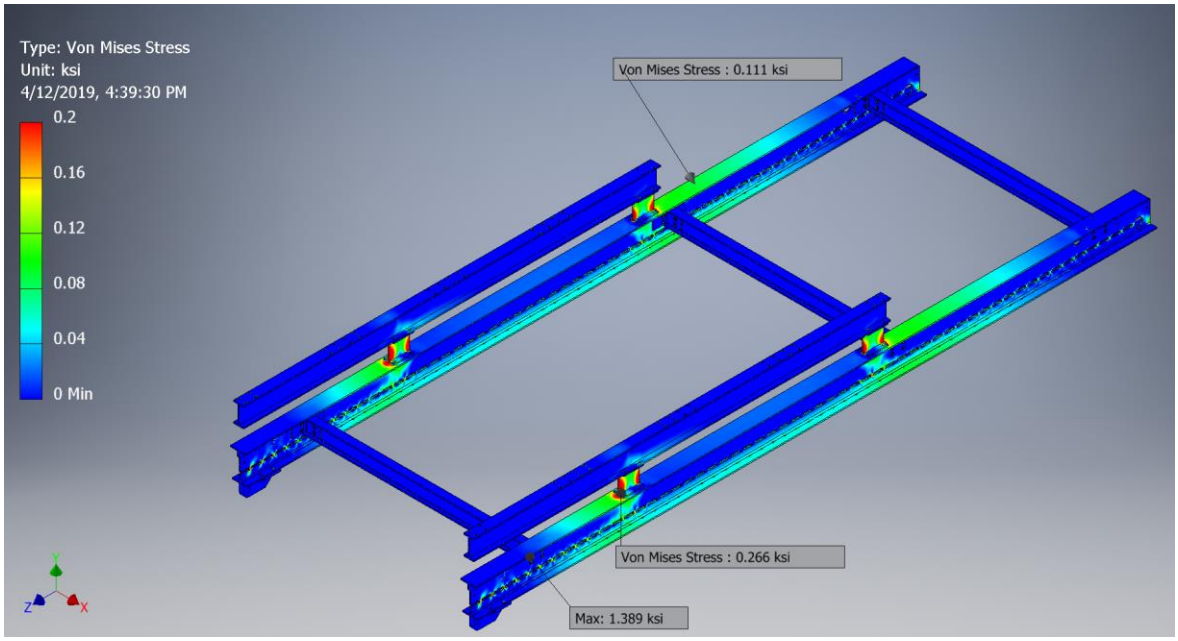

Figure 64 – Stresses Load Case #3

4.7 EndWall Analysis

End Wall Assembly for DUNE consists of 8 panels. One top panel with hanger plates and 7 baseline panels hanging from it. This load case was simulated using ANSYS workbench. The EW Panels consist of 2 FRP Box beams connected to each other by FR4 plates and G10 pins. There are 58 Aluminum Profiles that pass through the cutouts of the Box-beams. Load from the profiles and ground planes was calculated and applied on the model at appropriate locations. Standard earth's gravity was applied on all the models.

Load Case	Description	Minimum Safety Factor
1	12m EW during installation	4.9 at FRP Pin holes
2	12m EW Hanging Dry	4.8 at FRP Box beam fillet
3	12m EW Hanging Wet	13.2 at FRP Box Beam hole

A FEA model was created using 4,560,582 quadratic solid elements. A very fine mesh was generated at the pins as shown in the figure below. The profiles are not structural members and were not modeled; the weight of the profiles were applied at the appropriate locations. Since the greatest loads/stresses occur at the top of the EW only the top two modules were modeled and the weight of the lower six were applied.

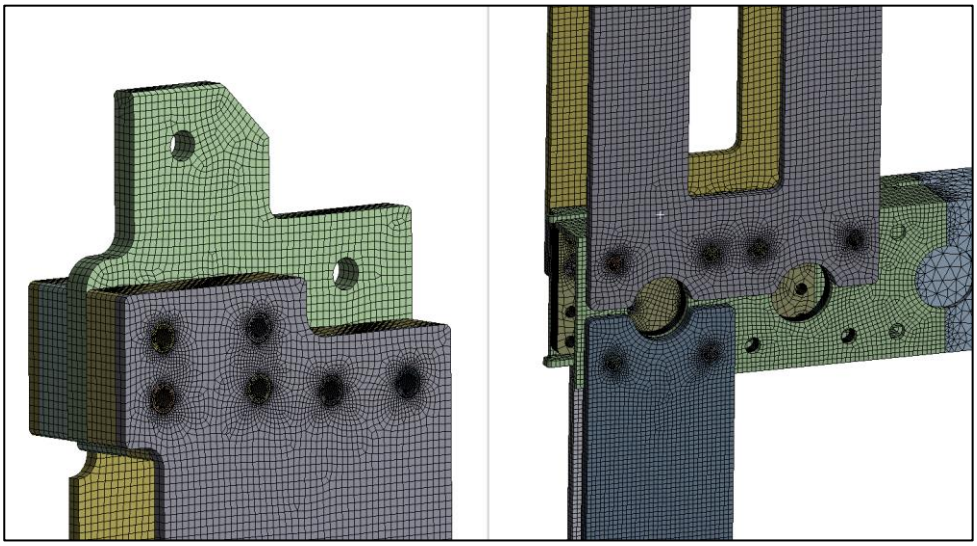

The boundary conditions are shown below:

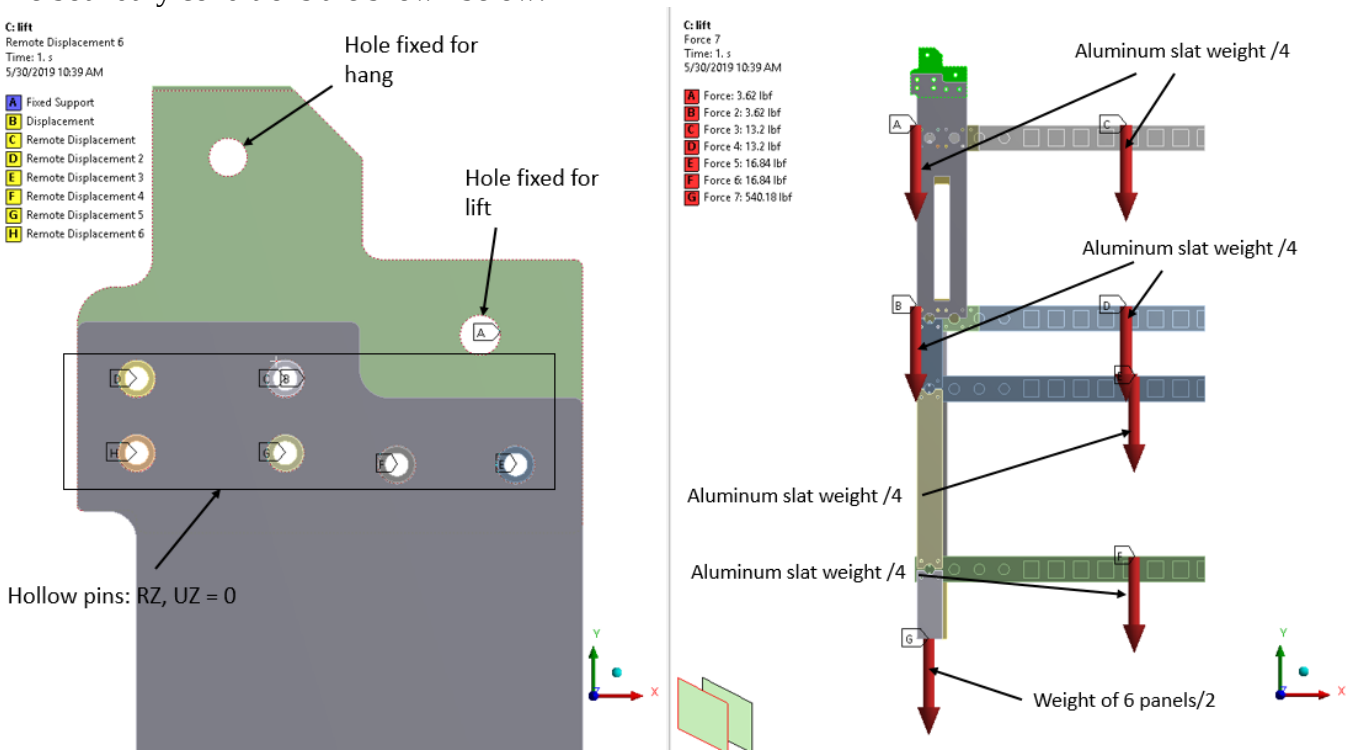

Load Case 1

The maximum deflections are shown below and were in the range of 5mm.

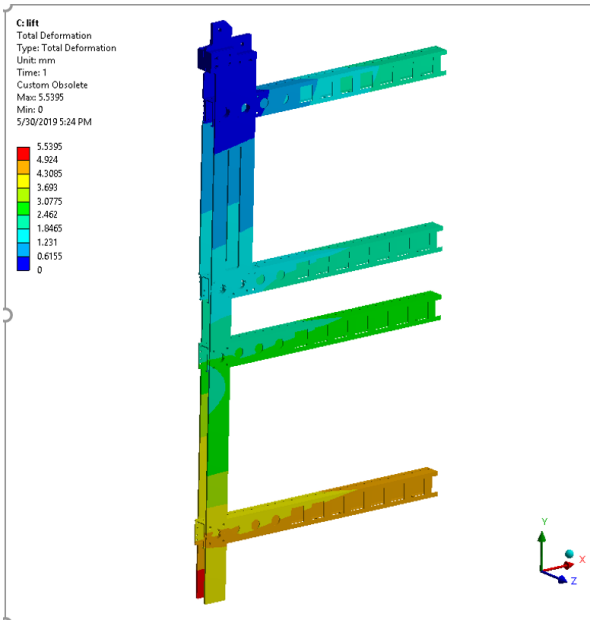

The highest pin stresses occurred at the top connection. The pins stresses are highly dependent on the assumptions and modeling. The pins were modeled with a 0.002" clearance and allowed to move and bend. The stresses therefore we dominated by the bending stresses. The 1st principal stress on the pins was 24.3MPa but this mainly due to bending because the stress in the Z direction, along the pin axis, is 22.5MPa. Using the FR4 allowable stress in the weak direction of 165.4MPa results in a pin safety factor of 7.35

FR4 (G10) Top Hollow Pins
Pins

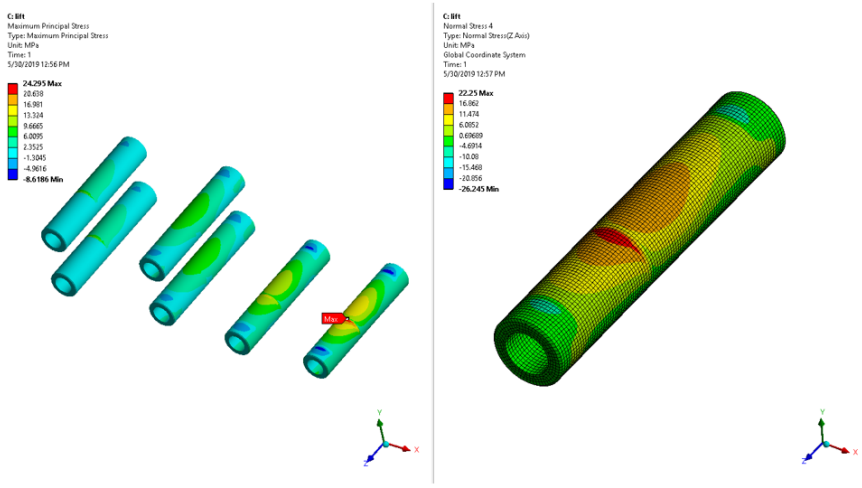

- **Maximum 1st principle stress in entire assy is 24.3 MPa on hollow pin.**
- **At that location σ_z = 22.25 MPa, i.e, predominant stress is in z direction due to bending.**
- **If this is strong direction, S_u = 200 MPa, if weak, S_u = 165.4**
- **Safety Factor = 165.4/22.5 = 7.35**

The center lifting plate was then examined. The max stresses occurred at the pin hole in the Y direction and were 18.1MPa. Using the weak direction ultimate stress we get a safety factor of 9.1

G10 Lifter Plate

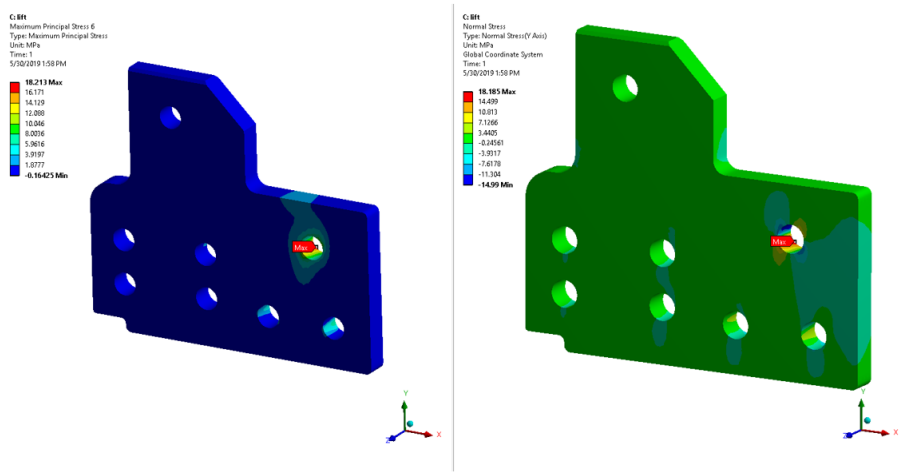

- **Highest1st principle stress in G-10 lifter plate is 18.21 MPa at pin hole.**
- **At that location σ_y = 18.15 MPa, i.e, predominant stress is in y direction(in plane).**
- **If this is strong direction, S_u = 200 MPa, if weak, S_u = 165.4**
- **Safety Factor = 165.4/18.21 = 9.1**

The FRP box beam had the highest stresses at the pin holes also and were 9.7MPa which results in a safety factor of 4.9

FRP Box Beams

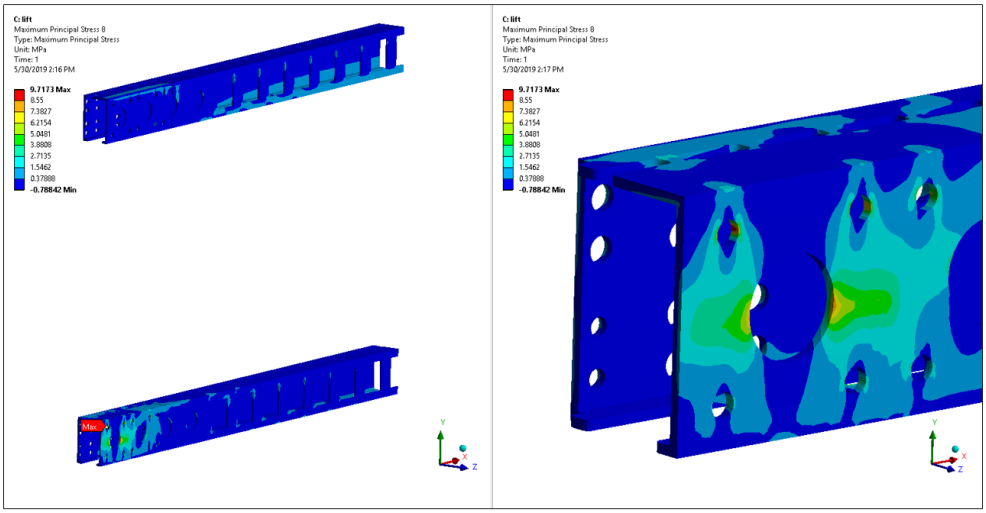

- **Highest 1st principle stress in box beam is 9.72 MPa at a pin hole.**
- **If this is strong direction, S_u = 206.8 MPa, if weak, S_u = 48.2**
- **Safety Factor = 48.2/9.72 = 4.97**

Finally the FRP connector plates had a max stress of 8.5MPa which results in a safety factor of 5.6

FRP Connectors

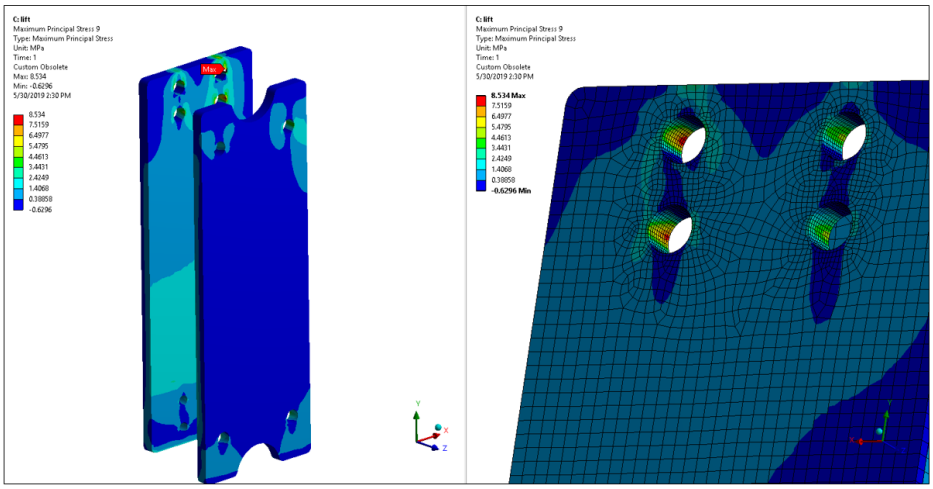

- **Highest 1st principle stress in the connectors is 8.53 MPa at a pin hole.**
- **If this is strong direction, S_u = 206.8 MPa, if weak, S_u = 48.2**
- **Safety Factor = 48.2/8.53 = 5.65**

Load Case 2

Load case 2 is the full EW hanging in the operating position.

The highest pin stresses occurred at the top connection. The pins stresses are highly dependent on the assumptions and modeling. The pins were modeled with a 0.002" clearance and allowed to move and bend. The stresses therefore we dominated by the bending stresses. The 1st principal stress on the pins was 11.2MPa but this mainly due to bending because the stress in the Z direction, along the pin axis, is 10.0MPa. Using the FR4 allowable stress in the weak direction of 165.4MPa results in a pin safety factor of 14.7

FR4 (G10) Top Hollow Pins

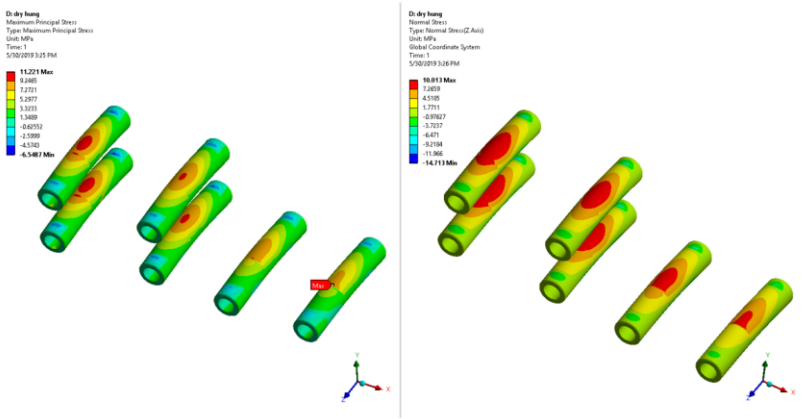

- **Maximum 1st principle stress in top hollow pins is 11.21 MPa on hollow pin.**
- **At that location σ_z = 10.01 MPa, i.e, predominant stress is in z direction due to bending.**
- **If this is strong direction, S_u = 200 MPa, if weak, S_u = 165.4.**
- **Safety Factor = 165.4/11.21 = 14.75.**

The center lifting plate was then examined. The max stresses occurred at the pin hole in the Y direction and were 10.7MPa. Using the weak direction ultimate stress we get a safety factor of 15.4

G10 Lifter Plate

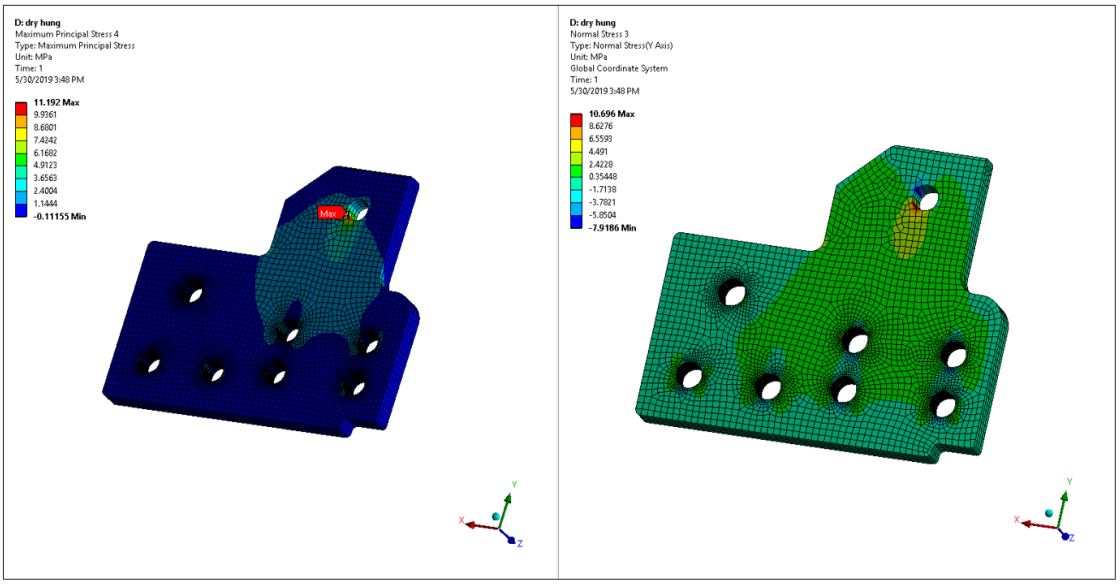

- **Highest 1st principle stress in G-10 lifter plate is 11.19 MPa at pin hole.**
- **At that location σ_y = 10.7 MPa, i.e, predominant stress is in y direction (in plane).**
- **If this is strong direction, S_u = 200 MPa, if weak, S_u = 165.4**
- **Safety Factor = 165.4/10.7 = 15.46**

The FRP box beam had the highest stresses at a fillet and were 9.9MPa which results in a safety factor of 4.8

FRP Box Beams

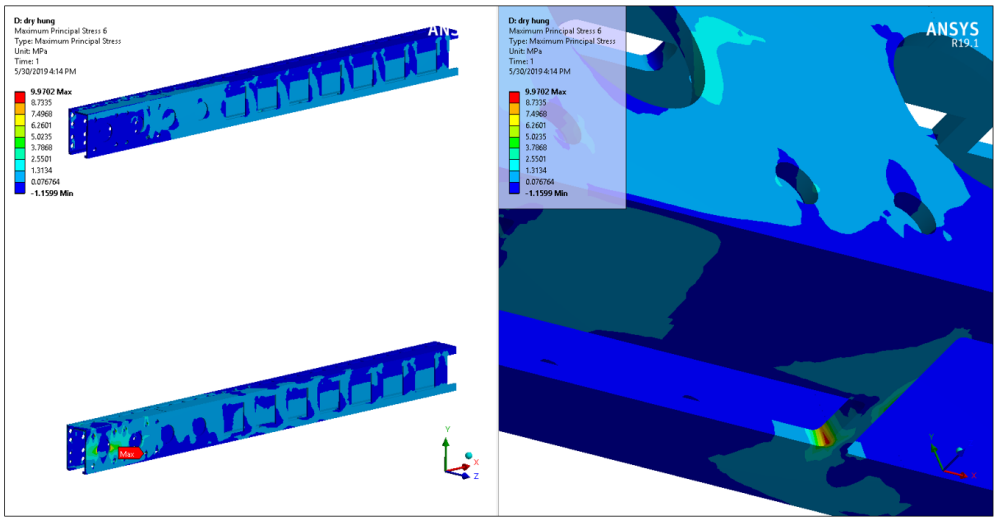

- **Highest 1st principle stress in box beam is 9.97 MPa at a fillwe.**
- **If this is strong direction, S_u = 206.8 MPa, if weak, S_u = 48.2.**
- **Safety Factor = 48.2/9.97 = 4.83.**

Finally the FRP connector plates had a max stress of 8.3MPa which results in a safety factor of 5.8

FRP Connectors

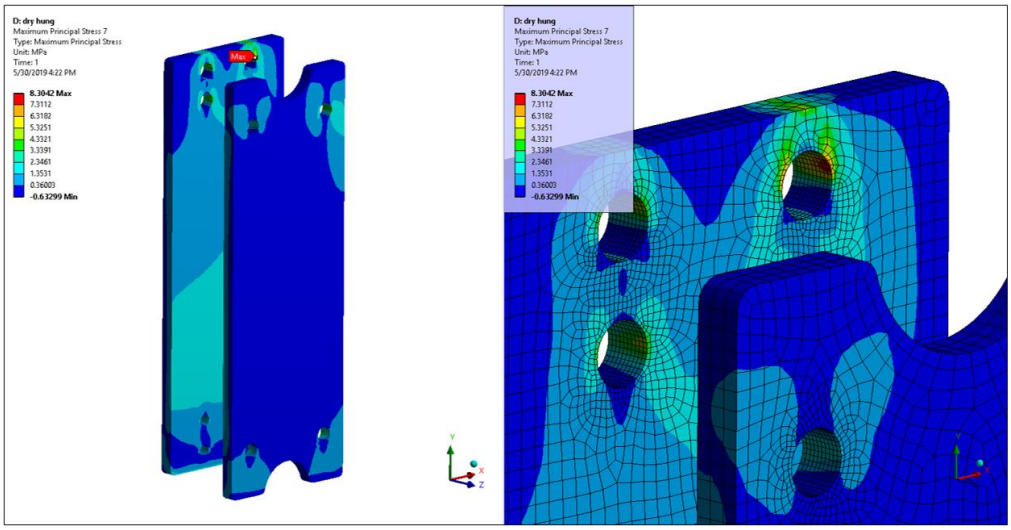

- **Highest 1st principle stress in the connectors is 8.30 MPa at a pin hole.**
- **If this is strong direction, S_u = 206.8 MPa, if weak, S_u = 48.2**
- **Safety Factor = 48.2/8.30 = 5.81.**

Load Case 3

Load case 3 is the full EW hanging in the operating position in liquid argon. The weights of all the components were adjusted appropriately to account for the effect of buoyance.

The highest pin stresses occurred at the top connection. The pins stresses are highly dependent on the assumptions and modeling. The pins were modeled with a 0.002" clearance and allowed to move and bend. The stresses therefore we dominated by the bending stresses. The 1st principal stress on the pins was 4.7MPa but this mainly due to bending because the stress in the Z direction, along the pin axis, is 3.6MPa. Using the FR4 allowable stress in the weak direction of 165.4MPa results in a pin safety factor of 34.8

FR4 (G10) Top Hollow Pins

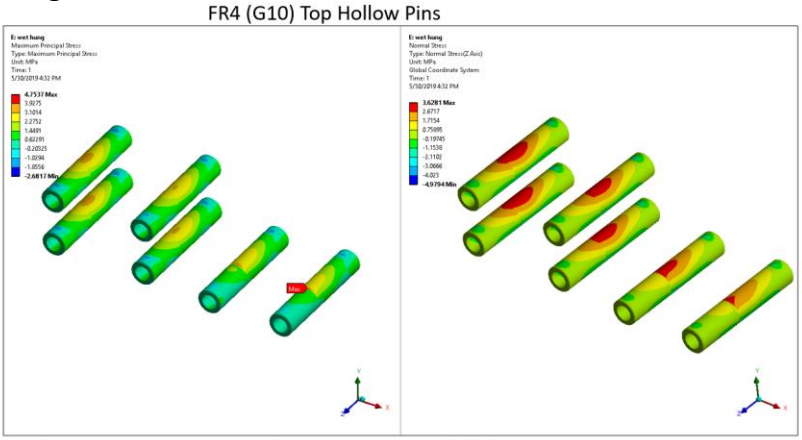

- **Maximum 1st principle stress in top hollow pins is 4.75 MPa on hollow pin.**
- **At that location σ_z = 3.631 MPa, i.e, predominant stress is in z direction due to bending.**
- **If this is strong direction, S_u = 200 MPa, if weak, S_u = 165.4.**
- **Safety Factor = 165.4/4.75 = 34.8.**

The center lifting plate was then examined. The max stresses occurred at the pin hole in the Y direction and were 3.6MPa. Using the weak direction ultimate stress we get a safety factor of 45.1

G10 Lifter Plate

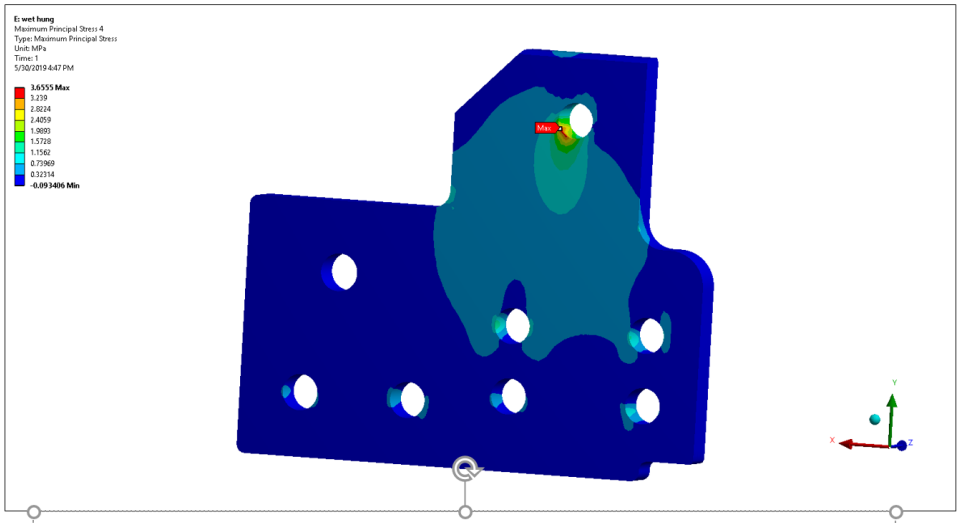

- **Highest 1st principle stress in G-10 lifter plate is 3.66 MPa at pin hole.**
- **If this is thickness direction, S_u = 165.4.**
- **Safety Factor = 165.4/3.66 = 45.1.**

The FRP box beam had the highest stresses at a fillet and were 3.6MPa which results in a safety factor of 13.3

FRP Box Beams

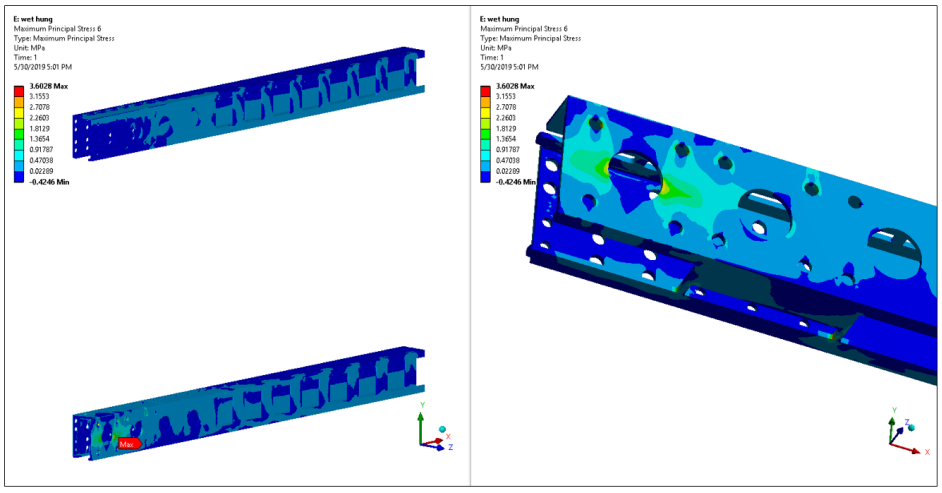

- **Highest 1st principle stress in box beam is 3.6 MPa at a fillet.**
- **If this is strong direction, S_u = 206.8 MPa, if weak, S_u = 48.2.**
- **Safety Factor = 48.2/3.62 = 13.3.**

Finally the FRP connector plates had a max stress of 2.6MPa which results in a safety factor of 18.2

FRP Connectors

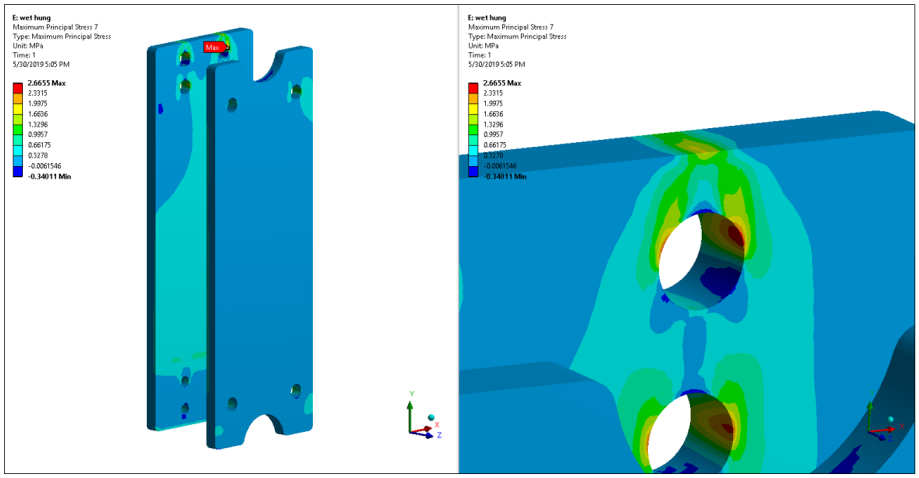

- **Highest 1st principle stress in the connectors is 2.65 MPa at a pin hole.**
- **If this is strong direction, S_u = 206.8 MPa, if weak, S_u = 48.2**
- **Safety Factor = 48.2/2.65 = 18.19**

4.8 Thermal Considerations

- Box beam/I-beam and Field shaping profiles:
  - For both Top/Bottom FC panels, field shaping profiles are only locked at one of the beams to allow for differential shrinkage. For Endwall FCs, one side has holes in profile and locks slip nut into place; other end slip nut is only help by friction/compression.

- To hold the Field shaping profiles onto the top/bottom beams, a stack of belleville washers sandwiched between two flat washers is used.
  - Since the epoxy is supposed to shrink a lot more than SS, 6 belleville washers provide a compressed spring with 1.5mm flexibility.
  - Vendor is not giving out details of the material or properties of epoxy as it is proprietary information.
  - Plan to cold test sections of FRP pieces to find the contraction at cryogenic temperatures.

- To hold field shaping profiles onto the box beams using the FRP angle, a spring washer and flat washer is used.

- Ground planes for Top/Bottom:
  - CTEs of FRP and SS are very close to each other.
  - Over the length of 3.5m the differential thermal contraction between stainless steel and FRP beams could be up to 3mm.
  - Over the width of ground plane (about 2.3m). The differential contraction will be about 2mm.

- Earlier design of ground plane had oversized holes 10mm in diameter. Ground planes holes have been changed to 6mm diameter. Need to open the ground plane holes to have oversized holes at certain places.

- A stack of two M10 belleville washers is used to connect the inner FRP vertical support pieces.

5 Installation of CPA and FC in the Cryostat

The CPA/Field Cage/End Wall installation is part of a more complex sequence for construction of the complete TPC also involving the APAs and the closing of the temporary construction opening (TCO). All the components of the TPC must be in the cryostat before the TCO is closed up. All lifting and access equipment that is remaining after the TCO is closed must be removed from the manholes. Details of the HV installation can be found in the DUNE-SP far detector TDR.

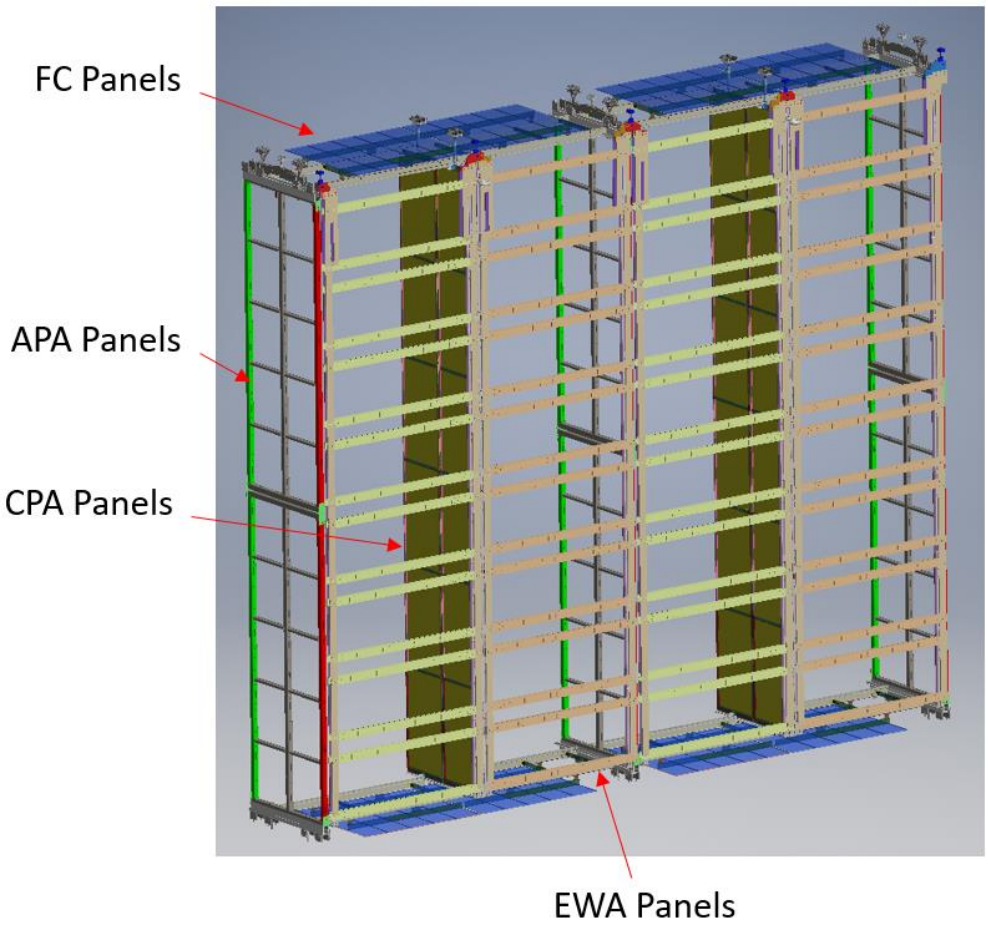

Figure 39--3-D view of the TPC

The CPA and top FC modules are assembled in parallel to the APA assembly. The sub-panels for the cathode plane are delivered to the airlock in crates that hold 4m long 1.15 m wide segments. After cleaning, the crates are brought into the cleanroom and opened. The panels inside are bagged to provide additional

dust protection. The sub-panels are lifted out of the crate and placed on the assembly frame using the cleanroom switchyard hoist. First one of the 1.15 m 4 m tall sections is assembled, followed by the second and third ones. The 1.15 m wide section is then lifted, connected to the installation switchyard, and moved to the TCO beam. The second 12 m tall section is then assembled like the first. The two 1.15m wide panels are then connected to make the 2.3 m wide unit, see Figure 40. A complete set of QC measurements are taken of all electrical connections between panels. The cathode assembly is then moved to a location in the switchyard where the diffuser fibers and top field cage modules can be installed. The top FC modules are then attached. In Figure 41, the completed assembly is shown with the lower FC modules also attached. This is an option, but present planning is to install the lower FC modules separately inside the cryostat.

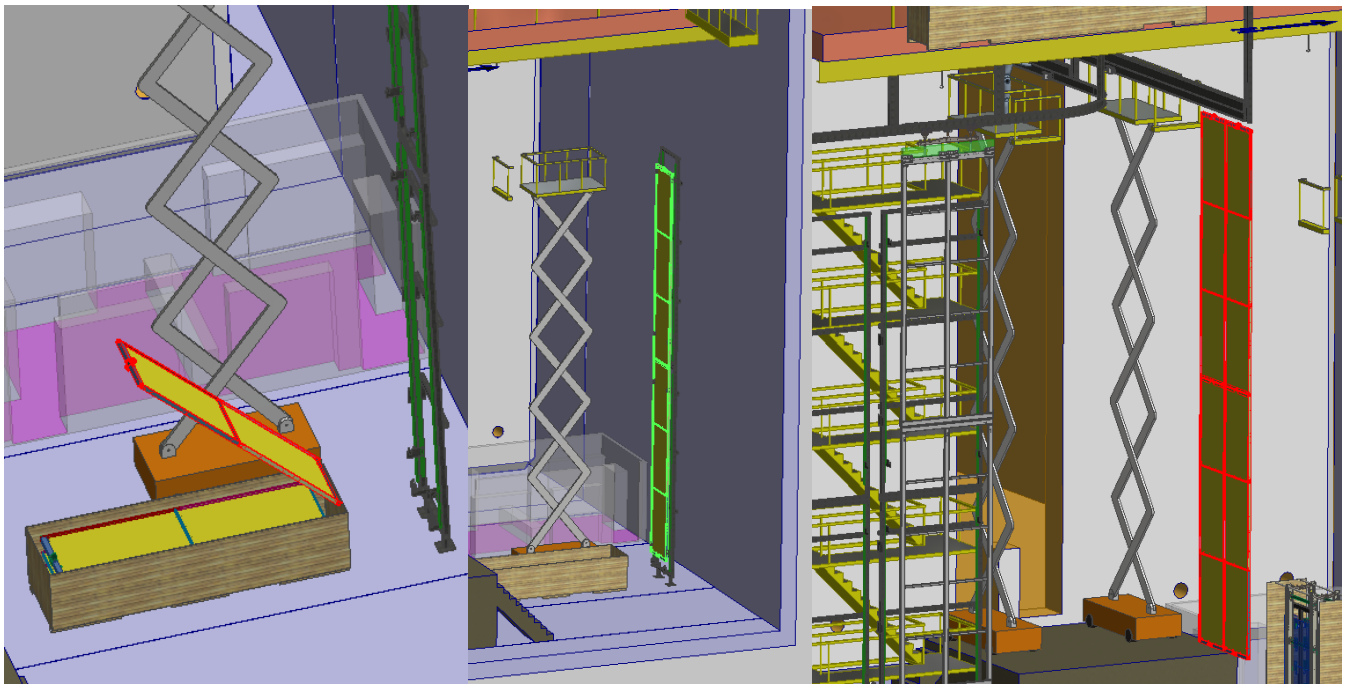

Figure 40-Assembly of CPAs

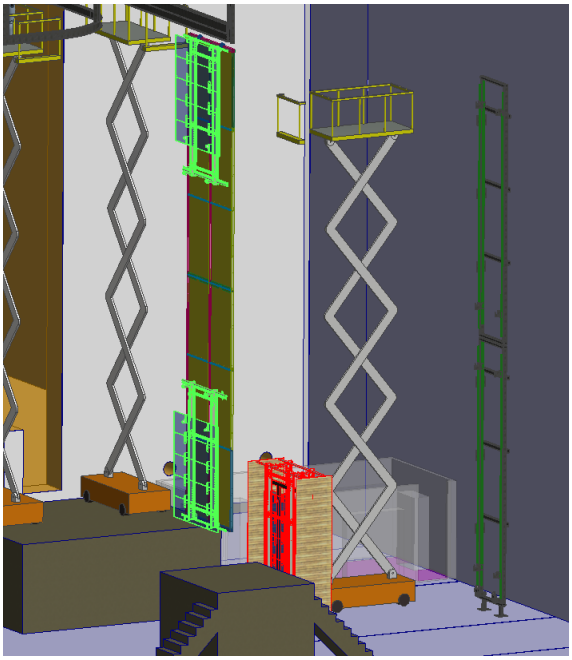

Figure 41-FC Attached to CPA Pair

The CPA/FC assemblies are brought into the cryostat using the overhead rails through the TCO. Inside the cryostat, they are moved into position using the DSS switchyard and DSS I-beams. Once in position, the load is transferred to the DSS beam, and the trolleys are removed. The CPA will wait in position until its APA pairs are fully tested, and then the FC modules could be deployed. The deployment sequence of the FC has not yet been fixed. If the FC are immediately deployed then the APA and FC can be tested in the final position. If one waits to deploy the field cages then the CE can undergo a longer burn in test and the opportunity to clean the cryostat near the end of the installation is available. The decision on the best time to deploy the FC will be made by the time of the installation final review. Figure 42 shows the equipment for deploying the FCs. The top FCs are raised by connecting a cable to the module and then using a pulley-winch assembly to lift the module, which latches to the APA mounts, see Figure 42.

A scissor lift is used to connect the cable to the module and also to control the winch. After the module is in place, the deployment tool is moved to the next APA and CPA sets. The lower FC is deployed using a custom frame that can be wheeled into position, see Figure 43. The cable from a small host is then attached to the FC module, and the module can be lowered. The hoist is on a linear slide, so the cable is always directly over the connection point. This keeps the CPA from swinging because of an induced moment. When the module is down, it latches to the APA frame much like the upper FC. The electrical connections to the HV bus are tested, and deployment is complete. In principal, the cathode/FC assemblies can be constructed faster than the APAs. In theory the cathode/FC assembly process could start later than the start of the APA assembly if the deployment is postponed. The risks and benefits of different deployment sequences will be evaluated near the start of installation.

Eight sub-panels are needed to build one complete 12 m tall EW panel. First a custom hoist is installed on the end of the DSS beam for lifting and assembling the sub-panels in place as shown in Figure 44. The endwall transport crates are then brought to the material airlock using a forklift where they are cleaned. Once clean, the crates are moved into the cleanroom and placed next to the TCO. Then a hoist running on the rails through the TCO lifts the endwall sub-panels onto the transport cart, which is then hoisted into the cryostat. The top endwall sub-panel is then attached to the installation hoist and lifted out of the cart. When the sub-panel is free of the cart, it is re-positioned so the second sub-panel can be attached to the first, and the pair is then lifted. This process is repeated until the full 12 m endwall FC panel is assembled and can be attached to the DSS. All the HV connections inside the panel can now be tested. The process is then repeated for the remaining three endwall panels comprising the east endwall assembly.

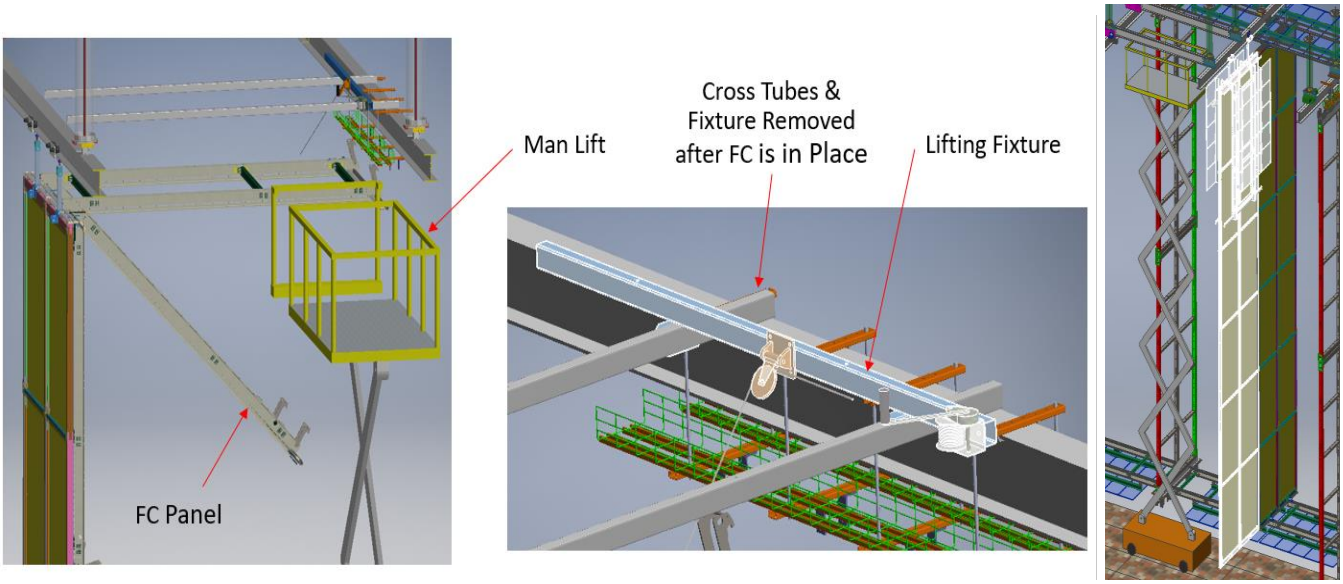

Figure 42-Deploying Top FC

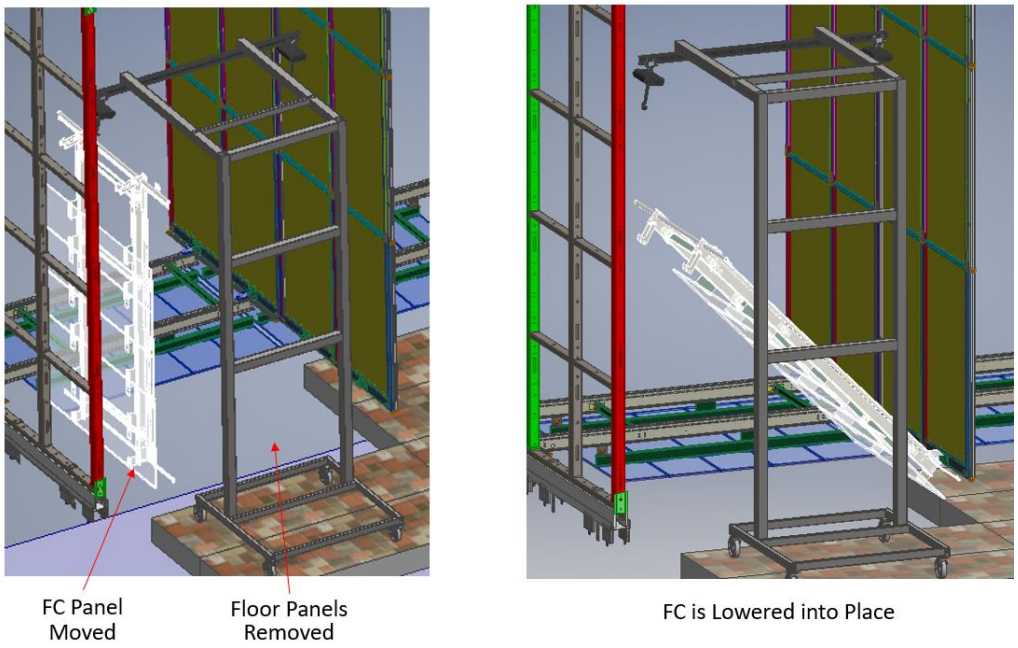

Figure 43-Bottom FC Deployed

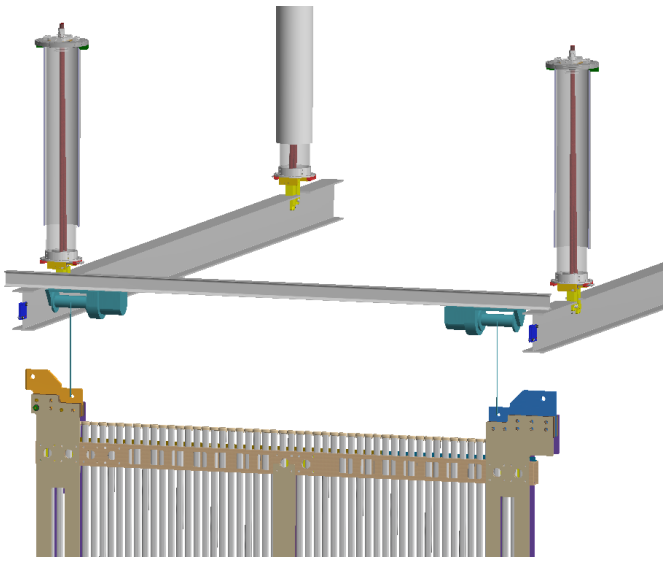

Figure 44-EW Deployed

5.1 Quality Assurance Plan and Quality Control Procedures for the CPA, FC and EW

A complete QA plan has been devised using QR or barcodes on removable plastic tags which will account for all HVS components linked to a particular position in the 10kt DUNE Far Detector. By using removable tags with barcodes, no additional material is introduced into the detector cryostat. QC checklists will be included in the scanned QR or barcode tags and will be stored electronically.

The plan starts with barcode or QR tags scanned and attached to the basic shipping units at the various HVS factories. The file associated with a QR or barcode contains QC checklist information obtained during assembly at the factories. A (paper) shipping tag will be attached to each shipping crate containing information about which units are included in the crate.

In the detector cryostat at SURF, a tag is attached to each position for an EndWall or CPA/FC unit on the DSS. It is planned to use cheap plastic "cattle tags" for all tagged items. These are large and will be bright yellow in color and temporarily attached to items with plastic loops (or cable ties). This will ensure that all tags are removed by visual inspection before the TPC is closed.

QC procedures done during the assembly of the TPC for each of the components involve visual inspections and in some cases measurements of dimensions and/or detector properties. The following example illustrates the QC implementation of the HVS QA plan starting with assembly of CPAs.

1. tag on each 2-module Unit (3 tags) (beginning of QC - individual parts for a 2-module Unit are not tagged - RPs, profiles, FSSs, frame pieces treated as identical). In shipping crate, have 6 2-module Units each with a removable barcode tag plus hardware package with a paper barcode.
2. barcode label on shipping crate (paper sticker) contains contents of crate (6 barcodes + barcodes of 2 hardware packages). This barcode is only used for shipping purposes - once the crate is opened at SURF, only the internal barcodes are scanned for continued assembly.
3. 1st CPA Panel from crate – single tag on Panel contains 3 tags of individual Units used to produce

- remove 3 Unit tags in this step.

4. 2nd CPA Panel from crate – single tag on Panel contains 3 tags of individual Units used to produce - remove 3 Unit tags in this step.
5. combine 2 Panels into CPA pair Plane- tag on Plane contains tags of 2 individual Panels - remove 2 Panel tags in this step.
6. Attach Top/Bottom FC units to both sides of CPA Plane – single tag on CPA/FC assembly contains tags of each FC unit (4 tags) and tag of CPA Plane (1 tag) - remove tags on FCs and CPA Plane in this step.
7. Move into cryostat - scan barcode of position tag on DSS and tag on CPA/FC assembly - remove tag on CPA/FC in this step. Remove DSS barcode tag also since now have a complete list of components and their checklists installed at a particular location in the cryostat.

At this point, have a sequence of linked QR or barcodes associated with QC checklists that tell which CPA and FC units are mounted in the DSS position with no material left in the cryostat. Details of the QC procedures and checklists are contained in docdb-10452.

6 Material Properties and Failure Criteria

The main materials for the detector are stainless steel, aluminum and what is called generically Fiber Reinforced Plastics (FRP). There will be two types of FRP material used in the detector. The CPA will be constructed using FR4 material which is a thermosetting industrial fiber glass composite laminate consisting of a continuous filament glass cloth material with an epoxy resin binder. The FR4 material will meet ASTM D709-16. This product, first introduced in the 1950's, has characteristics of high strength, low moisture absorption, excellent electrical properties and chemical resistance. These properties are maintained not only at room temperature but also under humid or moist conditions. NEMA FR4 was the designation given to Glass Epoxy sheet composite by the National Electrical Manufacture Association (NEMA) to specify a consistent product between manufactures.

For the Field Cage we will be using fiber-reinforced plastic (FRP) pultruded structural elements, including I-beams and box beams. Pultruded FRP material has all of the reinforcing fibers running along the main axis of the section being used. The FRP material will meet the International Building Code classification for flame spread and smoke development of a Class A, as characterized by ASTM E84.

Both the FRP structural shapes and FR4 bar material shall be fire resistant but can be halogenated.

FR4 laminate sheet is made up with bifunctional or trifunctional epoxy making up the bulk of heavy sheet and then using finer glass cloth with high temperature resistant tetra-functional epoxy giving a high performance outer finish. FR4 sheets are orthotropic due to the glass fiber fabric (2D weave) contained in the epoxy matrix. The weave is shown schematically in Figure 45. The perpendicular fiber directions are identified as “Fill” and “Warp” with the warp direction generally running the roll direction as shown in the figure. Most fabrics are stronger in the warp than the fill because higher tension is placed on the warp fiber keeping it straighter during the weaving process. FR4 material is generally provided in large sheets where the longer direction (length or L) corresponds to the warp direction and the narrower direction (width or W) corresponds to the fill direction. The material strength and stiffness is dominated by the fibers. As there are no fibers running along the thickness direction (P), the strength in this direction should be expected to be much lower than the L or W directions particularly in tension. Also shown in is the coordinate system used to define the orthotropic material properties used in the analysis.

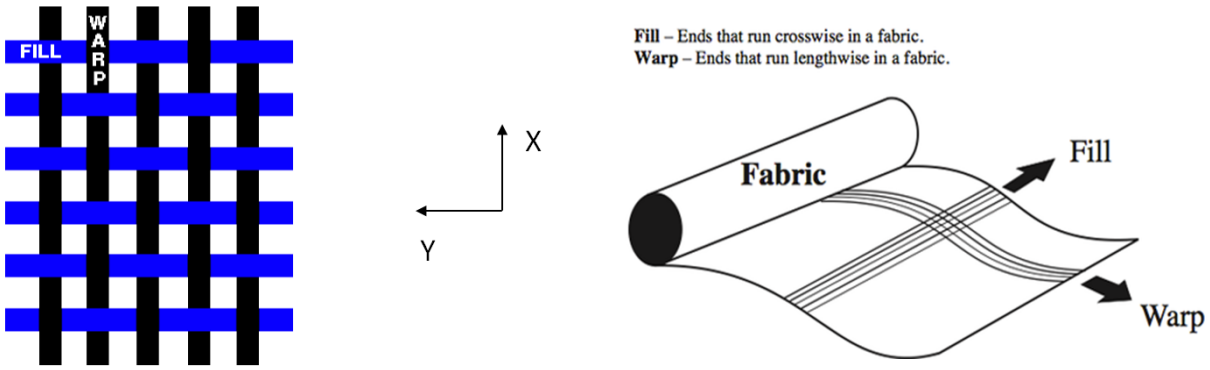

Figure 45 Schematic view of fiber weave as well as the corresponding orientation of the Fill and Warp directions

The Field Cage will be using pultruded FRP I-beams, angles and box sections which have their fibers oriented in a single direction. The strength of the pultruded sections is different from FR4 formed in sheets. I-beams and Box Beams are used as the structural elements in the top, bottom and end wall field cage assemblies, supporting the aluminum metal profiles and stainless steel ground planes for the TPC of proto-DUNE. The material for these structural components should be non-conductive and strong enough to withstand the loads of field cage and ground plane between the temperature range of -150C and 23C.

I-beams and box beams are supplied by Mc Master Carr but the manufacturing source is Bedford Reinforced Plastics. Testing on the samples was done by Intratek Plastics to make sure they meet the required standards was done by Intertek plastics. Tested fiberglass material met the MIL-PRF 62419A standards for flexural strength. It should be noted that the lowest strength of the material (48.2MPa) which is when loads are applied crossways are used to calculate the factor of safety. NASA (National Aeronautics and Space Administration) Technical Paper 3663 about Low Temperature mechanical testing of Epoxy Resin composite materials should be referred for the cryogenic temperature behavior of the materials. According to the paper the epoxy resin composite materials have better resistance to micro cracking at cryogenic temperatures and hence they have more strength as compared to room temperature. Therefore, the use of room temperature properties is considered conservative. The material strength provided by vendors is consistent with what has been measured in tests, see Section 7.

The material properties used for calculations were:

FR4:

Thermal expansion Coefficient Normal at 87K	29.4 x 10^-6 cm/cmK
Thermal expansion Coefficient Warp at 87K	9.7 x 10^-6 cm/cmK
Modulus of Elasticity	18.6 GPa (2,770ksi)
Ultimate stress Weak	165.4 MPa (24ksi)
Ultimate stress Strong	200 MPa (29ksi)
Ultimate stress Thickness	64.7MPa (9390psi)
Density	1.8 g/cm^3

FRP Pultruded Sections:

Thermal expansion Coefficient Lengthwise	5.2 x 10^-6 cm/cmK
Modulus of Elasticity	19.1 GPa (2,770ksi)

Ultimate stress Weak	48.2 MPa (7ksi)
Ultimate stress Strong	206.8 MPa (30ksi)
Density	1.8 g/cm^3

Stainless Steel 304:

Thermal expansion Coefficient at 87K	13.3 x 10^-6 cm/cmK
Modulus of Elasticity	214.3 GPa (31000ksi)
Yield stress	215 MPa (31ksi)

Aluminum:

Thermal expansion Coefficient at 87K	10 x 10^-6 cm/cmK
Modulus of Elasticity	75.83 GPa (11,000ksi)

The thermal expansion coefficients were obtained from NIST data for liquid argon temperatures. http://cryogenics.nist.gov/materials/materialproperties.htm

Vendors that can provide this material are:

Liberty Plastics http://libertyplastics.com/
Professional Plastics http://www.professionalplastics.com/

All stainless steel bolts and screws will be a minimum of SAE Grade5/ASTM A449 strength bolts. All pins will meet ANSI B18.8.2-1995 specification.

Failure Criteria

A failure criteria and evaluation methodology needs to be defined for the FR4 material because it is brittle and does not exhibit ductile failure and a defined yield stress like stainless steel. Eurocode 3 is a Load and Resistance Factor Design (LRFD) methodology which is based on ductile failure and the load and resistance factors have been developed over time based on statistical evaluation of ductile steel failure and therefore are not applicable for evaluating a brittle fiber reinforced plastic material.

CERN utilizes the JRC Science for Policy Report "Prospect for New Guidance in Design of FRP" as a guide for designing FRP structures. This report is focused on buildings in the construction sector and the examples provided in Section 2 of the Report are all large civil structures. The Report also is only applicable for temperatures down to -20C. The CPA and FC structures are much smaller and specialized, must support only their own weight and no external loads such as wind. The Report will be used as a guide for the stress analysis of the CPA and FC.

The brittle nature of failure in FR4 is typically evaluated using an allowable stress design (ASD) methodology for evaluating the strength of members. Brittle materials typically rupture and have a fractional reduction in area due to tensile strain of less than 0.05. For brittle materials it is recommended that the modified Mohr Theory of Failure be used which states that the principle tensile stresses be less than the ultimate stress of the material, see Shigley Standard Handbook of Machine Design, third edition. However, the CERN recommended "Prospect for New Guidance in Design of FRP" does not specifically address the brittle nature of the material and recommend any special methodology. The geometry and loading of the CPA and FC are very simple and the first principle stress will in general align with the loading direction.

Stress concentrations are also a concern for brittle materials and care should be taken to avoid sharp corners and other areas of stress concentrations. Shigley also defines stress concentration factors which are multipliers for geometric areas where stresses are higher and is a common method for evaluating high stress areas.

Safety factor for the AISC ASD and Eurocode 3 for ductile steel construction is 1.65 and is not applicable to the design of brittle fiber reinforced material. A safety factor of 3.75 will be used for all of the stresses calculated based on Section 2.3.2 of "Prospect for New Guidance in Design of FRP" and accounting for the effects of temperature, humidity, creep and variation in material properties. See section 1 of Appendix 1 for calculation of safety factors. All of the connections within the CPA and FC will be tested and test results compared to the stress analysis of these joints.

7 Material and Physical Testing

Physical testing of material has been performed to confirm published data from material suppliers. In addition, testing of specific joints and connections that are part of the CPA and FC design have also been tested in order to confirm their strength and the safety factors used.

7.1 Material Testing

In an effort to determine the ultimate strength of the FR4, samples of different thicknesses were tested. Since the material is anisotropic all tests were conducted in the X and Y direction as follows.

FR4 Destructive Testing 8" Long Samples

Direction	Cross-Section	Rupture	Stress
Y	0.255 x 1.002	8771#	34327 PSI
Y	0.255 x 1.002	9191#	35971 PSI
Y	0.255 x 1.002	9261#	36245 PSI
X	0.255 x 1.005	6730#	26261 PSI
X	0.255 x 1.005	6596#	25738 PSI
X	0.255 x 1.005	6862#	26776 PSI
Y	0.378 x 1.006	12309#	32369 PSI
Y	0.378 x 1.006	12666#	33308 PSI
Y	0.378 x 1.006	13223#	34773 PSI
X	0.38 x 1.004	10295#	26984 PSI
X	0.38 x 1.004	9257#	24263 PSI
X	0.38 x 1.004	9318#	24423 PSI
Y	0.500 x 1.003	15155# *	30219 PSI
Y	0.502 x 1.003	15014#	29819 PSI
Y	0.503 x 1.003	15248# *	30223 PSI
X	0.504 x 1.002	12505#	24762 PSI
X	0.503 x 1.001	12682#	25188 PSI

X	0.505 x 1.002	12581#	24863 PSI

* Specimen split axially also

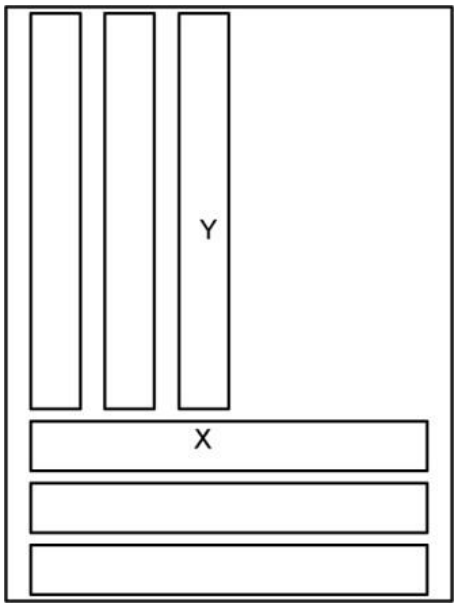

The material is anisotropic due to the way the woven material is fabricated into sheet form, it comes on a roll and is layered. The layers of weave are built up in the epoxy until the desired thickness is achieved. The lengthwise (Y) direction off the roll is stronger due to the way the fibers are woven and consistently they are layered in the same direction.

The low stress in the Y direction is 29819 PSI and in the X direction is 24263 PSI. These numbers should be considered in the design with a safety factor. When possible high stress members should be fabricated out of the material in the X direction.

Tensile Strength Testing in thickness (Perpendicular) direction

This sections of FR4 will be used in the detector. Material properties through the thickness is not provided by FR4 producers to tests were performed to evaluate the strength of the material in the thickness direction which could then be used in the stress analysis.

In order to determine the tensile strength in the thickness (perpendicular) direction, tensile test specimens were from a thick block of FR4 as shown in **Error! Reference source not found.**. The original block was 3 ” thick, 2.4” wide, and 96” in length. The figure shows the length dimension of the original block as indicated by an arrow marked on the block and a finished specimen is shown in the orientation that it was cut from the block. The specimen dimensions are shown in Figure 47. The gage length of the samples is 1 inch. The specimen dimensions determined following the general requirements for test specimen in ASTM D3039/D3039M-14. The specimens were loaded in tension using a Tinius Olsen universal test machine using a fixed bottom grip and compliant top grip. The testing was performed using displacement control of the crosshead at a rate of 0.05 in/min. An extensometer was not available for this gage length and so the displacement is taken from the crosshead position. The grips are the self-centering locking wedge type grips such that some of the displacement of the crosshead is taken up by wedge movement during tightening. The specimen data and test results are given in Figure 49**Error! Reference source not**

found.. Figure 50 shows the Force versus crosshead displacement plots for perpendicular specimens. An extensometer appropriate for the gauge length was not available and with the evident compliance in the grips as seen in the plots, an accurate determination of the modulus from these specimens is not possible. However, the plots do reveal the brittle nature of the failure with no significant material yielding. The tested samples are shown in Figure 46. The average failure stress of 10 samples was 9390 psi.

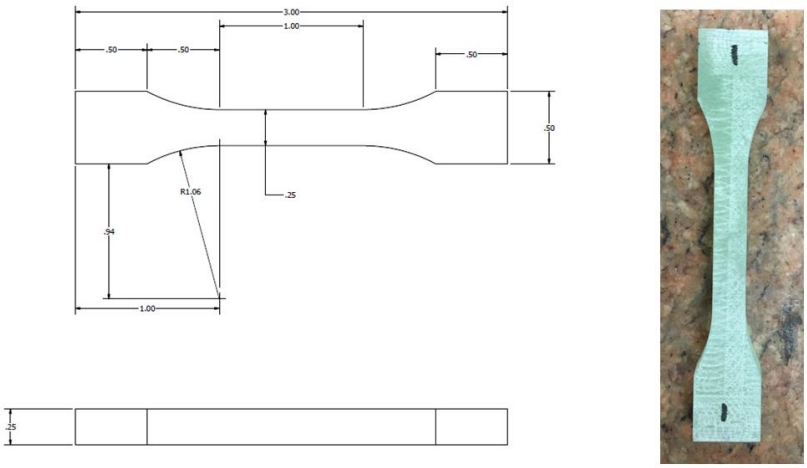

Figure 46 Specimen dimensions

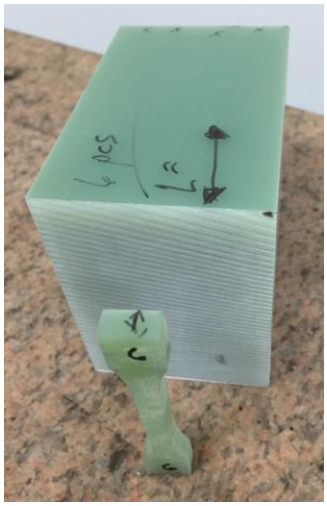

Figure 47 Specimen orientation as cut from 3 inch thick block. Arrows on block indicate the long dimension of the original piece.

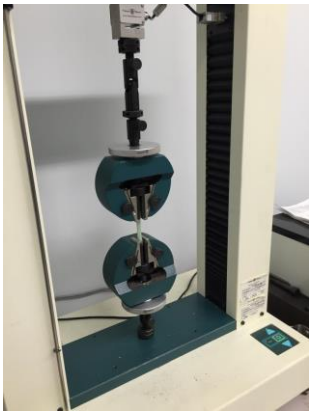

Figure 48 Specimen in grips of the tensile test machine.

Table 1 Sample data and test results.

Sample	Width [in]	Thickness [in]	Area [in^2]	Failure Load [lbf]	Failure Stress [psi]
1	0.243	0.24	0.05832	558.9	9583
2	0.242	0.24	0.05808	461.1	7940
3	0.241	0.24	0.05784	598.2	10343
4	0.243	0.24	0.05832	563.8	9667
5	0.243	0.239	0.05808	684.5	11786
6	0.254	0.250	0.0635	543.0	8560
7	0.247	0.251	0.0620	577.0	9300
8	0.244	0.254	0.0620	458.0	7390
9	0.245	0.251	0.0615	571.0	9290
10	0.251	0.253	0.0635	638.0	10040

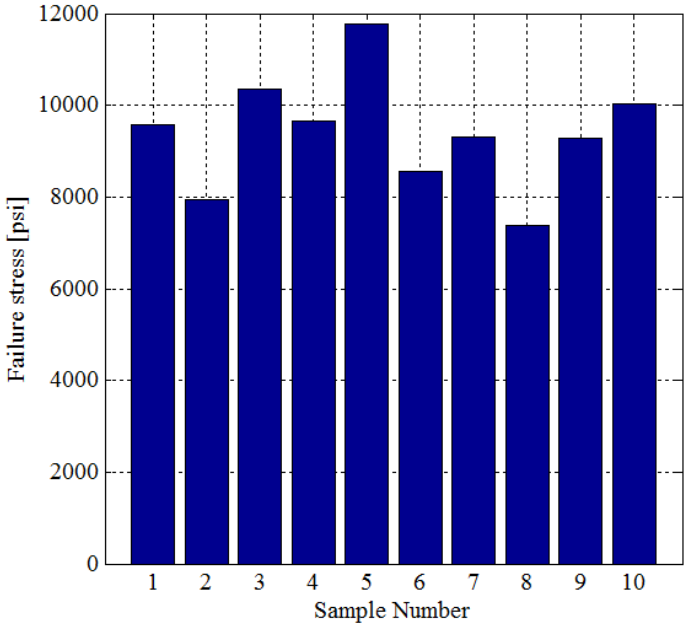

Figure 49 Plot of UTS for five samples.

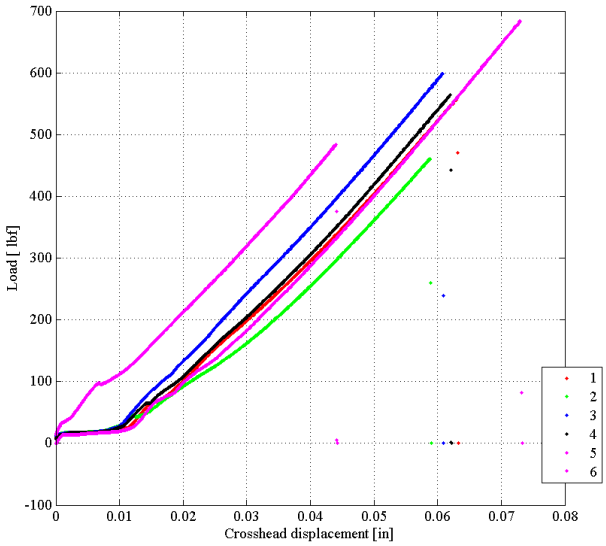

Figure 50 Force versus crosshead displacement plots for perpendicular specimens. While compliance in the grips is evident

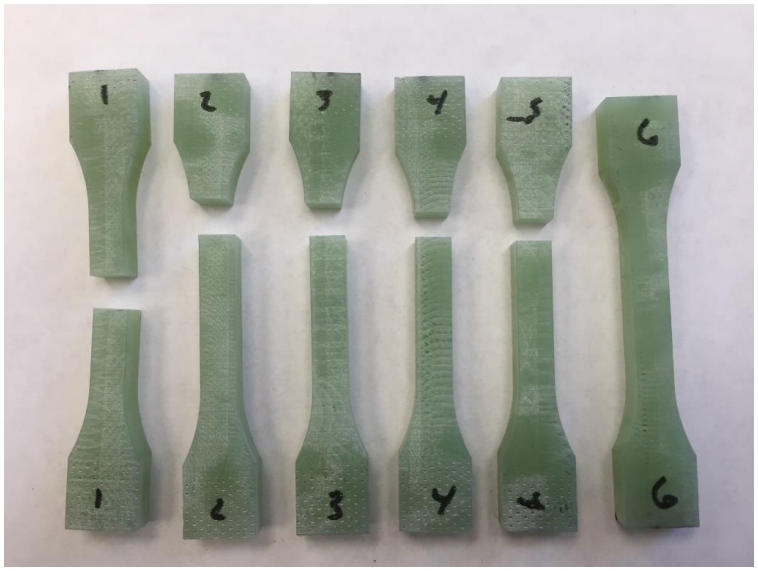

Figure 51 Specimens (1-5) after being pulled to failure and an untested specimen (6).

7.2 CPA Connection Testing

The CPA connections are shown in Figure 52 for ProtoDUNE-SP and identified in Table 2. The geometry of the connections 3 and 6 are identical as are connections 4 and 5. The loadings are different. For DUNE, there are a total of 9 connections – 1,2,and 3 are the same as for ProtoDUNE-SP, 4 and 5 become 4-8 for DUNE, and 6 becomes connection 9. The detail of the connections (except the center tab which is more complex) are shown in Figure 53 to Figure 55. The detail views show the two connecting points in top and side views. The red arrows in the figures indicate the line of action through the connection.

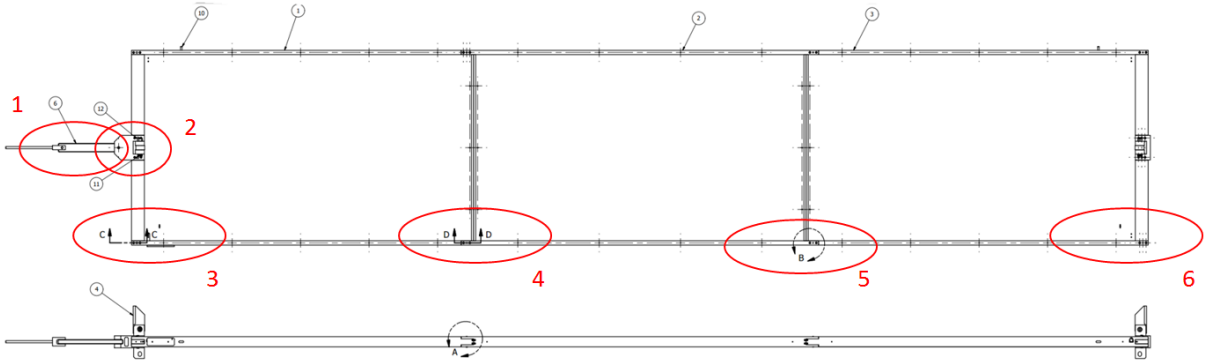

Figure 52 CPA Module identifying the connections that require testing.

Table 1 Identification of the CPA connections.

Connection number	Description	Reference Drawing(s)	Load [lbf]
1	Hanger Assembly	DUNE-4	1036Do these need to be re-evaluated for 12m Panel?

2	Center Support Tab	DFD-20-A401	
3	Upper Panel to Main Support Bar	DFD-20-(A,B,C)100	298
4	Middle Panel to Upper Panel	DFD-20-(A,B,C)100	272
5	Middle Panel to Middle Panel	DFD-20-(A,B,C)200	
6	Middle Panel to Middle Panel	DFD-20-(A,B,C)200	
7	Middle Panel to Middle Panel	DFD-20-(A,B,C)200	
8	Middle Panel to Lower Panel	DFD-20-(A,B,C)300	246
9	Lower to Bottom Support Bar	DFD-20-(A,B,C)300	220

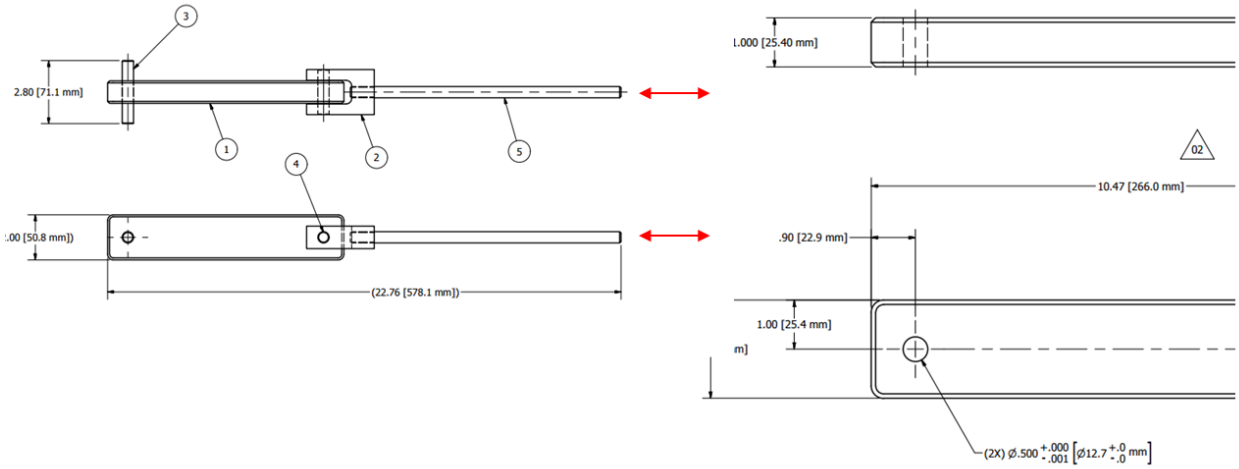

Figure 53 Connection 1: Hanger assembly (DUNE-4) and pin hole connection detail for FR4 extension bar.

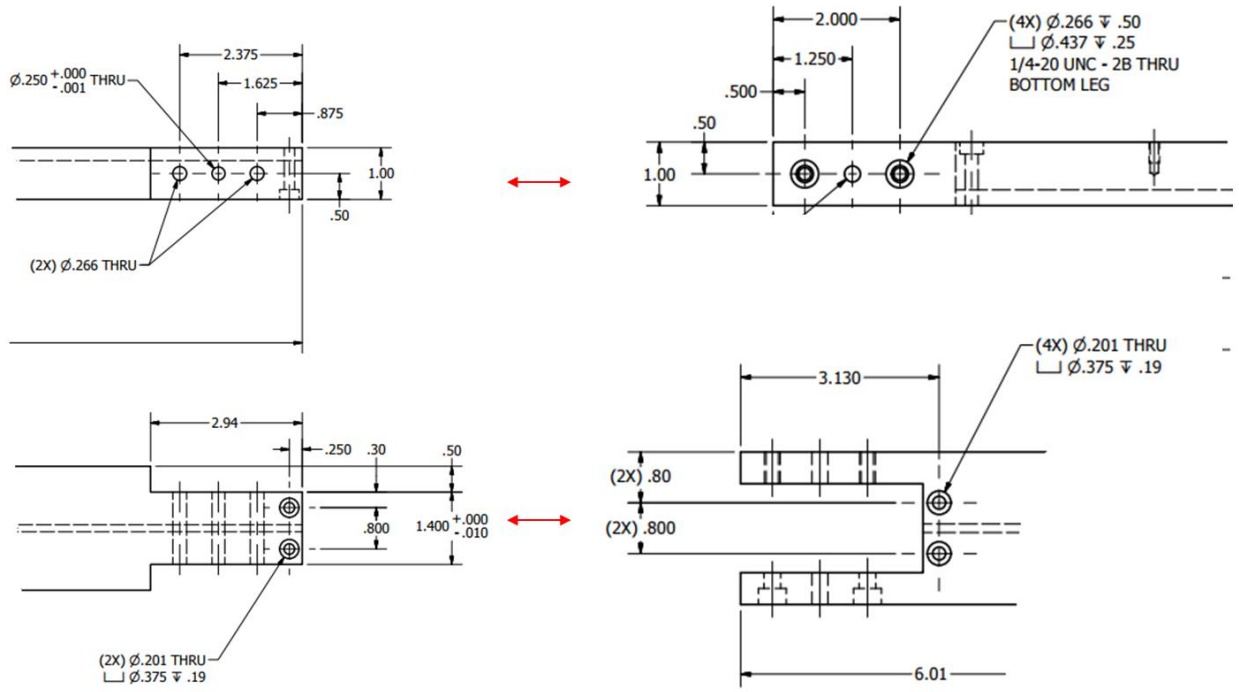

Figure 54 Connections 4 and 5 which connect the Upper-Middle and Middle-Lower panels respectively are identical.

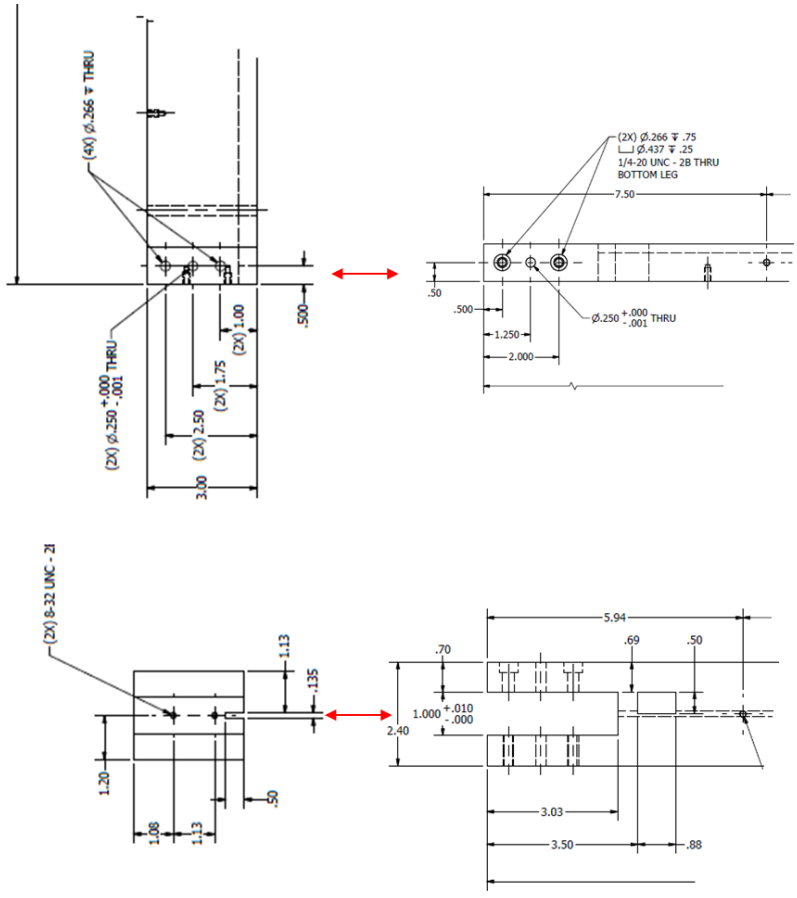

Figure 55 Connections 3 and 6: Upper panel to main support and Lower panel to lower support bar.

Figure 56 shows the details of the specimen used for the pin test connection. Due to the anisotropic behavior of the FR4 sheet, it is important to understand the sensitivity of the strength in various orientations. There are four principle orientations for a piece to be cut from a sheet and these are illustrated and identified in Figure 57. The most concerning orientations are shown by Specimens C and D where significant tensile stresses can develop in the weak thickness (Z, perpendicular to the fiber mat) direction of the sheet. As noted above, there are multiple pin connections following different details and orientation. The specimen hole size and spacing was developed based upon connections 4,5 (see Figure 52). Connections, 1,3, and 6 have similar geometry but have either additional hole clearance or cross sectional area such that they are all stronger than the test specimen. One of each type of the pin test specimens (A,B, and D from Figure 56) was initially tested on a tensile test machine with a maximum capacity of 2000 lbf. None of the samples broke. This value exceeds the load on connection 1 by a factor of two and greatly exceeds the load on connections 3-6 (> factor of 6). While the pin test specimen does not have the make-up of a traditional dogbone, an extensometer was placed on the specimens during testing to provide data for the modulus of elasticity. The stress versus strain is plotted in Figure 59. It is noted that this run was over a relatively small strain range (< 0.1% strain) and so this should be considered before interpreting these results. It is interesting that there is no apparent difference in the modulus when comparing the orthogonal sheet directions (L and W). The test specimens have been sent to Princeton to be tested in a load frame with greater capacity to determine the ultimate strength of the test specimen.

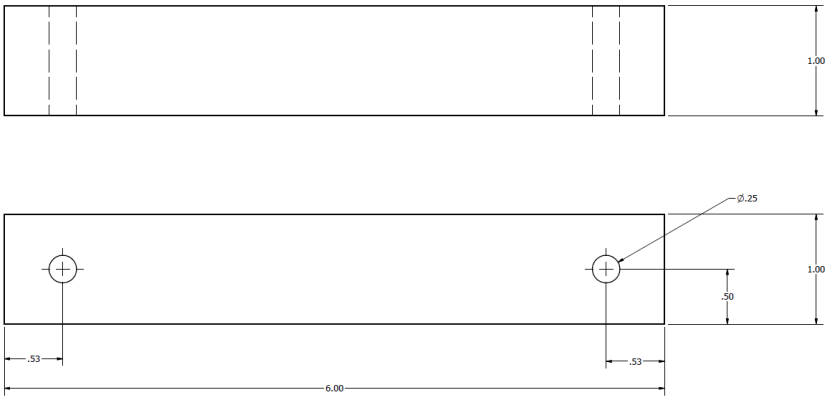

Figure 56 Pin connection test piece

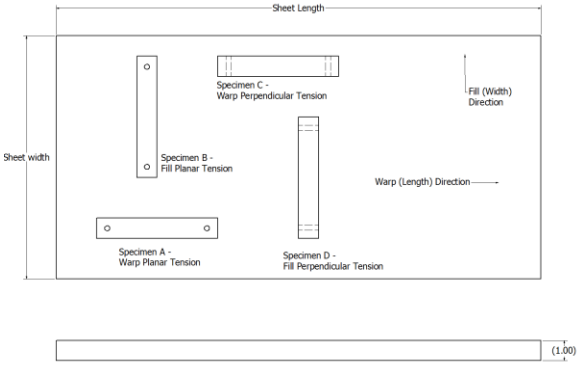

Figure 57 Orientation of pin connection specimens relative to the FR4 sheet directions.

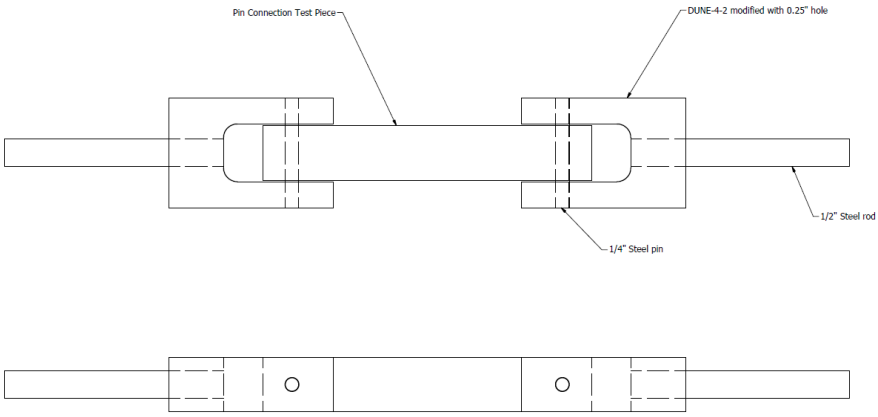

Figure 58 Pin test fixture configured for ¼" pin test.

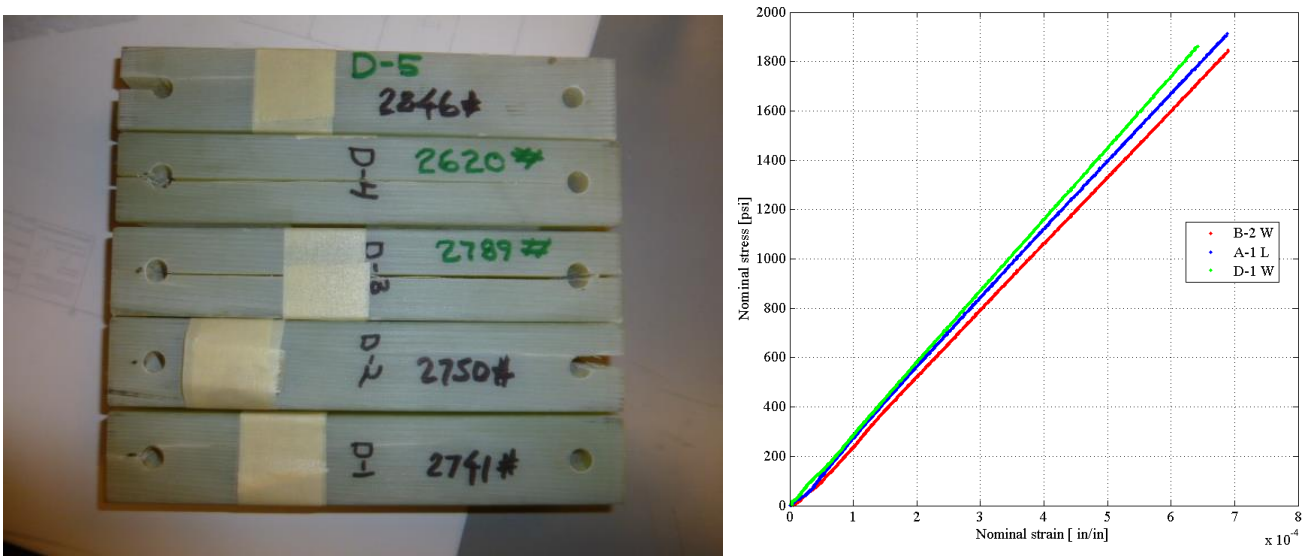

Figure 59 Stress vs. Strain plot using 2" gauge length extensometer in pin connection specimen.

The initial sample A test piece with a ¼" diameter pin failed at the pin at 6100 lbs, see Figure 60. The load is far in excess of any anticipated load on the pin in the CPA frame (max tensile load expected is 780 lbs during installation). The high strength of the connection occurred because the pin hole is perpendicular to the plane of the fibers, therefore, block shear can only occur by tearing the fiber mesh. The test with the ¼" diameter pin was also conducted with Sample D and the failure was due to shear in the FR4 material. The results are shown in the table below and broken pieces can be seen in Figure 62. Failure occurred in the FR4 material at a lower load with the D samples because the pin hole is aligned with the plane of the fibers and block shear is only resisted by the epoxy resin; the plane of shear occurs in the epoxy layer between fiber layers.

Specimen D -- 1/4" Pin

Sample #	Force
1	2741
2	2750
3	2789
4	2620
5	2846
Average	2749.2
Std Dev	83.2

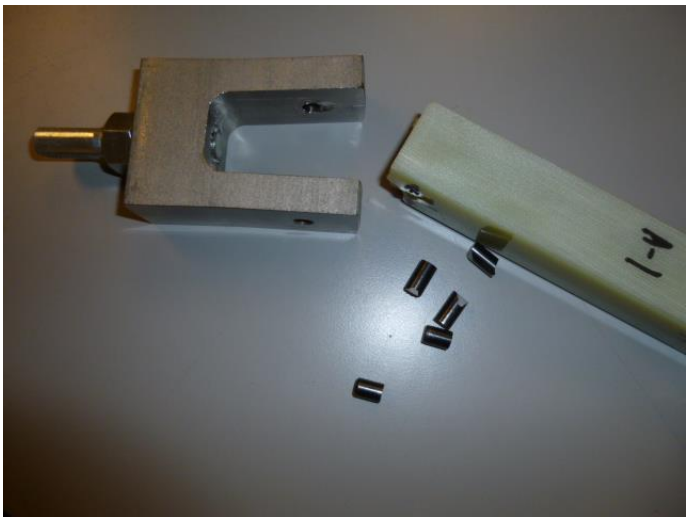

Figure 60 Failure of Sample A with 1/4" Pin

Figure 61 Failure of Sample D with 1/4" Pin

The A and B samples that has the pin hole perpendicular to the plane of the fibers has a much higher strength as shown in the tables and figure below. Failure occurred due to tension of the reduced area around the bolt rather than shear failure at the pin which occurred in the D sample. All of these test samples

are representative of the CPA connections and the worst case hole-to-edge distance. The maximum load these types of CPA joints are expected to withstand is 350 lbs. There is a large safety factor on the joint loading even with if the pin is oriented parallel to the plane of fibers (Sample D). When ordering the material for the CPA the plane of the fibers will be specified to ensure the strongest connection.

Specimen A -- 1/2" Pin		Specimen B -- 1/2" Pin	
Sample #	**Force**	**Sample #**	**Force**
1	10898	1	8925
2	10923	2	9263
3	10692	3	9237
4	10917	4	8753
		5	8904
Average	10857.5	Average	9016.4
Std Dev	110.8	Std Dev	223.5

Figure 62 A and B Samples

These initial tests of pinned joints were followed up with a test that mimicked exactly the CPA joint. A tensile test sample was made of two pieces that had the geometry of a joint but was held together only by the single pin. The two bolt holes have clearance and do no contribute to the tensile strength of the joint until deformation occurs at the pin. Therefore, it is felt that this is a worst case for this joint.

The test of individual pins was followed up by a test of the actual CPA joint. A tensile specimen was fabricated to mimic exactly the geometry of the joint. In the worst case only the pin carries the load so when pulled in tension only the steel pin was in place and the bolts were not. The bolt holes and counter bores were in the tensile specimen to see if they had any effect on the joint. In the first set of samples the fiber mesh was parallel to the axis of the pin. A typical failure is shown in Figure 63. The joint was then tested with the pin perpendicular to the mesh and significantly, higher strength was achieved. Results are listed in the table below and failed pieces are shown.

CPA Joint Test

Sample #	Force
1	3361
2	3202
3	3119
4	3610
Average	3323
Std Dev	216.1

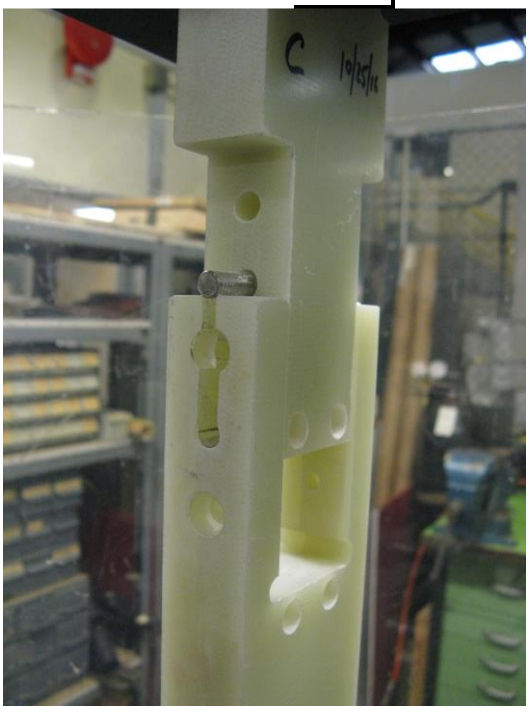

Figure 63 CPA Joint Test

	Failure Load (lbs)	
#	Room Temp	LN Temp
1	6641	9102
2	7135	9252
3	6666	8835
4		9034

7.3 Testing of FC Connections

This test is to obtain mechanical strength of FR4 shear pins and fiberglass screws used to join field cage frames, and verify mechanical integrity of field cage frames.

Two types of tests are to be performed: 1) shear test of FR4 shear pins and fiberglass screws to obtain mechanical strength of the FR4 shear pins and fiberglass screws, and 2) loading test of field cage frames to verify mechanical integrity of field cage frames.

Field cage consists of field cage frames and extruded aluminum and/or stainless steel profiles. The field cage frame is constructed from pultruded FRP I-beams and box beams, which are joined with FR4 shear pins and/or fiberglass screws. The weight of field cage and all other loads exerted on the field cage are supported by the field cage frame. The strength of FR4 shear pins and fiberglass screws is therefore of vital importance to ensure the integrity of the field cage. In its service condition, the entire field cage assembly is submerged in liquid Argon (LAr). Previous research [1] has shown that epoxy resin composite materials become slightly stronger at cryogenic temperature than at room temperature. Therefore, tests performed at room temperature can be considered as a conservative measurement of the strength of FR4 shear pins and fiberglass screws.

Two types of tests are designed: 1) shear test of FR4 shear pins and fiberglass screws to obtain mechanical strength of the FR4 shear pins and fiberglass screws, and 2) loading test of field cage frames to verify mechanical integrity of field cage frames. In a shear test of FR4 shear pins and fiberglass screws, a test unit with FR4 shear pin joints or fiberglass screw joints are assembled in a configuration similar to that in an actual joint in field cage frames. The test unit is loaded with tensile force using a universal testing machine until any of the joints fails.

Shear test of FR4 shear pins and fiberglass screws

There are two types of FR4 shear pins used in field cage frames: through hole FR4 shear pins and threaded hole FR4 shear pins. Through hole FR4 shear pins are used in top and bottom field cage frames and threaded hole FR4 shear pins are used in endwall field cage frames. Through hole FR4 shear pins are cut from a circular rod or tube with outer diameter of 1/2". A 6.5mm diameter hole is drilled at the center of the pin through its length. Threaded hole FR4 shear pins are cut from a circular rod or tube with outer diameter of 5/8". A 3/8"-16 thread is tapped at the center of the pin through its length. There are four different lengths of through hole FR4 shear pins (1/2", 3/4", 7/8", 1") and two different lengths of threaded FR4 shear pins (1" and 1 1/4"). Figure 64 shows four types of test units of through hole FR4 shear pins (Type 1, 2, 3 and 4), and Figure 65 shows two types of test units of threaded hole FR4 shear pins (Type 5 and 6).

As an alternative way of joining the field cage frames, FR4 shear pins are replaced with fiberglass screws to join the field cage frames. Three sizes of fiberglass screws are to be tested. Figure 66 shows the three types of test units of fiberglass screws (Type 7, 8 and 9).

Each test unit has two FR4 shear pin or fiberglass screw joints that are assembled in a configuration similar to that in an actual joint in field cage frames. Shown in Figure 67 is the drawing of an aluminum test bar, in which the material thickness, T, and the hole diameter, D, vary for different test units.

Bill of material of test units of through hole FR4 shear pins are shown in Tables 1, 2, 3 and 4. Bill of material of test units of threaded hole FR4 shear pins are shown in Tables 5 and 6. Bill of material of test units of fiberglass screws are shown in Tables 7, 8 and 9. The test units are loaded with tensile force using a universal testing machine. Increase the applied tensile force slowly until any of the two joints fails. The rupture force is recorded for each test, and pictures of failed test units are taken.

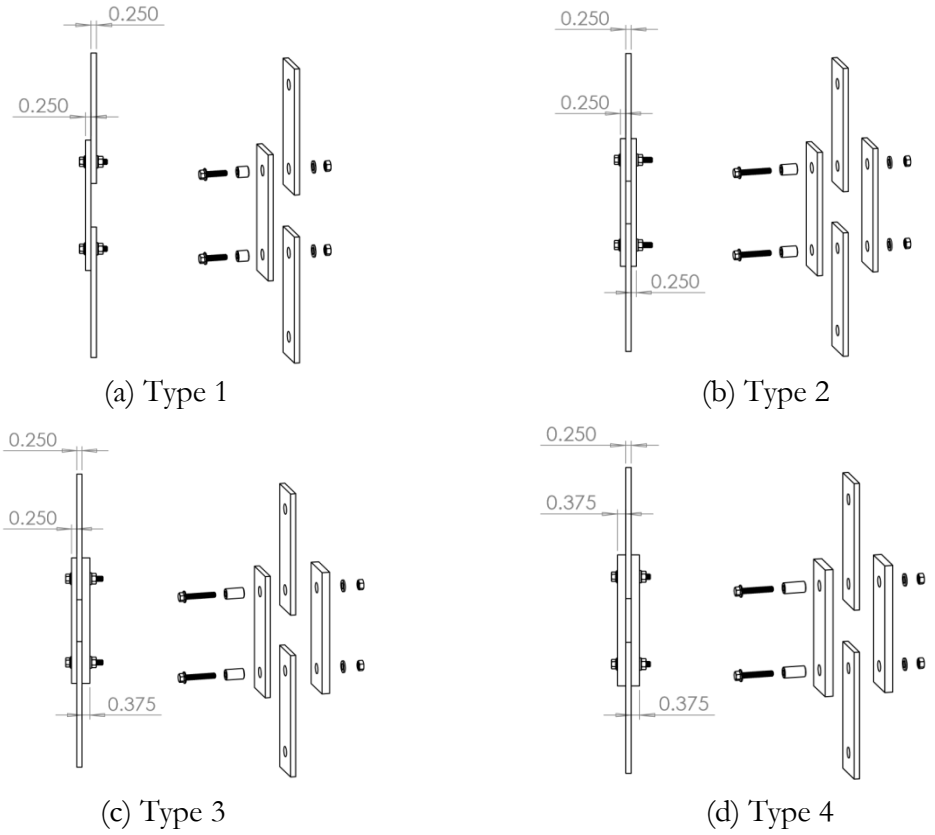

(a) Type 1 (b) Type 2

(c) Type 3 (d) Type 4

Figure 64 Test units of through hole FR4 shear pins: (a) Type 1

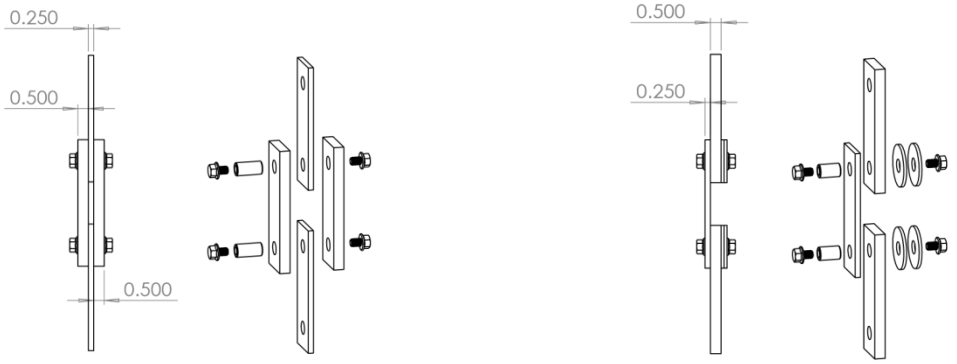

(a) Type 5 (b) Type 6

Figure 65 Test units of threaded hole FR4 shear pins

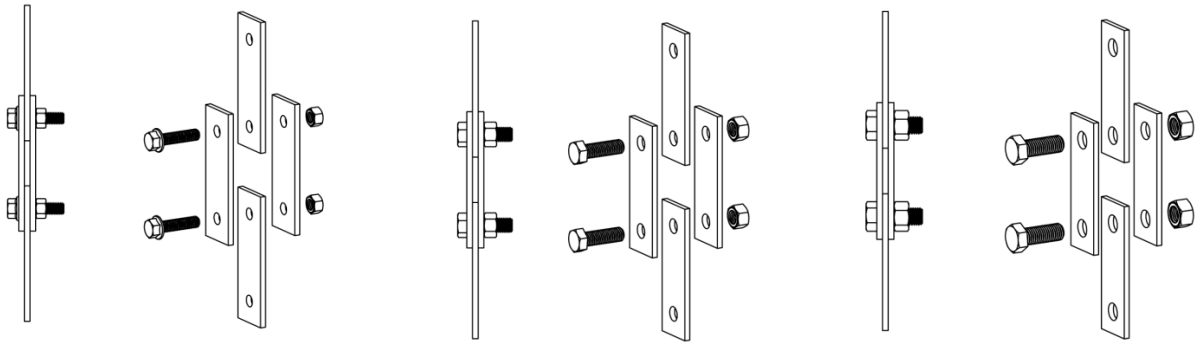

(a) Type 7 (b) Type 8 (c) Type 9

Figure 66 Test units of fiberglass screws

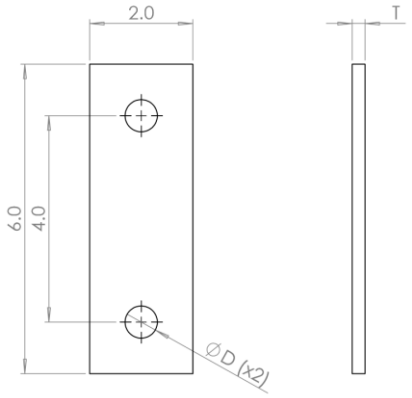

Figure 67 The drawing of the aluminum test bar.

Table 1 Bill of material of test unit of 1/2" through hole FR4 shear pin.

TEST UINT of 1/2" THROUGH HOLE FR4 SHEAR PIN (TYPE 1)				
Item #	Description	Qty	Dimensions	Comment
1	Top test bar-0.25"	3	2" x 6" x 0.25"	
2	Through Hole FR4 Shear Pin-0.5"	2	0.5" Dia, 0.5" Long, 6.5mm center thru hole	

3	Fiberglass Hex Head Cap Screw, Flanged	2	1/4"-20 Thread, 1" Long, Fully Threaded	McMaster P/N: 91345A688
4	Fiberglass Flat Washer	2	5/16" Screw Size, 0.312" ID, 0.562" OD	McMaster P/N: 93493A235
5	Fiberglass Hex Nut	2	1/4"-20 Thread Size, 7/16" Wide, 7/32" High	McMaster P/N: 91395A029

Table 2 Bill of material of test unit of 3/4" through hole FR4 shear pin.

TEST UNIT of 3/4" THROUGH HOLE FR4 SHEAR PIN (TYPE 2)				
Item #	Description	Qty	Dimensions	Comment
1	Top test bar-0.25"	4	2" x 6" x 0.25"	
2	Through Hole FR4 Shear Pin-0.75"	2	0.5" Dia, 0.75" Long, 6.5mm center thru hole	
3	Fiberglass Hex Head Cap Screw, Flanged	2	1/4"-20 Thread, 1-1/2" Long, Fully Threaded	McMaster P/N: 91345A692
4	Fiberglass Flat Washer	2	5/16" Screw Size, 0.312" ID, 0.562" OD	McMaster P/N: 93493A235
5	Fiberglass Hex Nut	2	1/4"-20 Thread Size, 7/16" Wide, 7/32" High	McMaster P/N: 91395A029

Table 3 Bill of material of test unit of 7/8" through hole FR4 shear pin.

TEST UNIT of 7/8" THROUGH HOLE FR4 SHEAR PIN (TYPE 3)				
Item #	Description	Qty	Dimensions	Comment
1	Top test bar-0.25"	3	2" x 6" x 0.25"	
2	Top test bar-0.375"	1	2" x 6" x 0.375"	
3	Through Hole FR4 Shear Pin-0.875"	2	0.5" Dia, 0.875" Long, 6.5mm center thru hole	
4	Fiberglass Hex Head Cap Screw, Flanged	2	1/4"-20 Thread, 1-1/2" Long, Fully Threaded	McMaster P/N: 91345A692
5	Fiberglass Flat Washer	2	5/16" Screw Size, 0.312" ID, 0.562" OD	McMaster P/N: 93493A235
6	Fiberglass Hex Nut	2	1/4"-20 Thread Size, 7/16" Wide, 7/32" High	McMaster P/N: 91395A029

Table 4 Bill of material of test unit of 1" through hole FR4 shear pin.

TEST UNIT of 1" THROUGH HOLE FR4 SHEAR PIN (TYPE 4)				
Item #	Description	Qty	Dimensions	Comment
1	Top test bar-0.25"	2	2" x 6" x 0.25"	
2	Top test bar-0.375"	2	2" x 6" x 0.375"	
3	Through Hole FR4 Shear Pin-1.0"	2	0.5" Dia, 1.0" Long, 6.5mm center thru hole	
4	Fiberglass Hex Head Cap Screw, Flanged	2	1/4"-20 Thread, 1-1/2" Long, Fully Threaded	McMaster P/N: 91345A692
5	Fiberglass Flat Washer	2	5/16" Screw Size, 0.312" ID, 0.562" OD	McMaster P/N: 93493A235
6	Fiberglass Hex Nut	2	1/4"-20 Thread Size, 7/16" Wide, 7/32" High	McMaster P/N: 91395A029

Table 5 Bill of material of test unit of 1" threaded hole FR4 shear pin.

TEST UNIT of 1" THREADED HOLE FR4 SHEAR PIN (TYPE 5)				
Item #	Description	Qty	Dimensions	Comment
1	Side test bar-0.25"	1	2" x 6" x 0.25"	
2	Side test bar-0.5"	2	2" x 6" x 0.5"	
3	Threaded Hole FR4 Shear Pin-1.25"	2	5/8" Dia, 1.0" Long, 3/8"-16 threaded hole	
4	Fiberglass Hex Head Cap Screw, Flanged	4	3/8"-16 Thread, 1/2" Long, Fully Threaded	McMaster P/N: 91345A694
5	Fiberglass Flat Washer	4	5/8" Screw Size, 0.625" ID, 2.000" OD	McMaster P/N: 90800A380

Table 6 Bill of material of test unit of 1 1/4" threaded hole FR4 shear pin.

TEST UNIT of 1 1/4" THREADED HOLE FR4 SHEAR PIN (TYPE 6)				
Item #	Description	Qty	Dimensions	Comment
1	Side test bar-0.25"	2	2" x 6" x 0.25"	
2	Side test bar-0.5"	2	2" x 6" x 0.5"	
3	Threaded Hole FR4 Shear Pin-1.25"	2	5/8" Dia, 1.25" Long, 3/8"-16 threaded hole	
4	Fiberglass Hex Head Cap Screw, Flanged	4	3/8"-16 Thread, 1/2" Long, Fully Threaded	McMaster P/N: 91345A694

Test results

A first batch of tests have been carried out in Princeton University. Tested in the first batch of tests are test units of Type 1, 2, 3, 4, 5 and 6. Three samples are tested for each type. Shown in Figure 68(a) are the six types of test units, which are Type 1, 2, 3, 4, 5 and 6 from left to right. Shown in Figure 68(b) are the test units after tests are done. Figure 69(a) shows a test unit clamped in a universal test machine ready for testing, and Figure 69(b) shows the test unit after the shear pin breaks.

Tabulated in Table 10 are the rupture force of the tested samples. Average rupture force are calculated as the strength of the shear pins. According to finite element analysis of the topmost endwall panels, which support all the weight of other three endwall panels, the maximum reaction force on the Type 5 pins is 78 lbs, which results in a safety factor of 5155 lbs / 78 lbs = 66. The maximum reaction force on the Type 6 pins is 7.4 lb, which results in a safety factor of 3695 lbs / 7.4 lbs = 499.

According to the results from the completed tests, all FR4 shear pins are strong enough to connect the field cage frames with safety factors of 66 and 499.

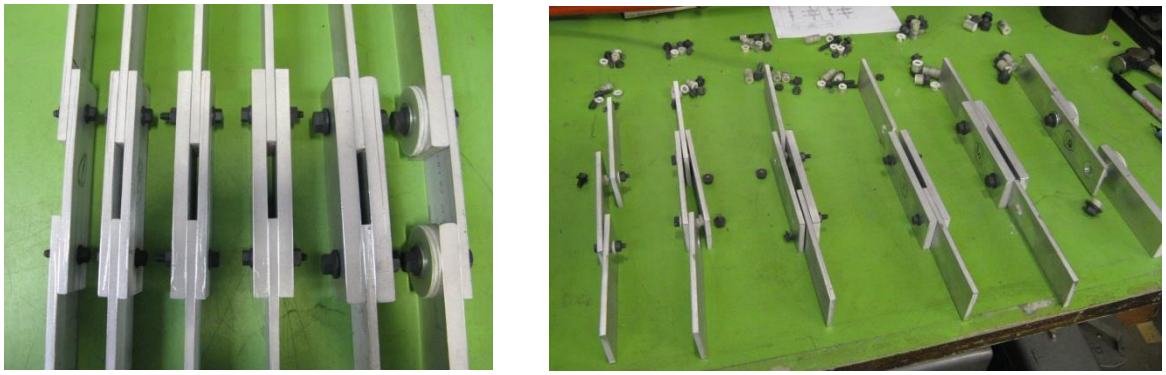

Figure 68 Test units of Type 1, 2, 3, 4, 5 and 6

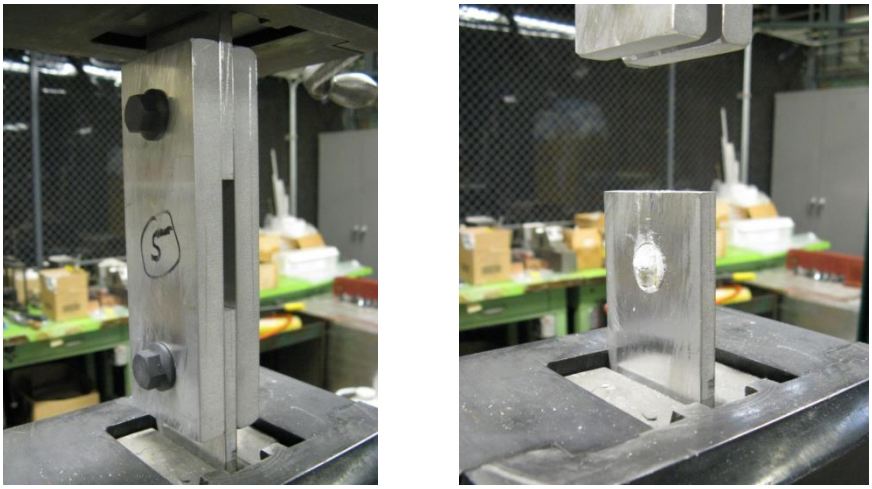

(a) (b)

Figure 69 Shear test using universal test machine

Table 10 Test results of test units Type 1, 2, 3, 4, 5 and 6.

Type	Rupture Force (lbs)			
	Run 1	Run 2	Run 3	Average

1	2174	2262	2220	**2219**
2	4857	4813	5027	**4899**
3	4888	4706	4925	**4840**
4	4804	4760	4971	**4845**
5	5177	4810	5477	**5155**
6	3673	3631	3781	**3695**

References:
[1] NASA Technical Paper 3663: *Low Temperature Mechanical Testing of Carbon-Fiber/Epoxy-Resin Composite Materials*, Alan T. Nettles and Emily J. Biss, November 1996

8 Cleaning Components

It is critical to clean all components and bag them during shipment. Individual pieces will be cleaned by alcohol or simple green plus a de-ionized water rinse during construction so that final assembly is free from dust and other particulates. This applied to the interior surfaces of all components as well. Components should be double bagged while still in clean areas prior to being exposed to dirty environments. Prior to taking components into the clean environment at CERN the outer bag will be removed. Once the component is in the clean environment, the inner bag will be removed.

Wires and cables will need to be wiped down with alcohol prior to being installed in the cryostat. After cleaning the wiring should be dried out to remove the majority of initial moisture. The wiring should be placed in a vacuum chamber for 48 hours and then double bagged.

9 Interfaces and System Analysis

There are both mechanical and electrical interfaces between components that make up the HV as well as interfaces between HV components and other systems in the detector. Not only must the interfaces be well understood but also how the entire detector behaves as a system.

Between HV components there are interfaces between the CPA and FC and between the CPA and HV. Electrical interfaces with the high voltage power supply and feedthrough consist of connections with the HV cup and HV bus on the CPA. In addition, there are interconnects between CPA modules and CPA Panels and connections between the CPA and FC components. The required mechanical interfaces are as follows:

- Metal contact plates on the cathode surface at each corner, with two captive screws in each used for making electrical contact with the HV bus and the resistor board for the frame field strips.
- Through holes for the 3-mm diameter cable in the sides of each frame adjacent to the contact plates to allow interconnection of the HV buss between CPAs.
- A means of securing the HV buss cable in place.

- Through-holes near the centers of the top and bottom frames for connecting the top and bottom field cage elements to the cathode, with corresponding metal contact plate on the cathode surface.
- Similar holes and metal contacts through the CPA side frames at each end of the TPC volume for connecting the EndWall FCs to the CPA.
- Electrical specifications for these parts and interfaces are given in the High Voltage Design Section.

Between the CPA and the Top and Bottom FCs the interface is at the hinge joint, ensuring that the CPA and FC are located relative to each other properly.

Interface drawings can be found in DocDb 6260.

The TPC components also have several interfaces with external components. These interfaces are formally defined by interface documents that can be found on the DUNE DOCDB. The external interfaces and defining EDMS number are listed in the table below.

DUNE Consortia to Consortia Interface Document Matrix

	SP-PDS	SP-TPC	JT-COM	JT-CAL	JT-DAQ	JT-HV	JT-CISC
SP-APA	2088735	2088736	2145145	2145136	2145158	2088738	2088739
SP-PDS		2088720	2145146	2145137	2088726	2088721	2088731
SP-TPC			2145147	2145138	2088713	2088706	2088715
DP-CRP			2145148	2145139	2145156	2088744	2088742
DP-PDS			2145149	2145144	2088747	2088746	2088748
DP-TPC			2145153	2145140	2088749	2145155	2088750
JT-COM				2145159	2145151	2145150	2145152
JT-CAL					2145141	2145142	2145143
JT-DAQ						2145154	2088741
JT-HV							2088740

10 Hazard Analysis

The hazards analysis process began early in the design process to assure that hazards were identified and mitigated early in the evolution of the design. A Hazards Analysis Report (DocDb 649) was developed early on to identify potential hazards and methods of mitigation throughout the design/construction and operation of DUNE. This report will be used as a guide to identify hazards and mitigation for the CPA, FC, and HV systems as well as the installation of the detector. Hazards and mitigation for these separate parts of the TPC are addressed separately in their specific sections of this design paper.

It is planned that the construction and assembly of CPA modules, FC modules and installation in the detector will be performed according to a set of Work Planning and Control (WPC) documents. These WPC documents will identify hazards associated work, specify PPE that may be required and have a detailed plan for performing the work that mitigates the identified hazards. Work planning and control (WPC) is the use of formal, documented processes for identifying and mitigating risks when planning, authorizing, releasing, and performing work. The purpose of WPC is to ensure adequate protection of workers, the public, and the environment, which would otherwise be put at risk by inconsistent and inadequate planning, authorization, and control.

The following steps will be followed to develop WPC documents for the discrete tasks needed during assembly, testing and installation.

- Define the work
- Identify and analyze hazards
- Develop and implement controls
- Authorize work
- Perform work within controls
- Feedback and continuous improvement.

The assembly of the CPA has two main hazards: exposure to mechanical hazards associated with the use of hand tools and basic assembly of mechanical components; and lifting/rigging of completed CPA modules.

The assembly of the CPA will require the utilization of basic hand tools and machining equipment. The design of the CPA considers these hazards and tried to minimize

The construction and assembly of CPA modules will be performed according to a set of Work Planning and Control (WPC) documents. These WPC documents will identify hazards associated work, specify PPE that may be required and have a detailed plan for performing the work that mitigates the identified hazards.

The construction and assembly of CPA modules presents the following hazards:

- Use of hand tools
- Pinching hazards
- Lifting hazards
- Overhead crane operations

The HV system has both high voltage and stored energy, and is composed of both commercial and custom-built equipment. Most of the custom-built parts are contained within the cryostat; the only custom-built parts partly or entirely outside the cryostat are the HV filter and the HV feedthrough. The entire system is designed to have no exposed HV during normal operation. Hazards can be divided into categories as follows: hazards arising from discharges in argon inside the cryostat, hazards from failure of HV components inside the cryostat, hazards from failure of custom-built HV components outside the cryostat, hazards from commercially supplied components outside the cryostat, and hazards arising during servicing or installation.

Hazards from a discharge through liquid argon within the cryostat are mitigated by placing all cryostat penetrations behind the ground planes and protecting cables such that discharges create currents only inside the surfaces of the cryostat. There should be no electrical signal cables placed such that a HV discharge could reach them. The possibility of direct discharge to the anode plane wires, potentially returning through the wire bias supply cables, is mitigated by the ground screen plane.

Hazards from failure of resistors, varistors, or connections is mitigated by having multiple parallel components on each resistor board. Complete failure of all components on a resistor board or of an electrical connection on the FC or CPA is unlikely; if it were to occur, it could create the possibility of a high potential that sustains a discharge over the break in the circuit, but would not create a hazard outside the cryostat unless it breaks were in the final connection to ground after the monitoring point at the end of the FC chain.

Particular attention must be paid to the monitoring point at the end of the field cage resistor chain: in the event that the final terminating resistances to ground were to be removed by a component failure or other agency, the monitoring point voltage would rise to the full drift HV. This would create high voltage on the monitoring point cable. This should be mitigated by having multiple parallel resistors and varistors on the monitoring point to ground connection.

The feed-through and HV filter designs are designed such that HV conductors in these systems will be insulated and contained within ground shields. The current monitoring toroids must be within the ground shield to function correctly, and are protected only by the insulation. The HV supply meets EU safety standards. These designs and their connections will be reviewed according Fermilab and SURF safety rules.

HV hazards during initial installation are mitigated by not applying HV at any time during installation.

Standard practices will be followed during servicing or replacement of any part of the HV system to ensure the supply is locked off and all parts of the system are fully discharged. This includes working on anode wire bias supplies or the final monitoring point. A low voltage at the supply indicates a discharged condition only if the resistive path to ground is complete, which can be evaluated using voltage or current at the final monitoring point; particular care with safe grounding should be taken if a break in continuity is suspected.

11 Quality Assurance/Quality Control Plan

The Quality Assurance (QA) plan is as set of activities for ensuring quality in the process by which products are fabricated and assembled. The quality is determined by how well the final product meets the defined requirements. The QA plan aims to prevent defects proactively by prototyping, testing, and documenting the process. The QA plan is designed to mitigate the Risks and Hazards described in the sections above.

A comprehensive QA plan for the production, shipping and installation of the DUNE TPC HV components has been developed based partly on Quality Control (QC) procedures developed and implemented on ProtoDUNE-SP and on successful use of barcode tagging for the NOvA experiment detector elements. QC is a set of monitoring activities for ensuring quality in product. The activities focus on identifying restrictions on the introduction of material into the cryostat – so no permanent tags or ink or paint markings are allowed on the detector components. A system of temporary tags containing QR or barcodes will be implemented. Scanning of a tag will bring up QC instructions and checklist forms linked to that coded tag. After performing the prescribed QC evaluations and filling out the checklists, the temporary tags are removed. The tag selection requirements are that the tags be large enough and of bright enough color to be seen from both ends of the cryostat. A particularly cheap and suitable choice is to use bright yellow “cattle tags”. These are 10-12 square inch plastic tags on which can be printed a QR or barcode and can be purchased very cheaply in quantities of hundreds to thousands. In this way, TPC components will be tracked from production through installation with all checklist measurements and test results for these components finally linked to a particular location in the TPC structure.

The first step for ensuring that the detector meets requirements is the creation of an integrated model of the entire TPC to evaluate interfaces and installation methods. This integrated model will facilitate the development of installation plans and ensure that all components fit together as expected.

The following activities will be performed to assure the CPA meets all design requirements as defined in the fabrication drawings and description in the sections above:

- Fabricate four prototype CPAs to test the design and fabrication and assembly methods.
- Installation test at Ash River:
    - Test the lifting and handling of the four prototypes CPA's.
    - Load the 4 prototype CPA's with FC modules and test and evaluate their installation.
- Develop a QC plan for inspecting fabricated part of the CPA frame to make sure they meet the dimensions and tolerances on the fabrication drawings.
- Develop a QC plan for inspecting and measuring each CPA module and completed CPA plane to ensure they meet the dimensions and tolerances on the drawings.
- Perform tests to evaluate joints in the CPA frame (see Section 3) to ensure that their design and strength meets the load requirements.
- Develop a QC for receiving the resistive panels. Measure the dimensions to confirm they meet the drawings and setup a plan and acceptance criteria to ensure that panel resistance is acceptable.
- Develop a QC HV test at SURF for evaluating side to side and top to bottom resistance for each completed CPA but after final assembly and after hanging during installation.

The following activities were performed to assure the FC (Top/Bottom and EndWalls) meets all design criteria as defined in the fabrication drawings and description in the sections above:

- Fabricate prototype FCs to test the design and fabrication and assembly methods.
- Installation test at Ash River:
    - Test the lifting and handling of the prototype FCs.
    - Mount the prototype Top/Bottom FCs to the CPA modules and test and evaluate their installation.
- Develop a QC plan for inspecting fabricated part of the FC frame to make sure they meet the dimensions and tolerances on the fabrication drawings.
- Develop a QC plan for inspecting and measuring each FC module and completed FC plane to ensure they meet the dimensions and tolerances on the drawings.
- Perform tests of each joint in the FC frame (see Section 3) to ensure that their design and strength meets the load requirements.

The following activities will be performed to assure the HV system meets all design criteria as defined in the fabrication drawings and description in the sections above:

- Develop a QC plan for inspecting fabricated part of the HV system to make sure they meet the dimensions and tolerances on the fabrication drawings. Fabricated parts not included in the CPA or FC QC plans include the following:
    - HV bus cables
    - Inter-CPA "pigtails" with lug connectors
    - Connection points on CPAs, with captive screws
    - Resistor-to-frame and frame-to-FC connectors
- Develop a QC plan for each completed HV bus cable segment to inspect for curvature or damage.
- Develop a QC procedure for HV cable post-annealing cooling test.
- Measure HV bus end-to-end and bus-to-CPA continuity and resistance after HV bus installation, compare to design values.

- Measure HV bus to frame continuity and resistance after frame electrode installation, compare to design values.
- Develop a QC a HV test at SURF for evaluating side to side and top to bottom resistance for each completed CPA, including HV bus, cup, and frames, but after final assembly and after hanging during installation.
- Performed HV test at 35-ton, including the following:
    - Tested ability to hold voltage at full scale;
    - Tested expected current and stability of current at all monitoring points;
    - Tested mechanical integrity of all components after full cool-down, warm-up cycle;
    - Tested discharge mitigation system using induced HV discharge.

12 HV Design

The TPC high voltage (HV) components include the HV power supply, cables, filter circuit, feedthrough, attachment to the resistive cathode plane arrays, the HV bus providing low-resistance connections between CPA Panels and modules, connections to the field cage, and devices for monitoring steady state and transient conditions of current and voltage.

A schematic of the complete TPC HV circuit is shown in Figure 70.

The cathode plane will be biased at −180 kV to provide the required 500 V/cm drift field. It will be powered by a dedicated HV power supply through an RC filter and feedthrough. The power supply for the cathode plane must be able to provide −200 kV. The output voltage ripple must not introduce more than 10% of the equivalent thermal noise from the front-end electronics. The power supply must be programmable to shut down its output at a certain current limit. During power on and off, including output loss (for any reason), the voltage ramp rate at the feedthrough must be controllable to prevent damage to the in-vessel electronics from excess charge injection. The high-voltage feedthrough must be able to withstand −250 kV at their center conductors in a 1 atm argon gas environment when terminated in liquid argon.

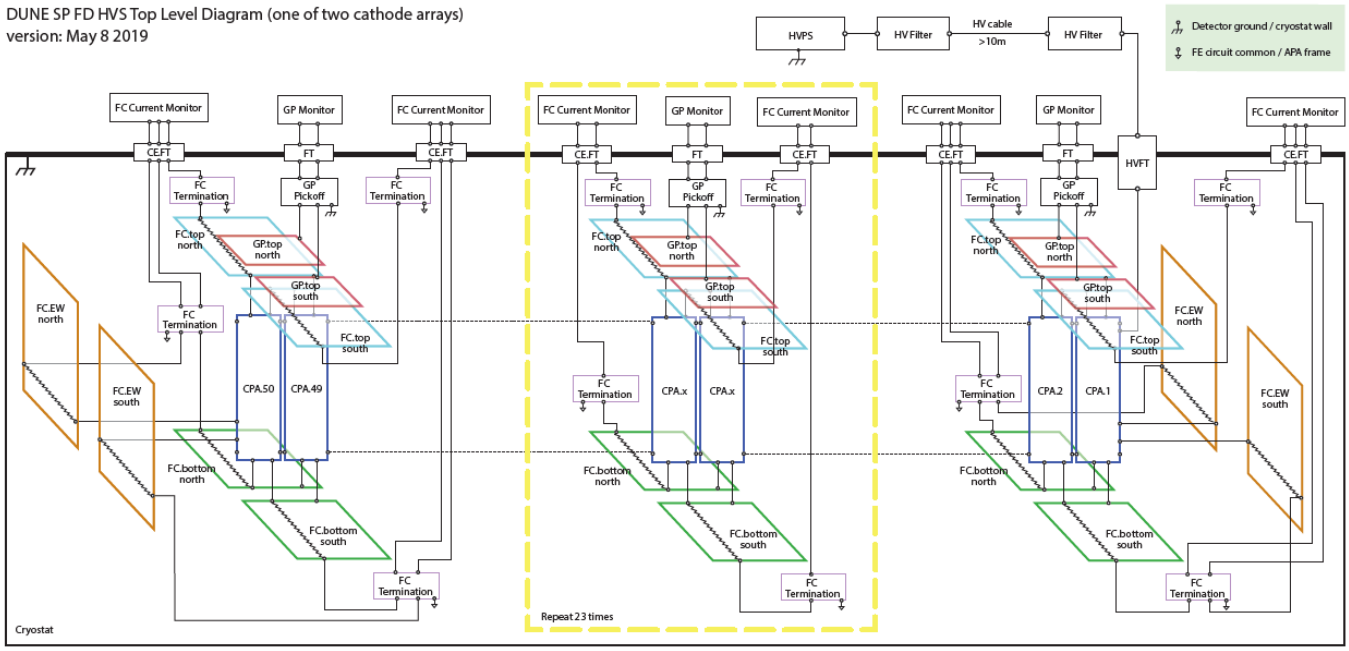

Figure 70 A schematic of the TPC high voltage circuit.

12.1 HV Requirements

		Parameter	Value	units
1	The HV system shall maintain a stable operational electric field for the TPC over the lifetime of the experiment.	HV-lifetime	20	years
2	The HV system shall automtically shut down in a manner that protects all detector components in the event of a discharge exceeding the specified percentage of the operating HV value	HV-Vtrip-level	10	%
3	The HV system shall automtically shut down in a manner that protects all detector components in the event of a discharge that results in a measurable change in the operating voltage lasting longert than the specified time.	HV-Vtrip-duration	1	s
4	The HV system shall automtically shut down in a manner that protects all detector components in the event of a rate of discharges exceeding the specified limit.	HV-Vtrip-Maxrate	2	/minute
5	The HV system shall have the capacity to automatically reset in a safe manner from any	HV-Vtrip-Autoreset		

		Parameter	Value	units
	discharge condition that does not trigger an automatic shutoff condition.			
6	The HV system shall be instrumented so that voltage changes at the HV filter output can trigger automatic shutoff or reset procedures.	HV-monitor-filter	1	
7	The HV system shall be instrumented so that voltage changes at the HV cup output can trigger automatic shutoff or reset procedures.	HV-monitor-cup		
8	The HV system shall be instrumented so that voltage changes at any cathode plane can trigger automatic shutoff or reset procedures.			
9	The HV system shall be instrumented so that voltage changes at any field cage module can trigger automatic shutoff or reset procedures.			
10	The HV system shall be instrumented with devices such as cameras that can detect HV discharge sparks created at any position within the cryostat held at HV.			
11	The HV system shall be capable of producing a constant field within the TPC fiducial volume up to the maximum value specified.	HV-Edrift-max	500	V/cm
12	The HV system shall be capable of producing a constant field within the TPC fiducial volume down to the minimum value specified.	HV-Edrift-min	250	V/cm
13	The HV system shall establish operating voltages that vary by less than the specified tolerance under DC operating conditions.	HV-Voltage-tolerance	1	%
14	The HV system shall maintain its operational voltage tolerance up to the maximum specified AC frequency.	HV-Frequency-range	100	Hz
15	The HV system shall provide stable HV at supply currents up to the specified maximum.	HV-Ioperating-max	5	nA
16	HV circuit shall have only one resistive path to ground through Field Cage in normal operation	HV-Ileakage-max	1	nA
17	HV circuit must hold drift field voltage-- overvoltage test	HV-max-voltage	150	percent
18	HV circuit must hold drift voltage-- max current at overvoltage	HV-max-ccurrent	1	nA
19	HV bus must have independent electrical continuity from HV cup to opposite edge of last CPA on both top and bottom buses	Max wire resistance	10	ohms

.

12.2 Power Supplies

In the present baseline option, the procurement of the power supply and HV cables and possibly the HV filtering scheme, will follow strictly the scheme adopted for the ProtoDUNE-SP prototype. The Heinzinger -300 kV power supply (with residual ripple less than 10^{-5}) and the related HV cable will be adopted, although used at lower voltage.

The filtering scheme and the monitoring system are essential to mitigate possible residual noise on the very sensitive front-end electronics. They will also be similar to the one under optimization on the ProtoDUNE-SP detector. In fact, despite the ripple specification of 10^{-5} from the Heinzinger power supply, the ripple amplitude is still too large for the TPC. The capacitive coupling between the cathode and the grid plane, assuming a simple parallel plate capacitor, is about 51 pF. About 20% of this coupling goes to the first induction plane (U). There are 800 U wires per APA, and each wire has half its length facing the CPA, yielding a capacitance between a U wire and the CPA of about 13 fF. To inject 100e noise into a U channel, it only needs about 1.3 mV of ripple on the cathode, while the power supply at 180 kV will generate ripple voltage of 1.8 V. Obviously for the SP TPC, further filtering of the HV output with attenuation factor of >2000 is needed.

This additional filtering of the voltage ripples is done through the intrinsic HV cable capacitance and series resistors installed inside the filter box. Established techniques and practices will be implemented to mitigate micro-discharges and minimize unwanted energy transfer in case of a HV breakdown.

12.3 Discharge Mitigation

The cathode plane of a Liquid Argon Time projection Chamber (TPC) is an equipotential plane held at a large negative voltage (about -180kV) to create the drift field for electrons created in the active volume. It presents a capacitance toward any other electrode of the TPC. The largest capacitance components are toward the membrane of the cryostat, held at ground potential or toward the ground plane near the liquid-gas interface which limits the electric field in the gas region. Depending on its location, the energy stored in the cathode plane electrodes may exceed 100J.

No definitive understanding of the cause of a breakdown of the liquid argon has so far emerged. A discharge could be caused by a local higher value of the electric field, perhaps due to a construction defect (“point effect”) and it may be triggered by a thermally generated bubble, or a microbubble caused by a cosmic ray or a radioactive decay. At any rate, a sudden and uncontrolled discharge, though not sufficient to damage the cryostat, can create considerable damage to the electrode structure or to the readout electronics. A cathode discharge (or a discharge of any electrode of the field cage) creates a voltage difference across adjacent electrodes much larger than the nominal operating voltage, which can damage the voltage divider resistors. The DUNE design uses varistors to limit the voltage difference across the divider resistor. A sudden discharge though couples capacitively to the wire planes, and it can damage the CMOS preamplifier in the front-end. A robust design for the Dune cathode plane needs to control the discharge, which can be achieved using two methods:

1. Segmenting the cathode, so the entire structure does not discharge at once, and
2. Using resistive elements to introduce long time constant to slow down the discharge.

Cathode Capacitance Model

The cathode plane sits between two wire Anode Plane Assemblies (APSs) and generates the field necessary to drift the electrons toward the anode wires.

Each Cathode Plane Assembly consists of a support structure (~2" structural tubes at the periphery, and other support structures in the middle) which hold in place conductive or resistive panels and defines an equipotential surface as depicted in Figure 71.

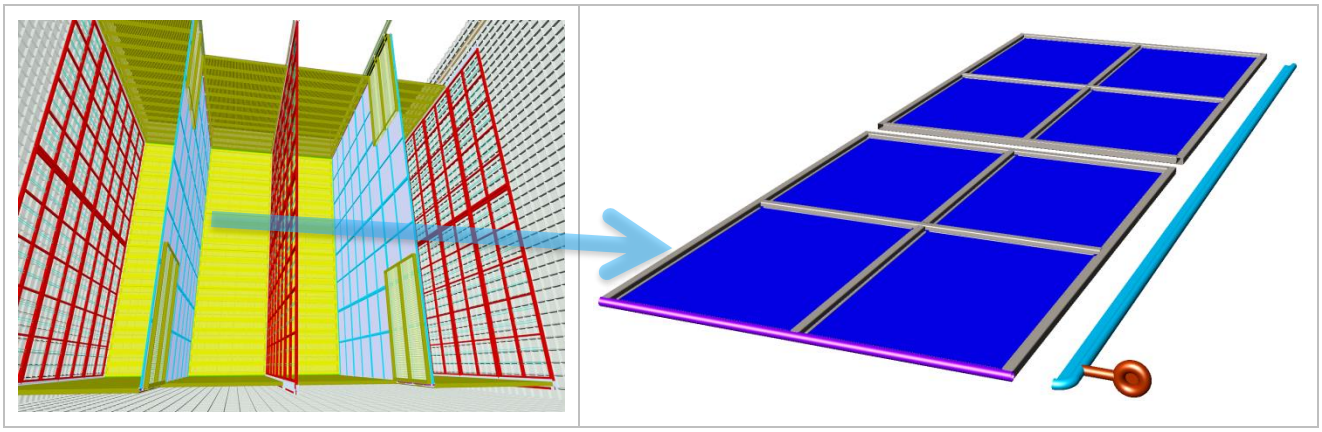

Figure 71 Cathode Plane Assembly of the Dune LAr TPC used in this early study

The cathode plane, even in the present design, where is not adjacent a cryostat wall, has a substantial capacitance the cryostat, which is held at ground potential and at the top toward the ground plane near the liquid-gas interface, which limits the electric field in the gas region. Some capacitance exists also toward the first few electrodes of the field cage. A smaller capacitance is toward the APA, which is 3.5m away. Most of the capacitance is toward the "grid" wire plane (not instrumented), but about 20% of the capacitance "leaks" trough the grid plane and couples the CPA to the first induction plane, whose wire are connected to the CMOS preamplifiers of the front-end electronics. This component of the capacitance cannot be neglected since it is the mechanism by which the cathode discharge couples to the preamplifiers and could cause a large voltage transient which could damage the CMOS front-end preamplifier.

Equivalent Electrical Model of the Cathode Plane

To study quantitatively the effects mentioned above it is necessary to devise an equivalent circuit model of the cathode plane. Borrowing from the Finite Elements method, one can imagine to subdivide the full 12m × 2.3m cathode plane into small 10cm × 10cm regions (cells). Each cell is modeled as resistors connected to adjacent cells and capacitors either to ground (modeling the cryostat capacitance) or toward other electrodes ("grid" wires, induction and collection wires) as represented in Figure 72.

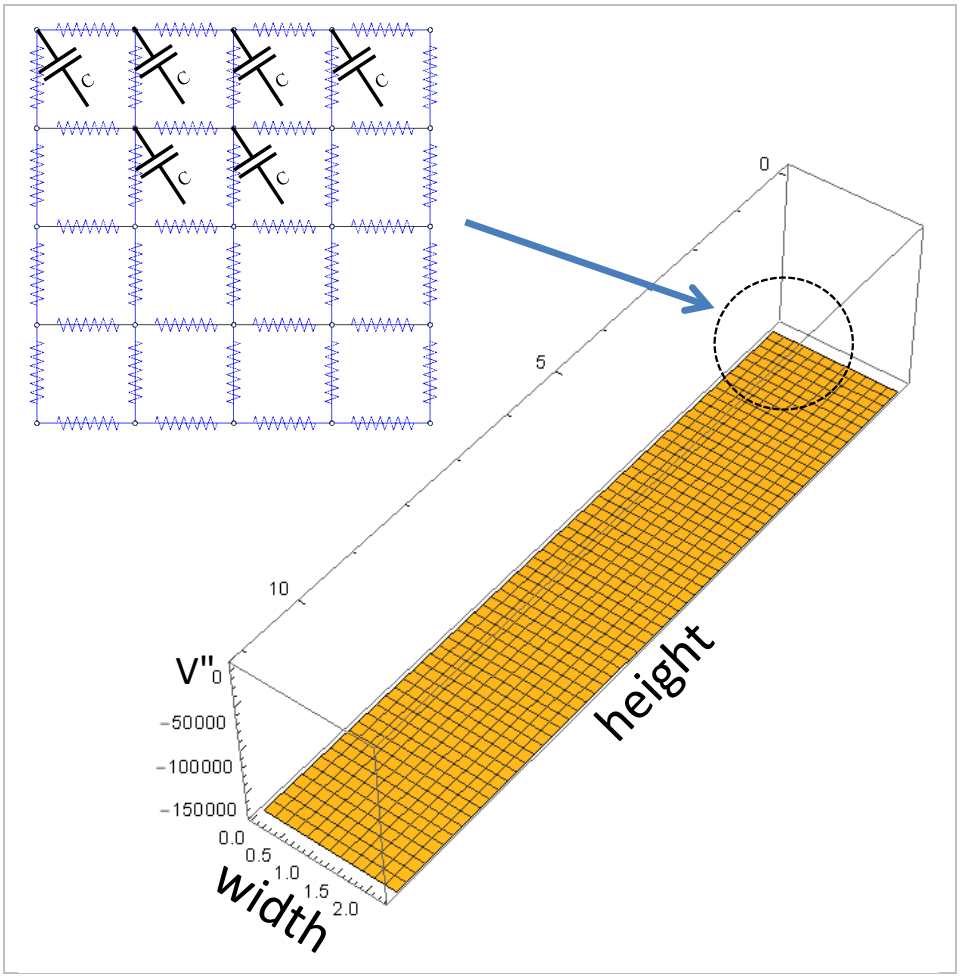

Figure 72 Equivalent circuit finite element method to model the cathode plane

Given the non uniform structure of the cathode plane, the resistor values can be different: for example lower resistor values may be used at the periphery to model the support structure, and higher resistor values in the interior to model the uniform resistivity of the panels. Also the capacitors are non uniform: in the Dune configuration most of the capacitance is at the periphery modeling the fringing field toward the cryostat walls or the screening ground plane on the top. A section of the equivalent circuit is depicted in Figure 73.

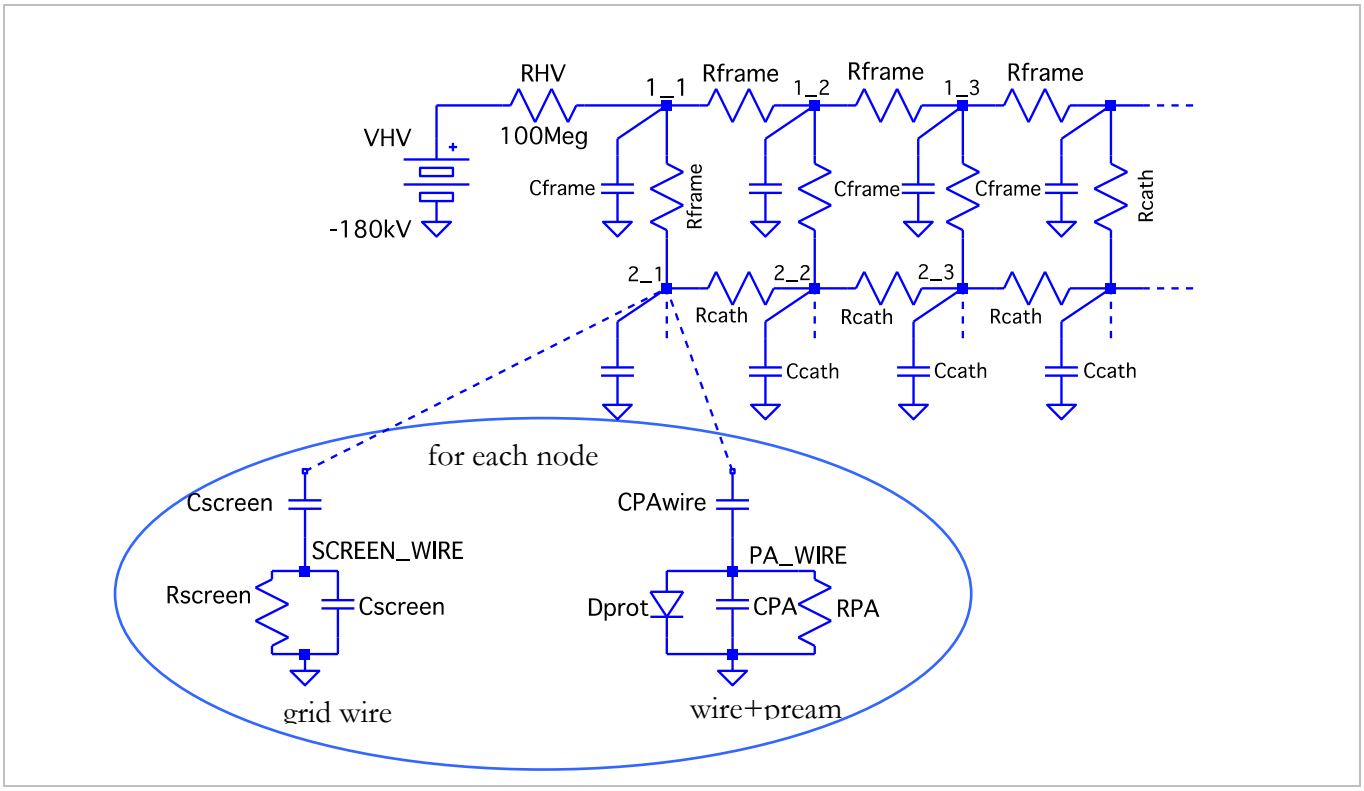

Figure 73 A section of the equivalent circuit of the cathode plane. Rframe and Cframe models the resistance and capacitance of the frame (support structure), while Rcath and Ccath model the resistance and capacitance of the cathode interior. Each node of the cat

R_{frame} represents the resistance of each 10cm section of the support frame. For example in the MicroBoone design 2.5cm stainless steel tubes, about 2.5mm thick were used, with a very low resistance of 14m□/m. Each resistor on the frame is connected to three adjacent cells (left, right and toward the interior). The R_{cath} resistors represent the resistance of each 10cm × 10cm cell of the resistive panels at the surface of the CPAs, typically with a different resistivity than the support frame. Each node in the finite element circuit model is also loaded by the capacitance toward the cryostat vessel (either Cf_{rame} or C_{cath}). Each node of the cathode finite element circuit model is also capacitively coupled to the APA by C_{screen} and C_{PAwire}. The diode and C_{PA} and R_{PA} model the preamplifier and its protection circuitry.

Calculation of the Maximum Cathode Resistivity

The minimum cathode resistivity is set by the dynamics of the discharge. It is necessary to slow down the development of a discharge in order to limit the maximum voltage transient on induction and collection wires, which are read out by CMOS preamplifiers.

Given the fact that for a deep underground detectors the rate of signal events either due to neutrinos being detected or by residual high energy cosmic rays is extremely low, the maximum resistance is set by the requirement to collect the DC current caused by ^{39}Ar radioactive decay within the volume of the TPC without causing a large voltage potential difference on the cathode.

The LAr properties used in the calculation are from the LBNE DOCDB, and are listed in Table 1.

Table 1 Properties of LAr (from LBNE DOCDB)

All values are on the liquid-vapor saturation line and at E=500 V/cm unless otherwise indicated.

Quantity	Symbol	Value	Units	Comments
Atomic number	Z	18		
Atomic weight	A	39.948(1)	g/mol	
Isotopic composition	A=36, 38, 40 stable; 39, 42 t1/2>1y			
Electron charge	q	1.602E−19	Coulomb	
Thermodynamic properties				
Normal boiling point	T_{NBP}	87.303(2)	K	
Density	ρ_{NBP}	1.396(1)	kg/L	
Response to ionizing radiation				
W-value for ionization	WI	23.6(3)	eV/pair	mip
W-value for scintillation	WS	19.5(10)	eV/photon	mip
Decay time	τ_{SCINT}	6(2),	Ns	
Charged particle transport properties				
Electron drift velocity	vD(e-)	1.60(2)	mm/μs	At TNBP
… variation wrt temperature	δLog(vD)/δT	-1.9	%/K	
… variation wrt field	δLog(vD)/δE	+0.094	%/(V/cm)	
Electron saturation drift velocity	vSAT(e-)	6.6	mm/μs	
Electron mobility at zero field	μ0	518(2)	$cm^2/V\ s$	At TNBP
Ion drift velocity	vD(Ion)	$8.0(4)x10^{-6}$	mm/μs	At TNBP
… variation wrt temperature	δLog(vD)/δT	+3.5	%/K	
… variation wrt field	δLog(vD)/δE	+0.2	%/(V/cm)	
Isotopic composition and radiological purity				
Isotope	Activity	Decay Mode	Half Life	Q-value (MeV)
39	1.01(8) Bq/kg	β^-	269□	0.565(5)

The rate of decay of ^{39}Ar per cubic meter is:

^{39}Ar decay rate = activity × ρAr × 1000 = 1.001 Bq/kg × 1.396 kg/L × 1000L/m^3 = 1.41×10^3 decay/(m^3 s)

The rate of generation of positive ion-electron pairs per unit volume is (worst case: disregarding scintillation and assuming all the energy of the electron generated in the □ decay goes into ionization):

Pair generation rate = decay rate × $E_{□}$ × $1/W_I$ = 1.41×10^3 decay/(m^3 s) × 0.565 Mev/decay × 1/23.6 1/eV =

$$33.75 \times 10^6 \text{ pairs}/(m^3\ s)$$

and the cathode current due to 39Ar generation (assumed uniform) is:

$$I_{39Ar} = q \times \text{Pair generation rate} = 1.602 \times 10^{-19}\ \text{C/ion} \times 33.75 \times 10^{6}\ \text{ion}/(\text{m}^3\ \text{s}) = 5.41\ \text{pA}/\text{m}^3$$

Since all the positive ion charge generated by 39Ar decay will be sooner or later collected, the volume to be considered is the total LAr TPC volume per CPA, not only the volume within the field cage. Therefore the 39Ar current per CPA is:

$$I_{39Ar,CPA} = I_{39Ar} \times L \times W \times H \cong 600\text{pA/CPA}$$

In the calculation it is assumed that this current is uniform over the cathode surface, and it correspond to a unit current per finite element 10cm × 10cm cell of 0.2pA/cell.

Furthermore it is possible to compute the ion space charge density in the LAr volume since the cathode positive ion current density is $\rho_p \times v_{dp}$ where $v_{dp} = 8 \times 10^{-6}$ mm/μs is the ion drift velocity.

$$\rho_p = \frac{I_{39Ar}}{v_{dp} \times W \times H} = \frac{600pA}{8.\times 10^{-3}\frac{m}{s} \times 2.5m \times 12m} = 2.5\,\frac{nC}{m^3}$$

Figure 74 shows the voltage profile (difference between the nominal value of -180kV and the actual value due to the positive ion current) on the CPA in the nominal condition, assuming the CPA high voltage is fed at the four corner via a 100MΩ resistor. A resistance of 10GΩ/m was assumed for the frame and 1GΩ/□ for the cathode interior. The maximum difference is about 0.6V or just 3.3ppm.

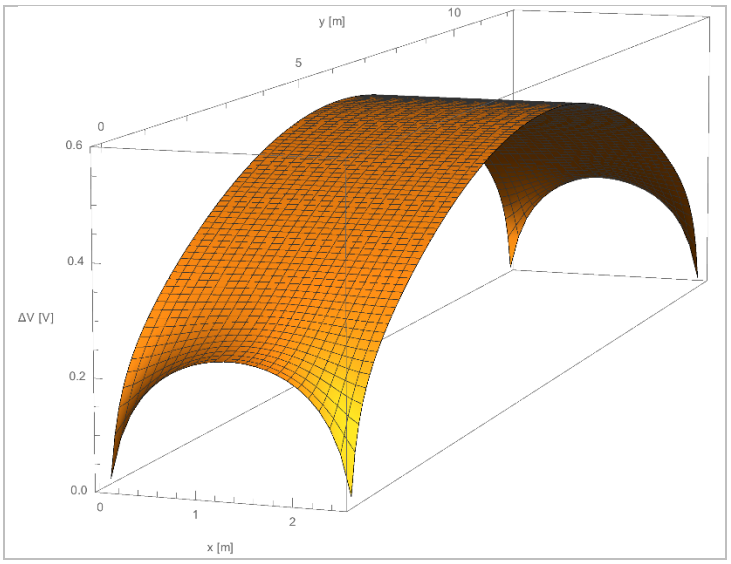

Figure 74 High voltage profile on the CPA in nominal condition

Even in the worst case (assuming failure of three feed points) in which the HV is fed on only one corner via a 100M□ resistor as depicted in Figure 75, the maximum voltage difference is still less than 3V, or just 17ppm.

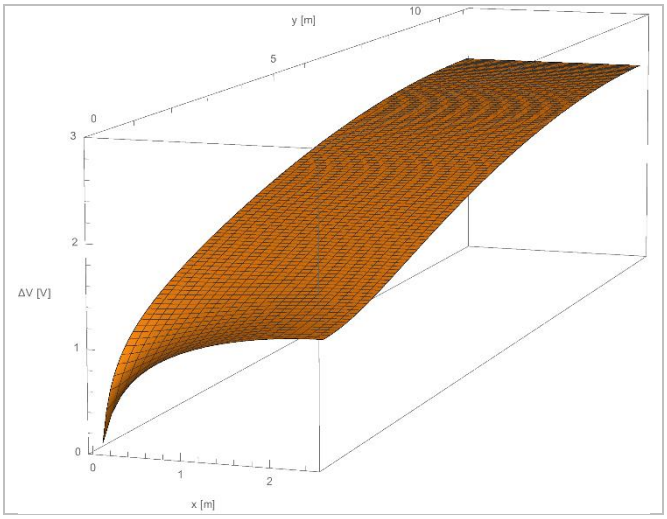

Figure 75 High voltage profile on the CPA in the worst case condition, assuming the HV is fed only on one corner.

Calculation of the Cathode Capacitances toward the Cryostat Vessel and Ground Plane

To reduce the cathode capacitance (and the electric field energy stored) the DUNE design has the cathode HV plane location in the interior of the vessel. Even with this modification, a substantial capacitance couples the CPA either to the cryostat bottom, the shielding ground plane just below the liquid surface limiting the electric field in the gas region or the vertical cryostat walls (first and last CPA).

The most precise simulation of the various components of the cathode capacitance (short of a full finite element model) can be extracted from the electric field maps, as in Figure 76.

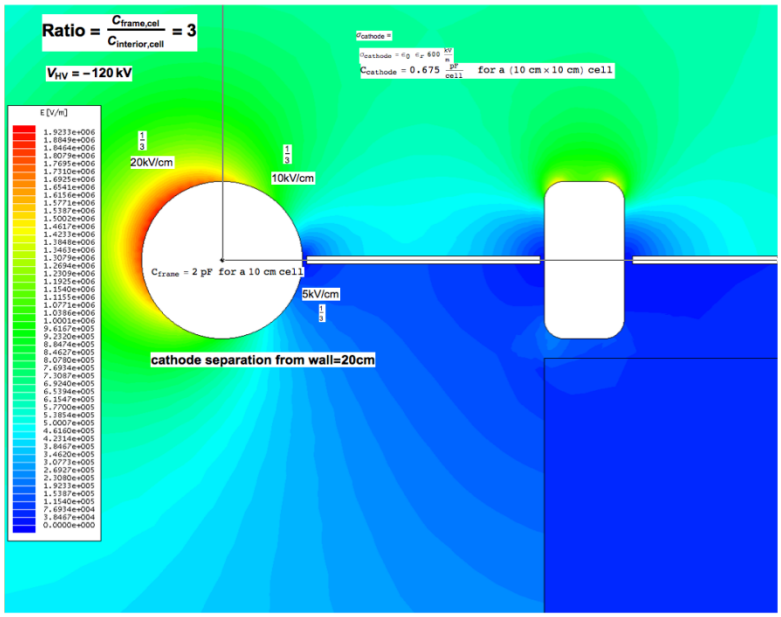

(From Bo Yu)

Figure 76 Electric field map of a CPA corner (older design: CPA near cryostat wall).

Electromagnetic theory holds that the E field is always perpendicular to a conductor. By applying Gauss law to a small cylinder perpendicular to the surface, one can compute the surface charge density as $\sigma = \varepsilon_0 \varepsilon_r E$. This quantity would bre the charge per unit area on the electrode of a capacitor whose value (per unit area) can be calculated as $C_{u.a.} = \sigma/V_{HV}$. For the case in Figure 76, V_{HV} = -120kV and the E field around the circumference of the CPA support tube can be approximated as being 1/3 at 20kV/cm (red), 1/3 at 10kV/cm (green) and 1/3 at 5kV/cm (lighter blue), which yields for the unit charge density:

$$\sigma = \varepsilon_0 \varepsilon_r (⅓ \times 2000 \text{ kV/m} + ⅓ \times 1000 \text{ kV/m} + ⅓ \times 500 \text{ kV/m}) = 2.5 \times 10^{-6} \text{ C/m}$$

which yields a capacitance of the CPA frame per unit length of :

$$C_{u.l.} = \frac{\sigma}{V_{HV}} = \frac{2.5 \times 10^{-6} \frac{C}{m}}{120 \times 10^{3} \frac{V}{m}} \cong 20\, pF/m$$

while the capacitance of the interior (assuming 20cm separation from the cryostat wall) would be C_{int} = 0.7pF/m^2.

The CPA capacitance can also be approximated by means of commonly used formulas. A few cases useful for the CPA calculation are summarized in Table 2.

Table 2 Capacitance Calculation

Configuration	Formula	Example
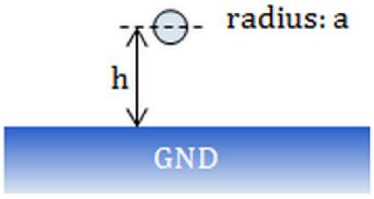	$Z_0 = \frac{60.}{\sqrt{\epsilon_r}} \text{Log}\left(\frac{h}{a} + \sqrt{-1 + \frac{h^2}{a^2}}\right)$ $C = \frac{\frac{1}{c/\sqrt{\epsilon_r}}}{Z_0}$	30 pF/m at radius a = 2.5cm h=20 cm from ground plane
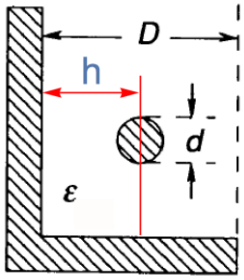	$z_0 = \frac{60.}{2.\sqrt{\epsilon_r}} \text{Log}\left(\left(\frac{D}{d}\right)^2 + \frac{D}{d}\sqrt{\left(\frac{D}{d}\right)^2 - 1}\right)$ $C = \frac{\frac{1}{c/\sqrt{\epsilon_r}}}{Z_0}$	35 pF/m at d = 5cm h=20 cm from ground plane
Parallel Plate	$C = \epsilon_r \epsilon_0 \frac{L \times W}{h}$	C = 67pF/m^2 20cm cathode separation from cryostat wall
Parallel Plate	$C = \epsilon_r \epsilon_0 \frac{L \times W}{h}$	C = 3.75pF/m^2 C cathode – wire plane Drift=3.6m

		$C_{cathode\text{-}wire} \cong 0.25pF$ (worst case: 12m wire, 5mm pitch)

For the rest of this report it assumed that C_{frame}=3pF/m (which corresponds to a cell capacitance of 300fF/10cm) and a capacitance $C_{interior}$=27pF/m^2 (which corresponds to a 10cm x 10cm cell capacitance of 270fF/100cm^2) which are roughly scaled from Figure 76 to allow for 50cm separation from cathode to cryostat wall.

Case 1: Conductive Frame, Resistive Cathode Interior

This case is the logical evolution of the TPC technology in use today. For example, MicroBoone uses a fully conductive cathode: to increase the time constant of a potential discharge the first line of attack is to increase the resistivity of the cathode surface, but preserving the frame structural support. In MicroBoone the cathode frame consists of 1" diameter steel tubes, 0.1" thick, which exhibit a resistance at LAr temperature of about 14MOhm/m. The resistance of the cathode is assumed 3.5MOhm/sq.

Figure 77 shows an animation of the cathode discharge process. The discharge starts at t=20ns, and in just one nanosecond the cathode frame is fully discharged (about 20% of the energy). Then the discharge proceeds toward the interior, and the potential distribution assumes a bathtub profile. By t=10ms the cathode is fully discharged. The discharge progresses so quickly because in effect the frame "shorts" the resistive interior and the path of least resistance is from any point of the cathode to the nearest point on the frame.

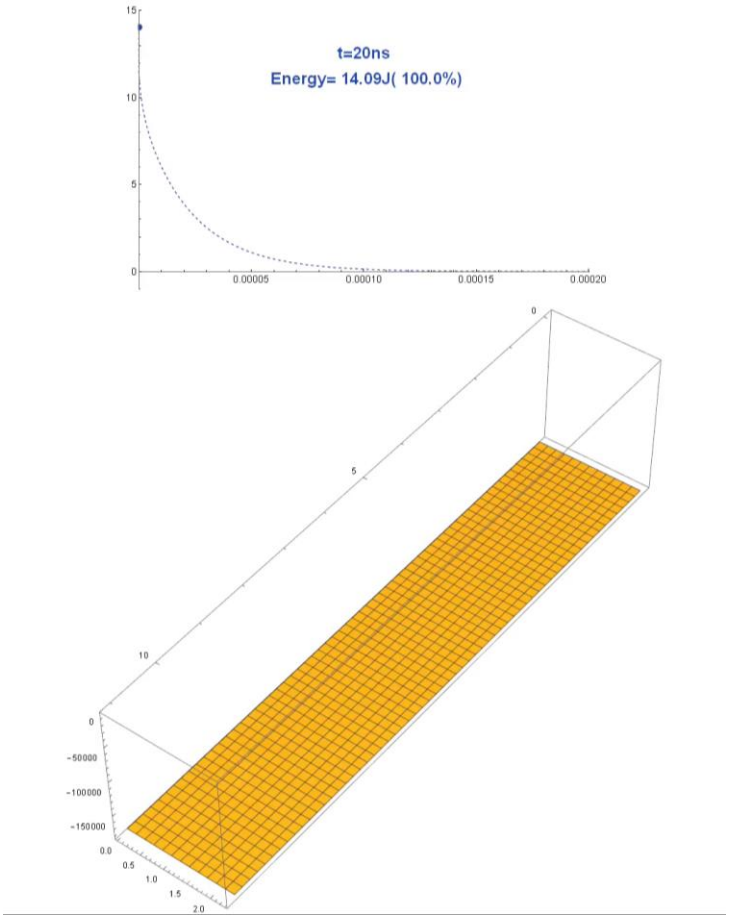

Figure 77 Cathode Discharge animation in the case of a conductive frame and resistive cathode interior. Parameters are: Rframe=14MΩ/m Rcathode=3.5MΩ/sq Cframe=3pF/m Ccathode=27pF/m2. The discharge starts in the middle of the shirt side at t=20ns. Notice that in j

Figure 78 shows the transient induced on the “grid” wire plane (uninstrumented). The fast discharge of the frame causes a 100V voltage spike on the 12m long wires.

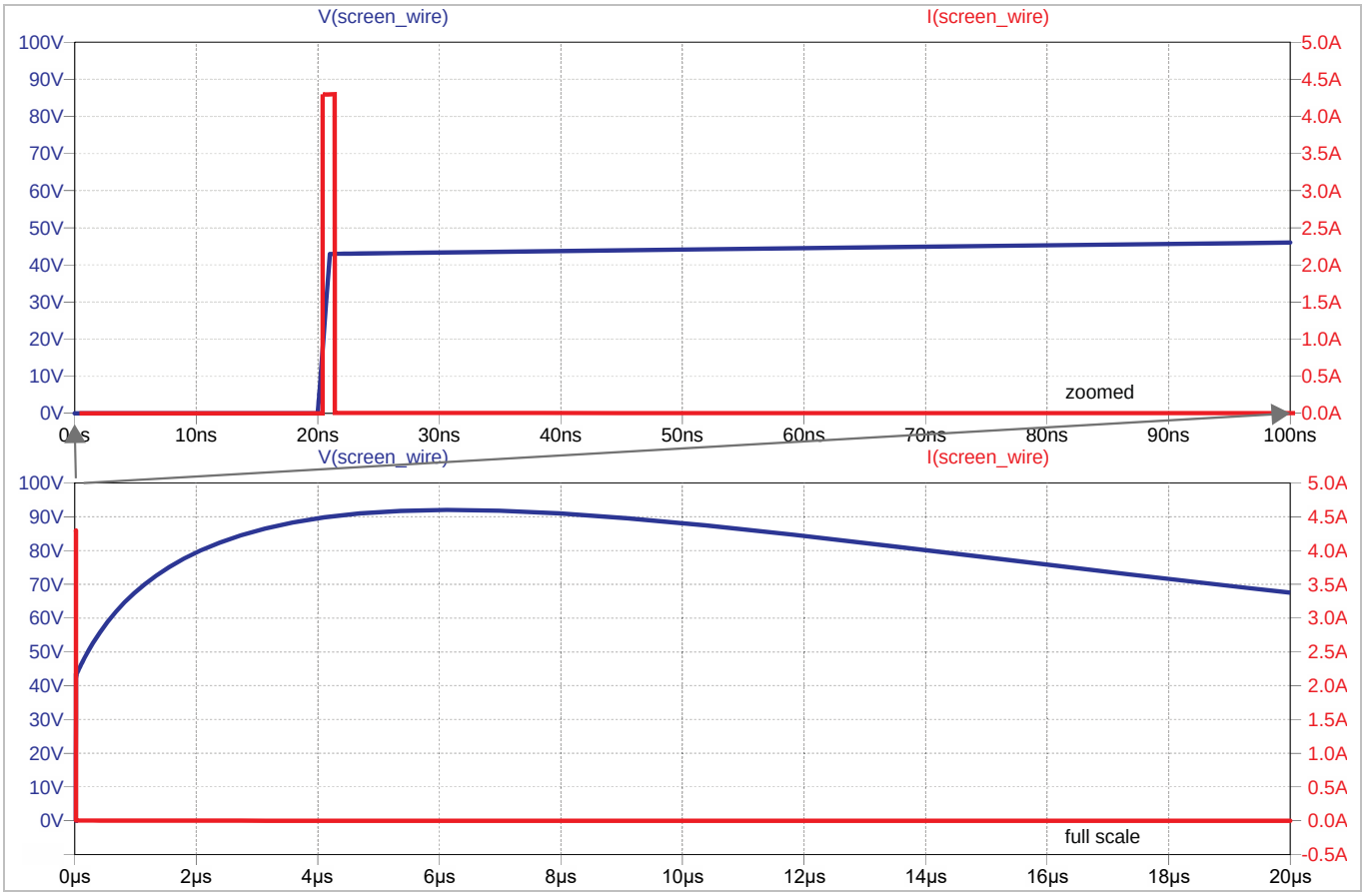

Figure 78 Voltage transient induced by the cathode discharge on the uninstrumented "grid" wire plane. Worst case: wire length is 12m. The fast frame discharge causes a maximum voltage of 100V.

Figure 79 shows the voltage transient on 12m long instrumented wire planes, connected to the front-end CMOS current sensitive preamplifier.

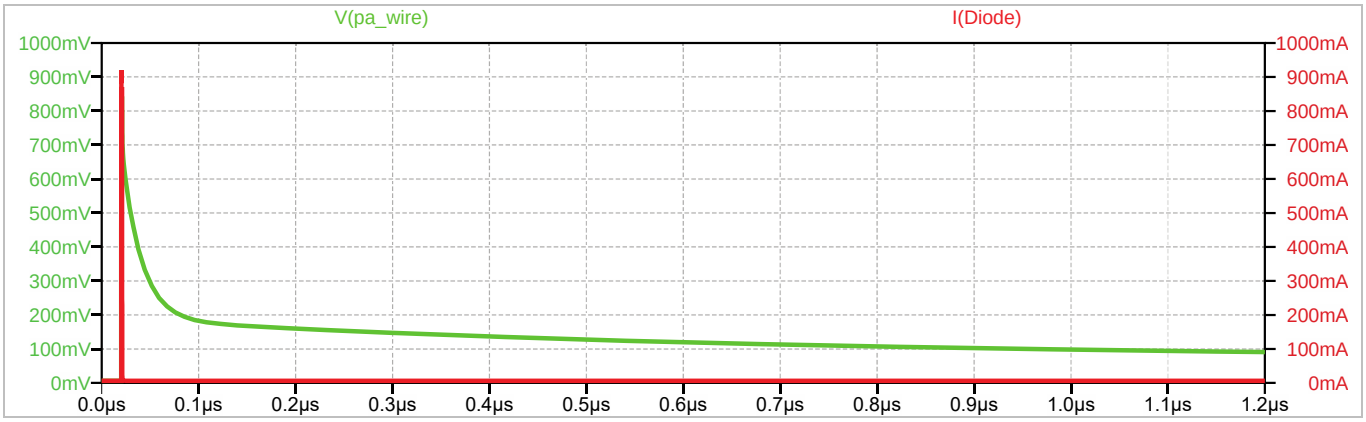

Figure 79 Voltage transient on the first induction wire plane. Worst case: 12m long wire. The voltage transient is limited to 900mV by the protection diode, which goes deeply into conduction, carrying a maximum current of almost one amp.

The maximum voltage excursion at the preamplifier input is limited by the protection diode to 900mV. The protection diode itself goes deeply into conduction, carrying a maximum current of 900mA. Such a large current requires an external diode since it could damage a monolithically integrated protection.

Low Resistance HV Bus and Resistive Cathode Frame

Using a resistive support frame would farther slowdown the cathode discharge and eliminate the transient due to the conductive frame discharge. This could be achieved in several different ways. For example, a mechanically strong resistive structural material could be used instead of stainless steel support frame. Or the conductive frame could be divided into shorter segments, interconnected by resistive elements. In the event of a discharge, only a short section would discharge with a short time constant, while the resistive connectors would introduce longer time constants to the discharge of the rest of the frame.

While technically feasible, these solutions introduce another problem. The Dune design is modular: each CPA module also feeds the resistive voltage divider of the field cage, both at the top and at the bottom. These resistive dividers need a current of a few microamperes and this loading would cause a voltage drop along the (resistive) top and bottom cathode frame.

To achieve both a low resistance path to feed the high voltage to the resistive dividers of the field cage and provide a resistive frame one need to use a coaxial structure for the top and bottom structural frame as depicted in Figure 80.

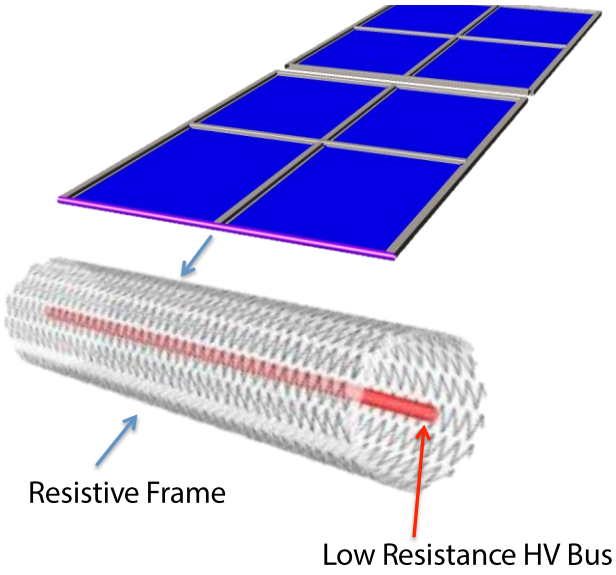

Figure 80 Coaxial frame concept. The structural members at the top and bottom are made with a coaxial geometry. The inner low resistance HV bus provides a conductive path to feed the field cage voltage dividers without any voltage drop, but are safely housed inside.

The HV bus would make contact with the resistive frame and the voltage divider chain for example at the left and right corner of each CPA. The resistive outer frame and the low resistance HV bus would be equipotential, so there would be no energy stored in the large capacitance of the coaxial structure. In the event of a discharge, there would be a large resistance both limiting the current and introducing a long time constant. It is a fact however that at the location of the discharge there would be an instantaneous potential difference between the resistive outer frame and the HV bus the interior volume need to be filled with a high dielectric strength material, for example the high density polyethylene used in the HV feedthroughs.

Fig. 81 shows an animation of the cathode discharge again assuming a zero resistance short in the middle of the short side assuming a resistive frame (10GOhm/m) and resistive cathode interior (1GOhm/m^2).

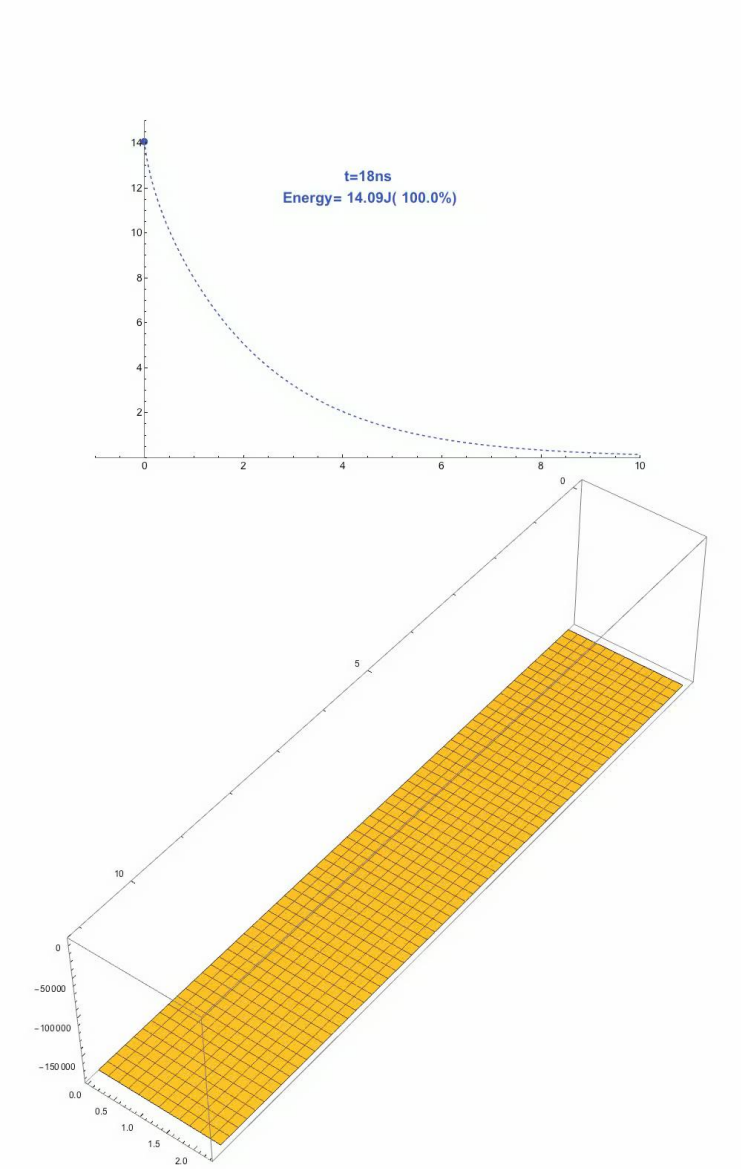

Figure 81 Cathode Discharge animation in the case of a resistive frame (10GΩ/m) and resistive cathode interior (1GΩ/m^2).

The first thing to notice in Figure 81 is the scale of the time axis: the discharge can be slowed down so much that it completes in several seconds, drastically limiting the current, the induced voltage and the probability of any mishap. Also the resistive frame (and interior) makes the discharge "smooth", eliminating the initial time constant.

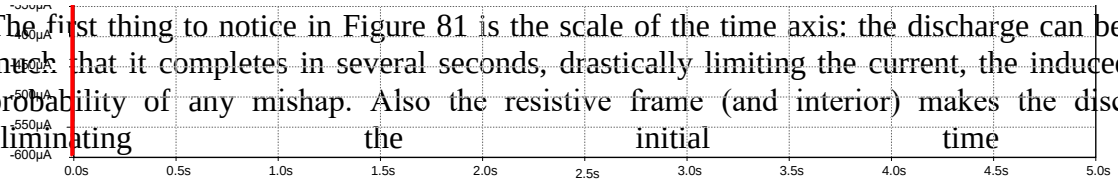

Figure 82 shows the discharge current, assuming a zero ohm short. Figure 83 shows the induced transient on a wire of the "grid" wire plane.

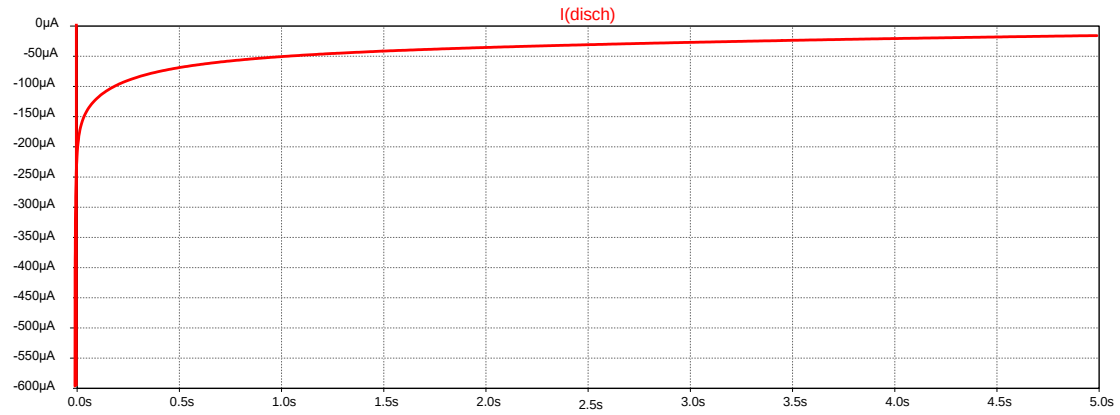

Figure 82 Discharge current. The maximum current is limited to well less than a milliampere by the resistive cathode structure.

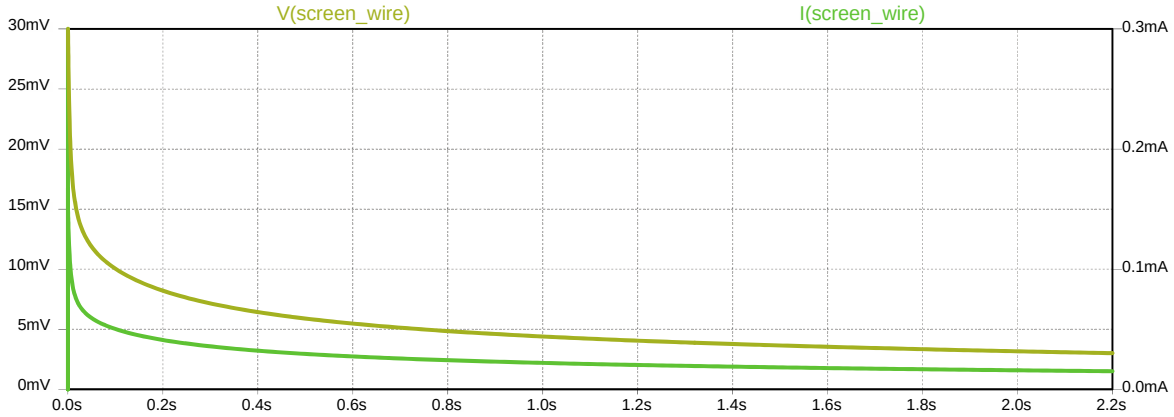

Figure 83 Transient induced by the discharge on a wire in the "grid" wire plane. Worst case: 12m wire. With a 10GΩ/m resistive frame and a 1GΩ/□ interior, the maximum voltage and current are greatly reduced, and the rate of the discharged is much lower.

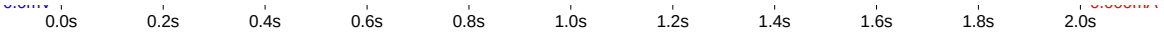

Figure 84 shows the discharge transient on the first induction plane. The transient has been so effectively reduced by the high resistance frame/interior that the protection diode does not turn on. The maximum current (≈50 uA) is enough to saturate the preamplifier (which will also provide a convenient mean to detect a discharge), but not to cause any damage.

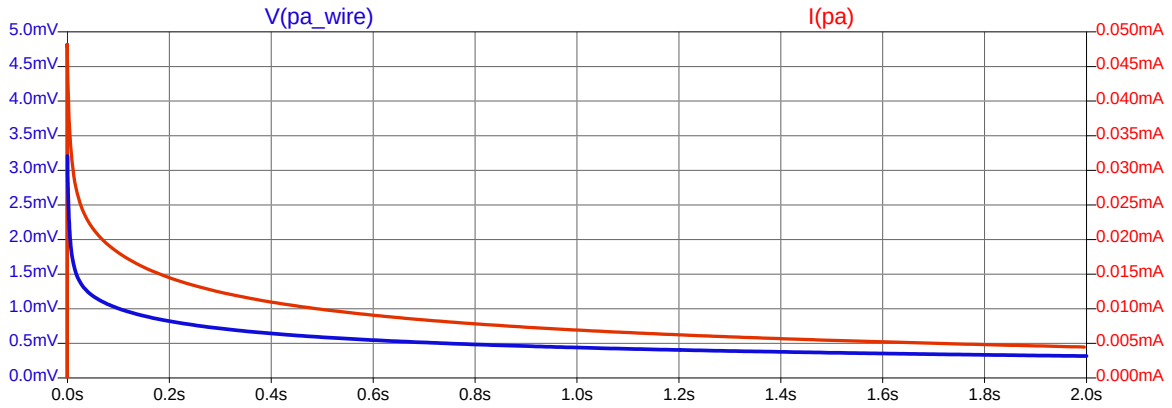

Figure 84 Discharge transient on a wire in the first induction plane. Worst case: 12m long wire. The transient has been so effectively reduced by the high resistance frame/interior that the protection diode does not turn on. The maximum current (≈50μA) is enough.

To study the time evolution of a discharge in a LAr TPC, an electrical equivalent model of the cathode and its coupling to the cryostat and the wire planes has been developed. It is based on a Finite Element equivalent RC circuit model. Each small section of the frame or of the cathode interior is modeled by its resistance to adjacent elements and its capacitance to the cryostat membrane as well as any other constant potential electrode (e.g. the ground plane at the liquid-gas interface). The interaction with the wire plane is modeled as a small capacitance from each node of the finite element cathode model to a wire of the "grid" wire plane or the induction/collection planes. A screening factor of 80% of the "grid" plane has been assumed, so that only 20% of the cathode-APA capacitance couples to the first induction plane. The use of a high resistance cathode plane with a conductive structural frame is not sufficient to control the discharge. Most of the cathode capacitance (and stored energy) is at the periphery, and 10-20% of the discharge energy is released in a very short transient. Besides the cathode also feeds the field cage voltage dividers: all the CPA must be electrically connected with low impedance, and a discharge in any CPA would quickly propagate to all of them. To effectively mitigate the cathode discharge it is necessary to also use a high resistance structural frame. To also feed the voltage dividers it is necessary to employ a coaxial frame on top and bottom, with a low resistance HV bus at the center which connects to both the resistive exterior and to the field cage resistive dividers. Since the frame resistive exterior and inner conductor are equipotential, no extra energy is stored in the system. A discharge will instantaneously ground a small region of the frame and to prevent an second inner discharge to the HV bus, the space needs to be filled with a high dielectric strength material (e.g. high density polyethylene, as used in the HV feedthroughs). In the event of a discharge, many long time constants are introduced, which both stretches the discharge over a long time (several seconds if resistances of the order of gigahoms are used) and limits the maximum voltage transient on the preamplifiers.

12.4 HV Bus

The purpose of the HV Bus is to connect the high voltage to each cathode panel at designated points without significant voltage drop between panels. As described in the section above, the cathode planes will be resistive, with electrical connections at distinct points. Connections between modules within a CPA Panel are made by tabs through the 5 horizontal edge frames. Across the CPA Panels, there is no direct electrical connection between the resistive panels. The HV Bus running along the top and bottom of the CPA Panels

provides this interconnection. The HV Bus conductor must be surrounded by a high dielectric strength material everywhere except at designated connection points in order to prevent direct arcing between a resistive panel and the HV Bus in the event of one of them having a discharge to ground.

The chosen design for the HV Bus is a loop of a high voltage cable placed along the edges of the entire CPA plane, hidden between the field shaping strips on the CPA frame and the main cathode resistive sheet. The chosen cable is Dielectric Sciences 2134 (Figure 85); we require only the central conductor and insulator, so the jacket and outer braid will be removed before installation. The cable within each CPA will be held in place by half-clips sized to allow the cable to contract and expand. The complete frame and field shaping strip geometry may be seen in figures in section 5.2, a 3d rendering can be seen in Figure 86 below, a sketch of electrical connections is in Figure 87, and a cross-section showing calculated potentials is in Figure 88.

Experience with this cable has been that it generally survives repeated cryogenic temperatures and thermal shocks, including rapid immersion in liquid nitrogen [H. Jostlein, private communication]. However, cracking has also been observed in the polyethylene insulator in cases where it was stressed or damaged. In order to avoid stresses in the cable, each segment of stripped DS2134 will be conditioned before installation by holding it straight in a metal cylinder and re-annealing the polyethilene insulator at 85 degrees C, as recommended by Dielectric Sciences [D.Leary, Dielectric Sciences, private communication]. Care will be taken not to bend or damage the polyethylene during installation.

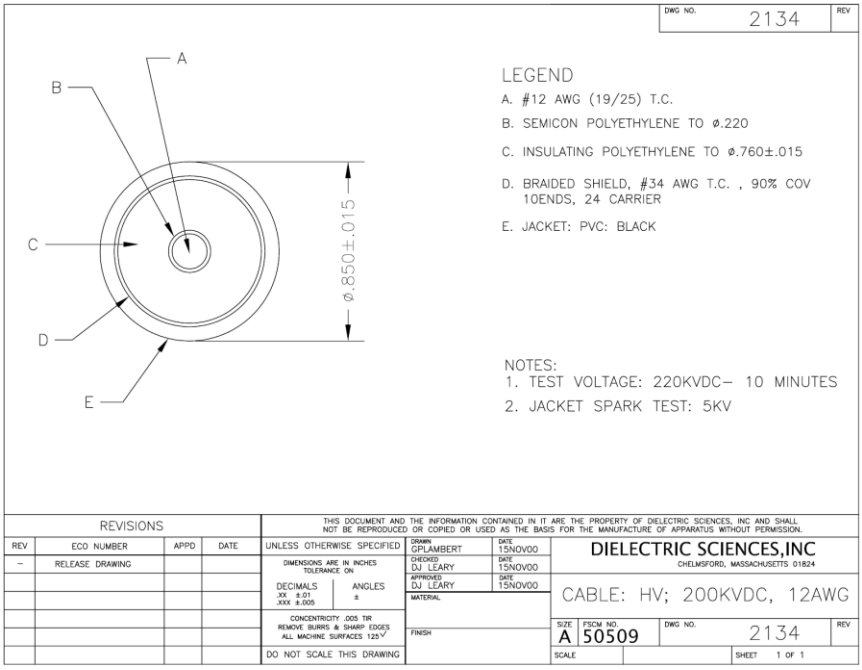

Figure 85 DS 2134 cable drawing, (c) Dielectric Sciences

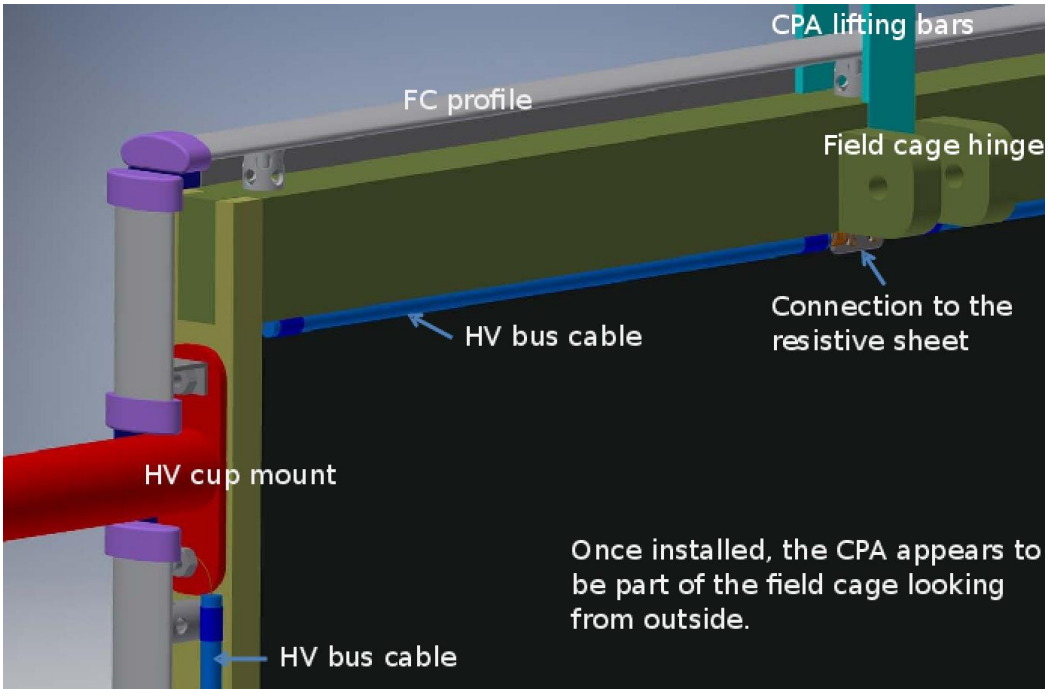

Figure 86 A perspective view of CPA frame showing the location of the HV bus cable and attachments to the HV cup and resistive cathode, with CPA frame electrodes omitted to make HV bus visible.

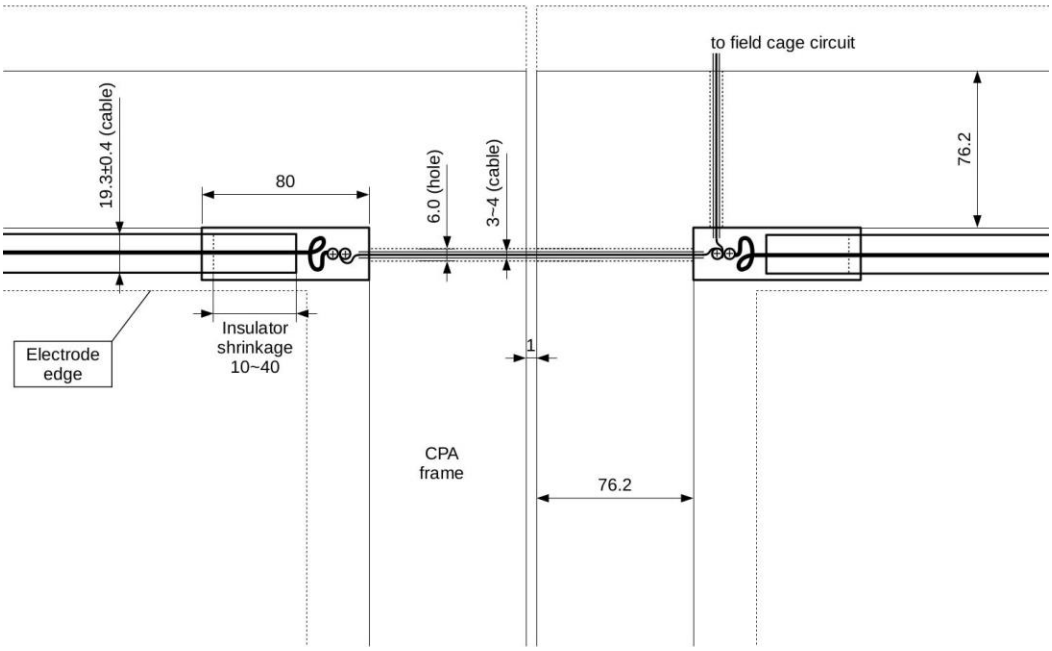

Figure 87 A sketch showing interconnection between two CPAs.

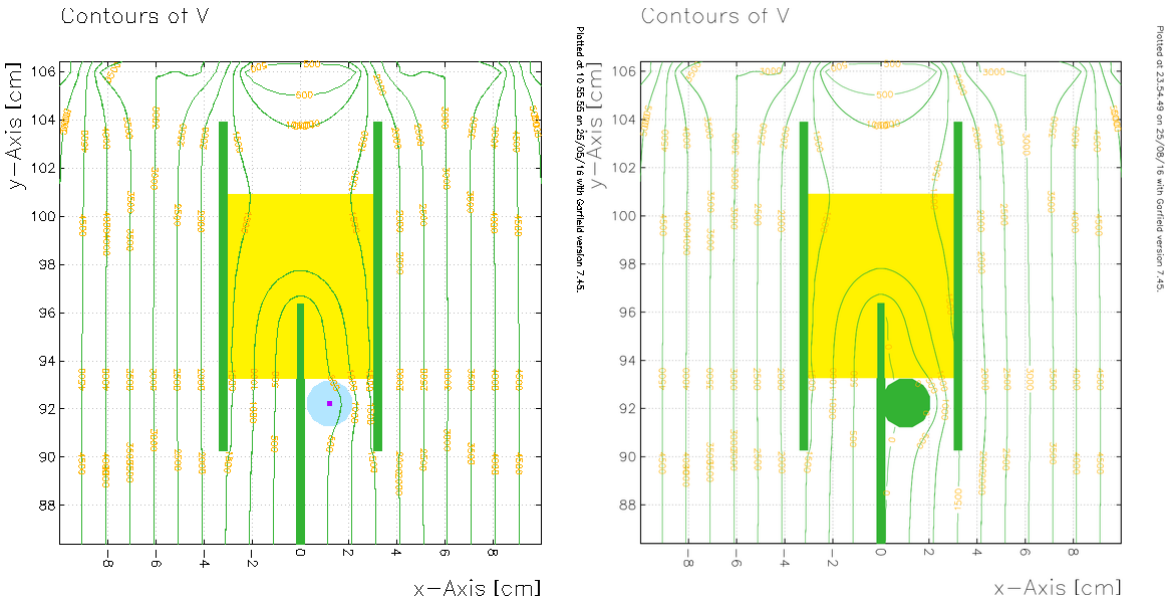

Figure 88 Equipotential lines around the HV bus and CPA frame at center (left plot) and around cable clip (right plot).

12.5 HV Feedthrough

The present design of the 300-kV feed-through, successfully adopted in ProtoDUNE SP and DP is based on the very successful construction technique adopted for the ICARUS HV feed-through, which was operated at 75 kV without interruption for more than three years without any failure. The ProtoDUNE SP feed-through was also successfully operated for several month at 180 kV without any weakness. The similar one constructed for ProtoDUNE DP was successfully tested for several hours at -300 kV in a stand alone LAr cryostat.

The design is based on a coaxial geometry, with an inner conductor (HV) and an outer conductor (ground) insulated by UHMW PE; the version of ProtoDUNE SP detector is shown in Figure 89. The outer conductor, made of a stainless-steel tube, surrounds the insulator, extending inside the cryostat up to the LAr level. In this geometry the electric field is confined in regions occupied by high-dielectric-strength media (UHMW PE and LAr). The inner conductor is made of a thin-walled stainless steel tube to minimize the heat input and to avoid the creation of argon gas bubbles around the HV lower end. The ultra-high vacuum tightness of the feed-through is ensured by the construction procedure based on the cryo/thermo-fitting technology developed in-house and based on many years of experience.

A contact, welded at the upper end for the connection to the HV cable and a round-shaped spring-loaded contact for the connection to the cathode, screwed at the lower end, completes the inner electrode. The warm end of the feed-though is mounted on a UHV CF250 Stainless steel flange (Figure 90-left), which includes, in addition to HV cable receptacle, also a HV chimney purging valve and a HV cable N2-Gas pressurizing/flushing valve to eliminate humidity in the surrounding of the HV cable insertion and contact. At the cold side, the spring loaded contact pushes on the inner surface of the donut shaped receptacle, connected to the CPA, (Figure 90-center) and can slide across to ensure electrical contact to compensate the changes in alignment due to the thermal contractions when the detector is cooled down at LAr temperature. Figure 90-right shows the electric field calculation in the vicinity of the HV feed-through (for

HV=-300 kV) indicating that the E-field will not exceed 30 kV/cm at the nominal HV value of ProtoDUNE SP (HV= -180kV).

The insertion of the HV feed-through in the ProtoDUNE SP cryostat is shown in Figure 91; similar concet is foreseen for DUNE. The width of the donut flat bottom is calculated to thake into account possible horizontal shifts during detector cool down. Smaller vertical displacements are compensated by the spring-loaded tip.

Special care is taken in the feed-through assembly to ensure complete filling with the PE dielectric of the space between the inner and outer conductors, and to guarantee leak-tightness at ultra-high-vacuum level.

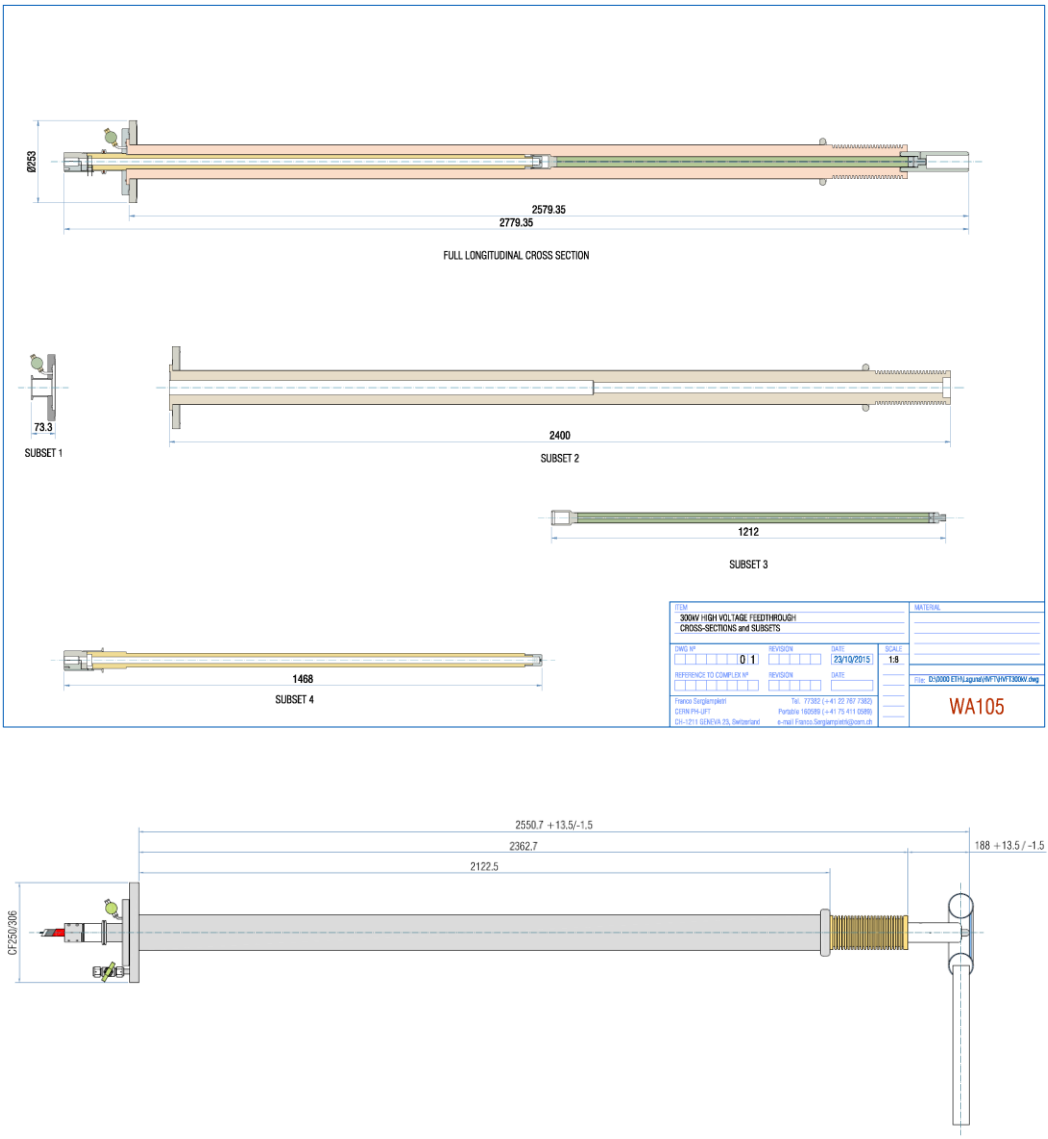

Figure 89 Top: preliminary design of the DP HV feed-through. Bottom: version with size adapted for ProtoDUNE SP and with spring loaded tip.

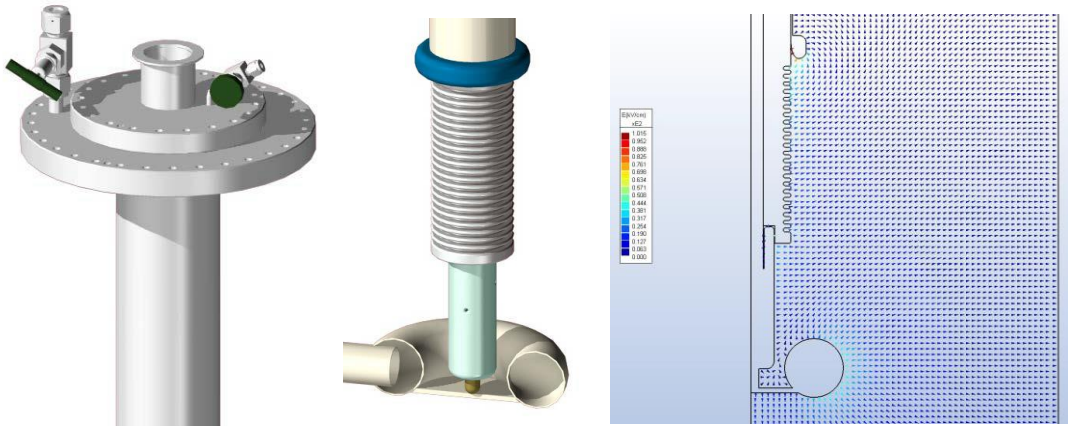

Figure 90 Details of the feed-through for ProtoDUNE. Left:. Top flange including purging valve and GN2 flushing valve. Center: spring loaded tip pushing on donut receptacle. Right: Electric field calculation in the vicinity of the HV feed-through (for HV=-300 kV) indicating that the E-field will not exceed 30 kV/cm at the nominal HV value of ProtoDUNE SP (HV= -180kV).

Figure 91 The insertion of the HV feed-through in the ProtoDUNE SP cryostat.

12.6 HV Cup and Connection to Frame

The feedthrough connects to a rounded, donut-shaped "cup" mounted on one side of the CPA at one end of the cathode plane, as shown in Figure 91. The cup is connected to the mounting point on the frame via a cylindrical tube in order to position the receptacle directly under the feedthrough flange. The electrical

connection to the top HV bus is made using the same pass-through hole and cable used for interconnection of adjacent CPA Panels. A section of HV cable runs along the inside of the frame down to the bottom of the end CPA, where it is secured at another mounting bracket and makes electrical connection to the lower HV bus.

12.7 HV Filter and Coronal Monitor

Despite the ripple specification of 10^{-5} from the Heinzinger power supply, the ripple amplitude is still too large for the TPC. In order to keep induced ripple in the SP TPC induction planes under 10% of equivalent thermal noise, further filtering of the HV output with attenuation factor greater than 2000 is needed.

Additional filtering of the voltage ripples is done through the intrinsic HV cable capacitance and series resistors installed inline with the cable inside a grounded enclosure. Figure 92 shows a design of a filter resistor cartridge used in ProtoDUNE. A toroidal transformer around the central conductor of the cable will detect fluctuations in the current. Figure 93 shows the equivalent circuit, and Figure 94 shows an exploded view of where the toroid is installed around inside the coaxial ground while maintaining safe insulation and continuous ground coverage.

Established techniques and practices will be implemented to eliminate micro-discharges and minimize unwanted energy transfer in case of a HV breakdown.

The design implemented in ProtoDUNE-SP make use of transformer oil to fill the gap between the insulators and the resistor in the filtered cartridge. This proved to be a weak point for long term operation given the small leak of the oil into the cable itself that required constant refill and eventually led to a degradation of the resistor properties. R&D with the polymer laboratory at CERN led to an optimized design where the oil is replaced by a solidified high rigidity polymer inserted under vacuum to guarantee no residual air gaps in the cartridge. Present operation of a prototype in ProtoDUNE demonstrates that the design is appropriate to avoid discharges and preserve the resistor properties.

Figure 92 filter cartridge design used for ProtoDUNE SP.

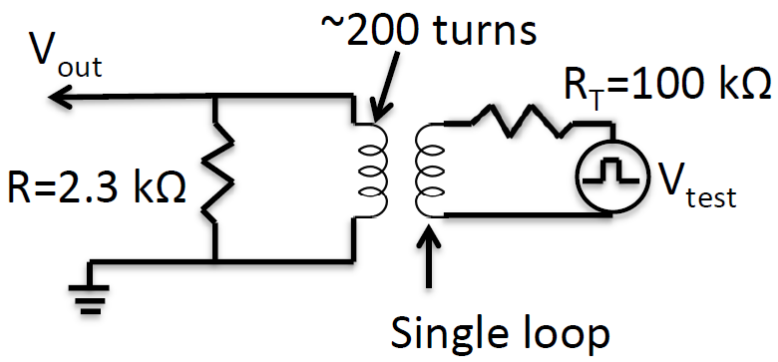

Figure 93 filter cartridge design used for ProtoDUNE SP.

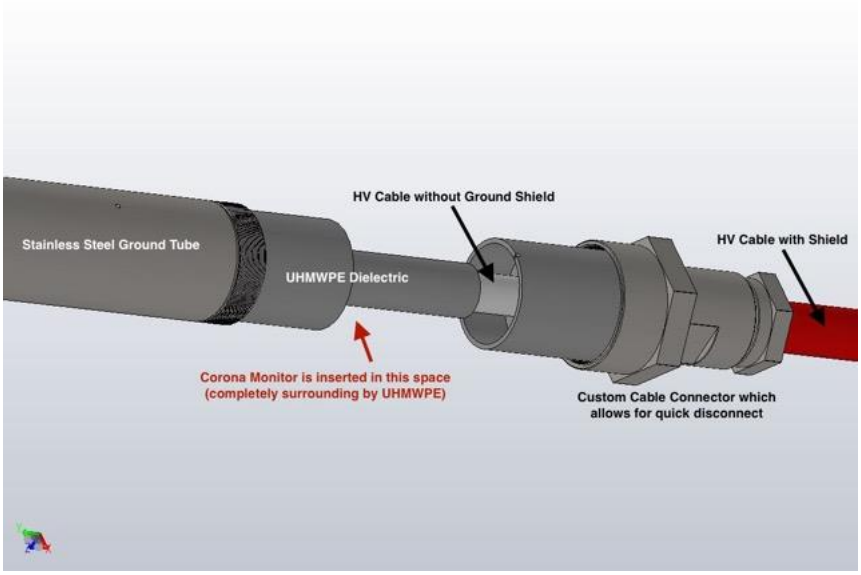

Figure 94 Exploded view of corona monitor plug design used for ProtoDUNE SP.

12.8 Resistor Divider Boards

The Resistor Divider Board consists of eight resistive stages in series. Each stage consists of two 5GΩ resistors in parallel yielding a parallel resistance of 2.5GΩ per stage. Each stage is protected against high voltage discharge transients by transient/surge absorbers (varistors). To achieve the desired clamping voltage three varistors are wired in series and placed in parallel with the associated resistors. A schematic of the Resistor Divider Board is shown in Figure 95.

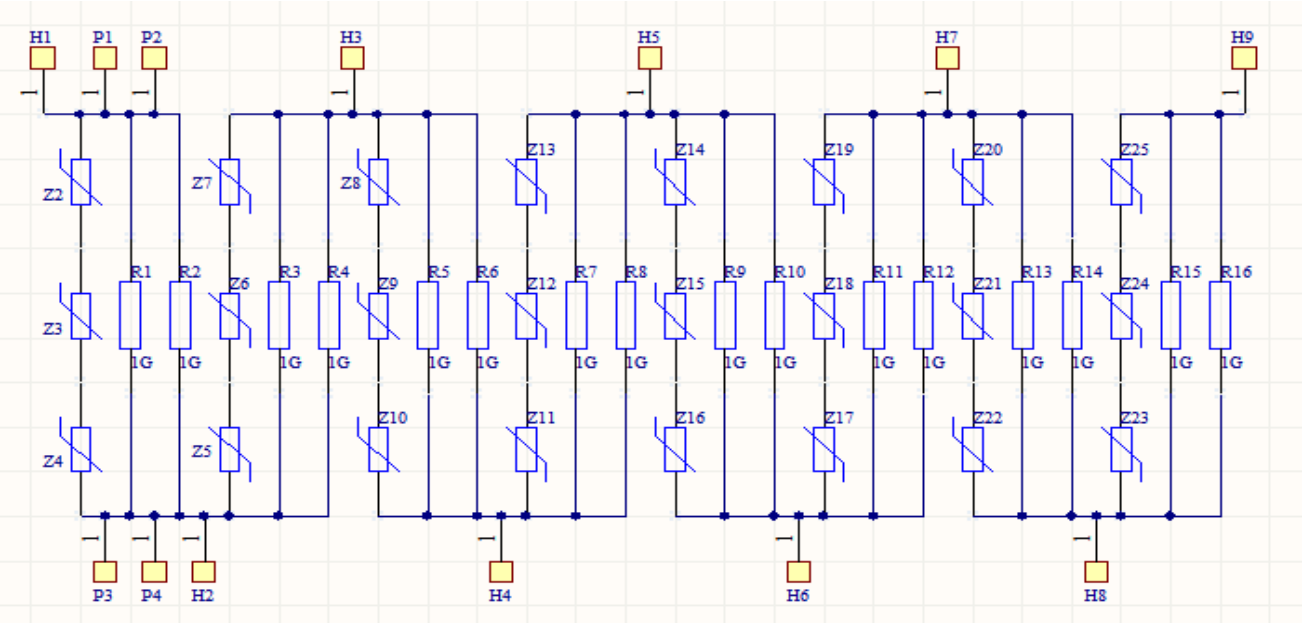

Figure 95 Schematic diagram of Resistor Divider Board.

Part numbers of components:

Resistors DigiKey p/n SM104FE-5000M-ND
Manufacturer Slim-Mox SM104035007FE
Transient/Surge Absorber DigiKey p/n P7227-ND
Manufacturer Panasonic ERZ-V14D182

The Resistor Divider printed circuit board is a two layer board fabricated from a 0.062 inch thick FR-4 laminate with 1 ounce weight copper cladding on top and bottom. Solder mask layers are present for top and bottom layers with openings in the mask for component pads and contact with the field shaping profiles. The FR-4 laminate is fire retardant and can be provided halogen free on request but at extra cost. The PCB's are manufactured by Advanced Circuits.

The printed circuit board is 520 mm wide and 80 mm high. Mounting holes are spaced at 60 mm intervals for connection to the field shaping profiles. The 60 mm spaced holes are designated as H1 through H9 in the schematic diagram. At one end of the board extra pads are provided for mounting additional resistors if different resistance values are needed at the cathode or anode end of the divider chain. The mounting hole accommodates an M4 size brass screw and a stainless steel nut. A curved washer and/or suitable coatings may be used to ensure electrical and mechanical integrity of this connection. The hole in the PCB is slightly oversized to accommodate slight dimensional variations. Electrical contact to the profile is made via the PCB bottom copper layer contacting the profile. The bottom conductive layer of the PCB is shown in Figure 96. Wire connections to the ends of the divider chain can be made via crimped ring terminals.

The resistors and transient/surge absorbers are tested prior to board assembly. A test stand has been built to evaluate the components at room temperature and at 77° K. All components will be serialized and tested.

V/I curves will be stored in a database. A sampling of components will be subjected to destructive testing by thermal cycling.

Bending jigs havw been developed for forming the resistor leads. The jigs will ensure consistency and reduce the likelihood of damage to the components. Components will be hand-soldered with leads trimmed to remove sharp points. Assembled boards will be visually examined for defects and resistance measurements made to verify electrical integrity.

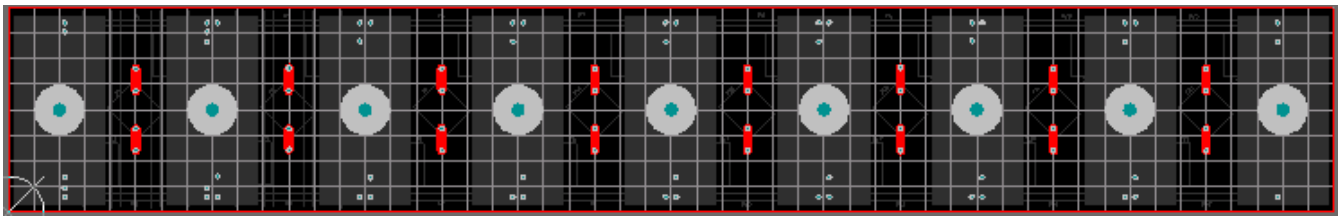

(a)

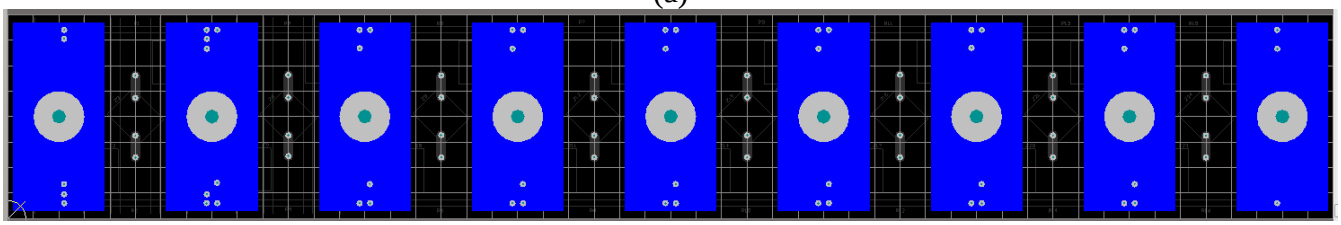

(b)

Figure 96 PCB Top Copper Layer(a) and Bottom Copper Layer(b) (X-ray view, i.e., looking through the board).

12.9 HV Frame Bias

The resistive strips on the CPA frame are located halfway between the cathode and the first FC element, and needs to be biased to a voltage halfway between their voltages. A resistor board containing two 5GΩ resistors in parallel will connect the HV bus to the frame electrodes at a top and a bottom corner of each CPA. (See Fig. 8.X) An identical board on the outer side of the field strip will connect the frame at that point to the first field cage element, with the connection from board to FC element made by a length of flexible conductor that runs vertically when the top FC is deployed (See figure below). A similar arrangement is made for each end-wall FC module. Because two CPAs attach to each FC module, the effective resistance between the HV bus and field strips is 1250MΩ, one half of a single stage of the FC resistor divider board; the same effective resistance is between the field strip and the first FC element, thus achieving the desired bias. The resistors will be protected by two varistors in series, placed in parallel with the resistors. The same parts for resistors and varistors are used as for the FC resistor boards:

Resistors DigiKey p/n SM104FE-5000M-ND
Manufacturer Slim-Mox SM104035007FE
Transient/Surge Absorber DigiKey p/n P7227-ND
Manufacturer Panasonic ERZ-V14D182

The printed circuit boards are 28 mm long and 51 mm wide.

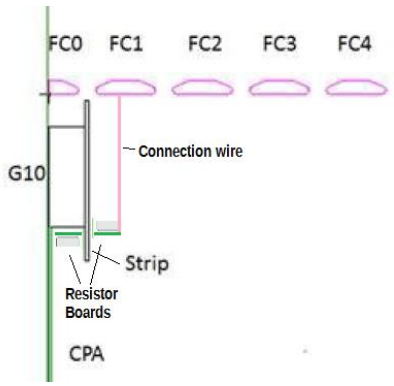

12.10 HV Current Monitor

HV circuit monitoring devices include the current reading of the power supply, the toroidal transformer to detect spikes and noise in the current draw described in the previous section, and a monitoring point at the end of the field cage resistor chain, which can be seen the schematic in Fig. 70.

The monitoring point is actually connected to a frame around the edge of the APA, and provides a means to control field-shaping around the edge of the APA by applying a bias voltage from an external supply; in this application, the current drawn can still be used to infer current through the FC resistor chain.

12.11 HV Slow Control Software

A possible setup of slow control monitor could be derived from that developed for ProtoDUNE-SP. Controls at single phase for the field cage terminations and monitoring are based on the OPC-DA (Open Platform Communications - Data Access) protocol communication with the hardware. In this way, one can turn on/off, set the voltage, current limit, current trip and monitor the status of each field cage terminations.

In the case of high voltage power supply, OPC-UA (Open Platform Communications - Unified Architecture) protocol is used to communicate with the cRIO (CompactRIO: http://www.ni.com/en-us/shop/compactrio.html) Heinzinger controller. The cRIO processes user input and sends commands to the power supply for the execution. Each command is executed inside the cRIO-FPGA in a 1ms loop. The data from the power supply is delivered to the slow control software by cRIO as well. All data is stored in an Oracle DB which allows also offline analysis.

The slow control software, DCS, that has been used at ProtoDUNE is based on the Siemens Simatic WinCC Open Architecture. Together with CERN's JCOP (Joint Control Project) and UNICOS (Unified Industrial Control System), it provides scalable multi-platform software.

DCS uses graphical user interface to allow to perform all required operations on the high voltage system components. The common functionalities include:

- Turning on/off the power supplies
- Setting the current limit

- Setting nominal voltage
- Setting ramping up/down rates
- Monitoring/Plotting the trends for voltage, current on the field cage and cathode power supplies, in addition to beam plug and ground plane monitoring

In addition to the common functionalities, Heinzinger slow control provides the following additional features:

- Setting the ramping rate
- Setting the ramping more
- Emergency stop
- Setting up the resistance in the system
- Function based current trip limits
- Auto recovery from the excessive current access (steamers)
- 3 data acquisition modes: slow, event log and fast acquisition
- Alarming with direct email and SMS

Figure 97 shows a screen-shot of the DCS for the Heinzinger power supply.

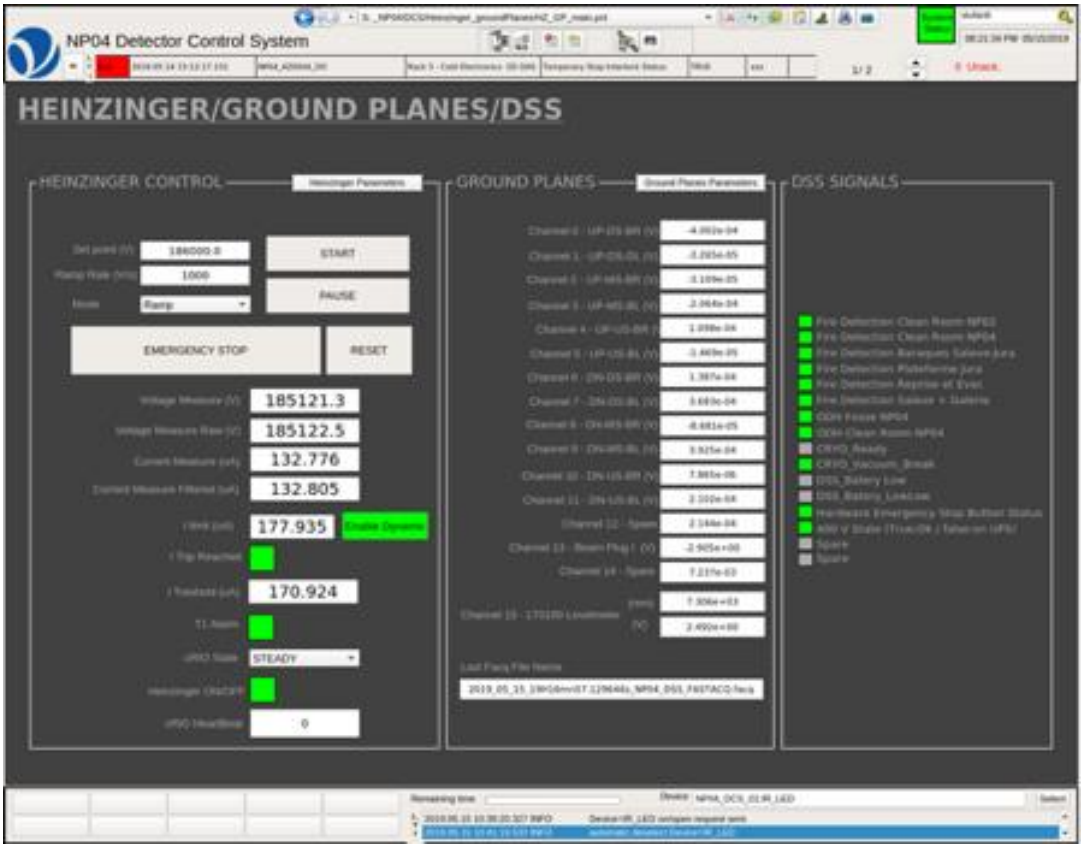

Figure 97 Screen shot of DCS for the Heinzinger HV power supply.

12.12 HV Assembly and Installation

Connections of the elements of the HV System are made during both component assembly and TPC

installation. During component assembly, connections are made on the CPA Units - HV Bus and FSS; and voltage divider boards on the EndWall and Top/Bottom FC modules. During installation, additional connections are made between adjacent CPA Panels, between CPA and Top/Bottom FCs and between CPA and EndWalls.

CPA Assembly

A schematic diagram of the electrical connections on the CPA is shown in Figure 98.

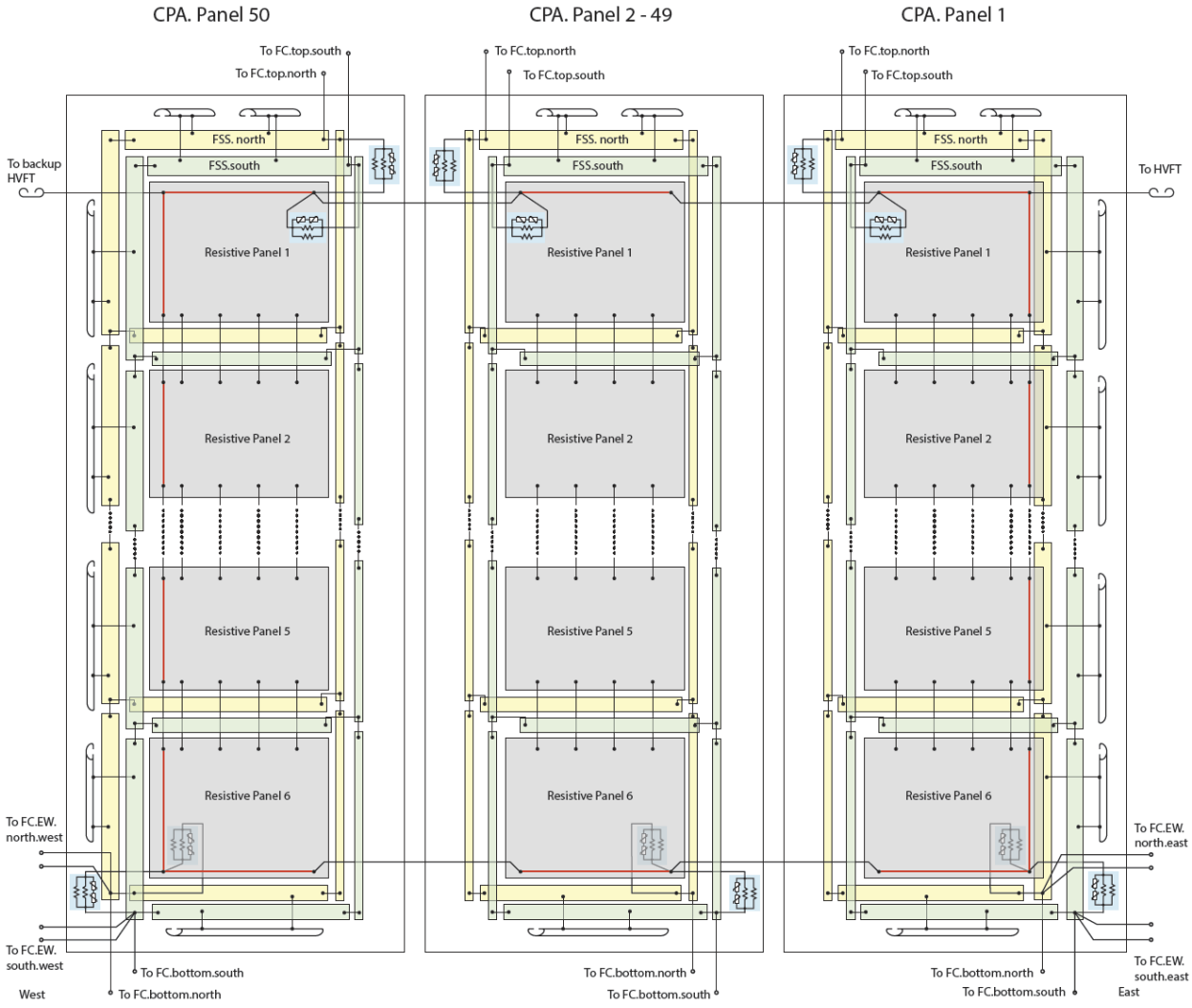

Figure 98 Schematic diagram of CPA electrical connections.

At the CPA production factories, HV connections on CPA Units will be completed and tested. These connections consist of elements of the HV Bus, connections between two resistive panels in a CPA Unit, connections between FSSs, mini-resistor board connections from the resistive panels to the FSS and finally, connections between the FSS and CPA profiles. In all cases, the connections are made with Brass plates, screws, flat washers and nuts (#8 or #10) and stainless steel disc spring (Belleville) washers.

For Upper (Lower) CPA Units, the HV Bus runs across the top (bottom) of the Unit under the FSS. The insulated cable bus is terminated with a #10 stainless steel ring lug which is attached to brass plates mounted on the front and back of the resistive panel with #10-24 Brass screws and two Belleville washers. In the case of the two CPA Panels at the end of the CPA Array, the HV Bus runs down the side of all 3 CPA Units and has similar brass plate connections as the Upper and Lower Units. For the (96) B-type CPA Panels, Middle Units have no HV Bus connections - the Upper (Lower) Unit has the HV Bus running also the top (bottom) of each Unit. The torque specification for these connections is 30.0 in-lbf. The front and back Brass plates supply HV to the resistive panels. In addition, four-fold connections are made between the resistive panels of the top and bottom module of each of the 3 CPA Units. These connections consist of a #10-24 Brass screw with a Brass nut and flat washer on the rear side and two Belleville washers and a flat washer on the front side under the screw head. The torque specification for these connections is 30.0 in-lbf.

FSSs are mounted to the CPA frames using #8-32 screws with a single #8 Belleville washer. At the junction between two FSSs, a Brass strap is connected to both FSSs with #8-32 Brass screws and two #8 Belleville washers. The torque specification for these connections is 25.0 in-lbf for the direct mounting screws and 25.0 in-lbf for the Brass straps.

The required voltage drop between the CPA Plane and the FSSs mounted on the CPA frames is 1/2 of the voltage drop between profiles of the FC. A mini-resistor board connecting the resistive panel to a FSS steps down the voltage to the required value. All connections are #8-32 Brass screws with nuts and Belleville washers. Stainless steel #8 ring lugs on a wire jumper connect the board to the Brass plate on the resistive panel. After the voltage drop, connection to the FSS is made with a #8-32 Brass screw with a nut and Belleville washers. This connection also includes a wire jumper with stainless steel #8 ring lug between the Belleville washers and the FSS - this jumper is connected to an additional resistor board that drops the voltage an additional l 1/2 step connected to the first profile of the Top/Bottom FC (described in installation section below).

At the top of each CPA Panel, an aluminum profile is mounted on either side of the Hinge Block. At the bottom of each CPA Panel, a single aluminum profile is mounted across the Panel width. These profiles are mounted directly to the CPA FR4 frames with special “Z” brackets. The voltage required on these CPA profiles is the same as on the FSSs. Jumper wires with #8 ring lugs are used to connect the nearest FSS to the mounting brackets of the Profiles. There are two connections per Profile to ensure proper voltage on these components.

The connection configurations and torque specifications for the CPA Units are summarized in Table 2. Standard torque screwdrivers are supplied to each factory to use in CPA production. The adjustable torque limit will be checked before each use.

Connection	Type	Torque (in.-lbf.)
HV Bus (cable to plate)	#10-24 Brass, 2 SS Belleville washers	30
RP section-to-section	#10-24 Brass, nut, flat washer, 2 SS B'ville	30
FSS fasteners	#8-32 Brass	25
FSS Brass Straps	#8-32 Brass, 2 SS B'ville	25
Mini-Electrical Board	#10-24 Brass, ring lug, nut, 2 SS B'ville	30
Mini-Electrical Board	#8-32 Brass, nut, ring lug, 2 SS B'ville	25
FSS to Profile	#8-32 Brass, nut, flat washer, 2 SS B'ville	25

Table 2 - List of CPA electrical connections with torque specifications.

Top/Bottom and EndWall FC Assembly

Figure 99 and Figure 100 show the schematic diagrams of the Top/Bottom FC module, and the EWFC module and an 8 module column. The interconnect between the adjacent field cage profiles are realized by a set of Resistive Divider Boards, described in 12.8, mounted on each profile.

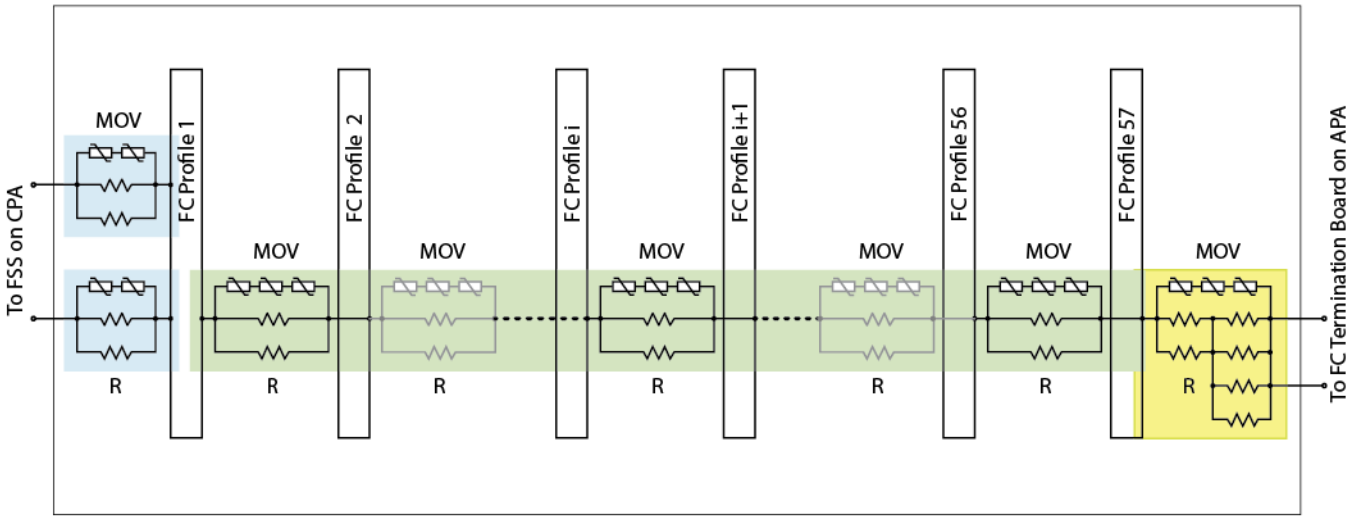

Figure 99 Schematic diagram of Top/Bottom FC Module electrical connections.

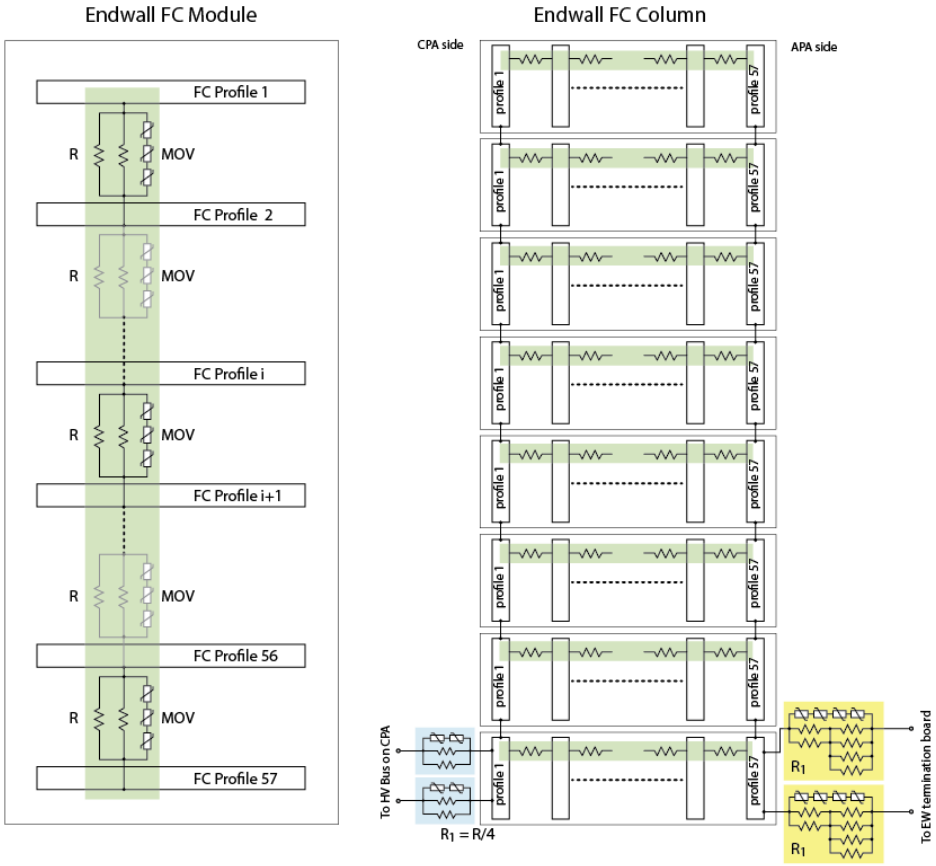

Figure 100 Schematic diagram of EndWall electrical connections.

Mounting of Resistive Divider Boards on the Field Cage Modules

The Resistive Divider Board (RDB) consists of eight resistive stages in series and hence connects to 9 field cage profiles electrically and mechanically. Figure 101 shows a cross sectional view of the board to profile connection.

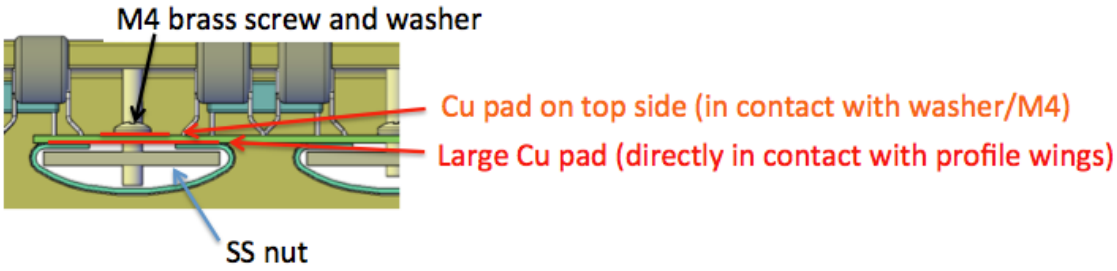

Figure 101 Cross sectional view of field cage profile, inserted stainless steel slip nut, M4 screw and washer as well as resistive divider board components.

A stainless steel (SS) slip nut with a tapped single hole (drawing: pDUNE-TPC-FC-W4-0047) is held by a M4 brass screw with a zinc plated steel washer (0.25" ID, 0.562" OD) inserted between the top surface of the PCB and the screw head. The screw is tightened with a torque specification of ~1 Nm.

The copper pad on the bottom side of the resistive divider board is pressed against the legs of the Al profiles which ensures a large area electrical connection. In addition, the washer placed underneath the M4 screw head is in direct contact with the copper pad on the top surface of the resistive divider board and electrically connects through the brass screw to the SS slip-nut which also presses against the legs of the Al profiles.

CPA/FC Installation

CPA Panels are shipped to SURF in crates containing two Panels making up a single CPA Plane. In the clean room at SURF, the CPA Units are removed from the crate and assembled into Panels. In addition to mechanical connections, Panel assembly involves completing the electrical connections involving resistive panels and FSSs. HV Bus segments on "A" and "C" Panels are connected at Unit boundaries with jumper wires between Brass plates. RP section-to-section connections are required between each of the 3 CPA Units, with connections as described in Table 2. FSSs at each Unit boundary are connected with "T"-shaped Brass straps connecting two vertical FSSs with a horizontal FSS. Once a CPA Panel is hung from the transport beam, electrical connections are checked on both front and rear sides.
Once both CPA Panels from a shipping crate are vertical, connections between the two Panels are made. At the top and the bottom wire jumpers are fed through holes in the frame to connect the HV Bus elements between Brass plates. The two-Panel assembly is called a CPA Plane and once connected, all connections are checked.

The next step in the installation procedure is to attach Top FC modules to the hinge blocks at the top and on both sides of the CPA Plane. Once hanging from the hinge block, the wire jumper from the voltage divider boards on the FC can be attached to the point where the mini-resistor board on the CPA makes contact with the FSS. The #8 ring lug is placed between the Belleville washers and the FSS and the screw is tightened with 25.0 in-lbf torque. There are two connections per FC module on each side of the CPA Plane. The CPA/FC assembly is then moved into the cryostat to its position in the TPC. Once the Bottom FCs are in place, similar connections between the CPA and Bottom FCs are made as those on the Top FCs.

For the first and last rows of CPA/FC assemblies, electrical connections must also be made from the CPA FSS to the first profile on the EndWalls. This is done in the same way as the connection from the CPA to the Top/Bottom FCs – a jumper from the voltage divider board mounted on the EW. There are two connections per EndWall section on each side of the CPA Array at the bottom of the TPC.

FC Termination on the APA

In the SP FD TPC design, the distance between the last T/B FC profile (#57) and the grid wire plane on the APA is 83mm. While the nominal bias voltage on the grid wires is -665V for a 500V/cm drift field, the effective average potential on the grid plane is about -623V. Therefore, the bias voltage on the last FC profile should be set at -4773V. We use a special short divider board with a 50% higher resistance than that between the other profiles (1.5*2.5G) to drop another 4500V before connecting to the FC termination board. This termination voltage of -273V is set by the resistance R_T on the termination board: R_T=227.5MΩ. This voltage is also brought out of the cryostat through a RG316 cable along the CE data/power cable bundles to the outside of the cryostat on the cold electronics feedthrough flange. This voltage line is used to measure the current flown through this FC module to monitor its stability. Figure 102 shows the schematic of the termination features of the TBFC modules.

The EWFC modules are stacked 8 high, each with its own RDB chain. To minimize the risk to the APA wires, we chose to short out all 8 of the RDB chains at their last profiles. The effective termination resistance on the termination board for the EWFC is $R_T/8$. This voltage is also brought out of the cryostat for monitoring purpose.

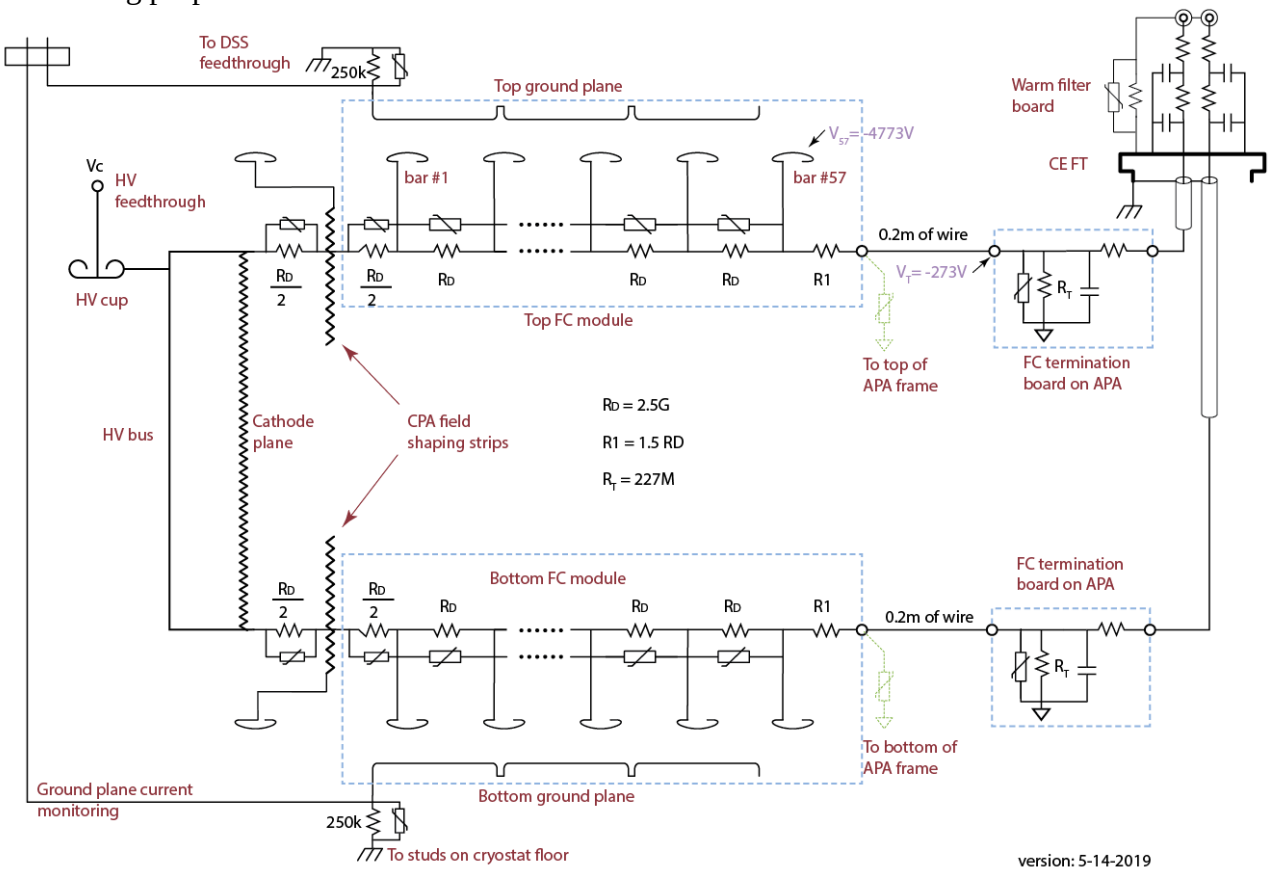

Figure 102 Schematic diagram of the terminations of the T/B FC.

The field cage termination boards, see Figure 103 for the NP04 version, are mounted on the top of the upper APA frame, and the bottom of the lower APA frame, between the banks of cold electronics boxes, near the TCO side of the APA. Each board has two termination channels. Unlike NP04, the FD center row of the APAs supports field cage modules on both sides. At the TCO side of the last APA, we'll need 4 channels of termination at that bottom corner of the APA by stacking two of the boards.

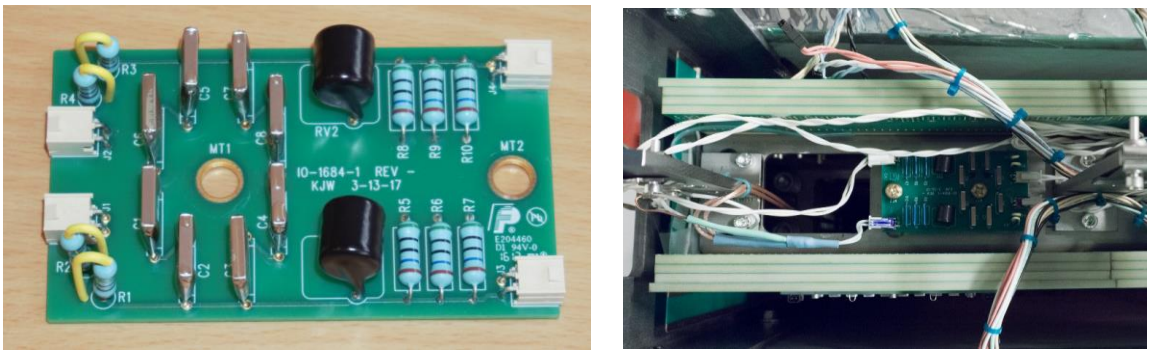

Figure 103 NP04 version of the FC termination board (left), and its mounting location on the APA.

13 Conclusion

A design of HVS system for the LAr-TPC of the DUNE single phase far detector has been developed, to meet the physics requirements. The design of the CPA and FC was built on experience learned from past experiments and extensive R&D test stands on material quality and performance as well as small scale LAr-TPC's.; the construction of prototypes have been performed to thoroughly understand the design. A first implementation of this design was realized and successfully tested in ProtoDUNE-SP. Full size mechanical prototypes are being constructed to evaluate the installation of the TPC into the far detector cryostat.

References

There are no sources in the current document.